

The role of CTCF in skeletal muscle homeostasis

Yuqing Yang

Division of Experimental Medicine, Faculty of Medicine and Health Sciences
McGill University, Montreal, Quebec, Canada

April 2022

A thesis submitted to McGill University in partial fulfillment of the requirements of the
degree of Master of Science

© Yuqing Yang 2022

Table of Contents

Abstract.....	4
Résumé.....	5
Acknowledgement.....	7
Contribution of Authors.....	8
1 Introduction	9
1.1 Skeletal muscle	9
1.1.1 Muscle architecture	9
1.1.2 Muscle fiber	11
1.1.3 Muscle contraction.....	13
1.1.4 Muscle metabolism	14
1.2 Muscle regeneration.....	16
1.2.1 Satellite cells	16
1.2.2 Minor trauma	18
1.2.3 Major trauma.....	19
1.2.4 Chronic regeneration.....	20
1.3 CTCF function	20
1.3.1 Role in transcription.....	21
1.3.2 Role in genome organization	24
1.3.3 Role in muscular diseases	25
2 The role of CTCF in skeletal muscle homeostasis	27
2.1 Introduction.....	27
2.2 Hypothesis.....	28
2.3 Objectives	28
2.4 Results.....	29
2.4.1 <i>HSA^{Cre/+}; Ctcfl^{l/+}</i> mice exhibit muscle defects	29
2.4.2 CTCF-deficient mice exhibit signs of muscle regeneration	33
2.4.3 The loss of CTCF in muscle causes collagen deposition.....	37
2.4.4 CTCF-deficient muscles do not exhibit signs of apoptosis	38

2.4.5	Muscles that lost CTCF exhibit weak signs of degeneration.....	38
2.4.6	The loss of CTCF in muscle leads to weak signs of inflammation	40
2.4.7	Transcriptome analysis in <i>HSA</i> ^{Cre/+} ; <i>Ctcf</i> ^{fl/fl} mice.....	42
2.5	Materials and Methods.....	56
2.5.1	Mice	56
2.5.2	Four limb hanging test	56
2.5.3	<i>Ex vivo</i> muscle contractility assay	56
2.5.4	Immunofluorescence.....	57
2.5.5	Histological staining	58
2.5.6	Real-time qPCR	59
2.5.7	Western blotting.....	59
2.5.8	Immunophenotyping	60
2.5.9	RNA-seq and analysis.....	61
3	Discussion	62
3.1	CTCF is necessary for muscle contraction	62
3.2	CTCF deficiency may influence muscle metabolism	63
3.3	The loss of CTCF may trigger unfolded protein response and mTORC1 signaling .	64
3.4	The potential mechanism of <i>Ctcf</i> mKO mice	66
4	Conclusion	68
5	References.....	69

Abstract

Skeletal muscle is one of the most dynamic human tissues and it is critical for the voluntary movement of the body. Muscle function is tightly linked to its delicate structure, which is mainly composed of myofibers and connective tissues. Muscle contraction is achieved by the cooperation of diverse types of myofibers, and supported by muscle metabolism that is dependent on robust mitochondria activity. When homeostasis is disrupted, skeletal muscle exhibits various strategies to deal with the injury, depending on the severity of the injury. Muscle regeneration has strong links with the activation of a muscle stem cell transcriptional program. CCCTC-binding factor (CTCF) is an indispensable protein in vertebrates and promotes a myogenic differentiation program in muscle cell line. It is regarded as a multifunctional epigenetic regulatory protein. CTCF was first identified as a transcriptional repressor. In addition to the regulation of transcription, it also plays a critical role as a genomic architectural protein. Recent studies indicate that CTCF is involved in muscle-related diseases. However, the role of CTCF in skeletal muscle *in vivo* homeostasis has not been explored. Our novel study investigated whether CTCF plays a role in skeletal muscle formation and function through employing a *Ctcf* knockout mouse, *HSA^{Cre/+}; Ctcf^{fl/fl}* mice. In this model, *Ctcf* expression is specifically reduced in skeletal muscle myonuclei, starting at 9.5 days *post coitum*. We found that these mice started to progressively lose weight and muscle mass at 8 weeks after birth, and demonstrated dramatic muscle wasting by 13 weeks. Meanwhile, CTCF-deficient mice also exhibit serious defects in muscle function and contraction. Furthermore, the loss of CTCF in skeletal muscles lead to signs of regeneration at 13 weeks, while these muscles only had a few degenerating myofibers. It suggests that CTCF-deficient muscle may suffer from continuous muscle injuries which trigger strong muscle regeneration. Transcriptome analysis provides insight that repression of genes involved in muscle contraction and homeostasis may underlie the muscle wasting observed in *Ctcf* knockout mice.

Résumé

Les muscles squelettiques sont parmi les tissus humains les plus dynamiques et ils sont essentiels pour les mouvements volontaires du corps. Les fonctions musculaires sont étroitement liées à leur structure délicate, principalement composée de myofibres et de tissus conjonctifs. La contraction musculaire est obtenue par la coopération de divers types de myofibres et soutenue par le métabolisme musculaire qui dépend de l'activité robuste des mitochondries. Lorsque l'homéostasie est perturbée, le muscle squelettique présente diverses stratégies pour faire face à la blessure, en fonction de sa gravité. Cette régénération musculaire a des liens étroits avec l'activation d'un programme de transcription caractéristique des cellules souches musculaires. *CCCTC-Binding Factor* (CTCF) est une protéine indispensable chez les vertébrés qui, entre autres, favorise un programme de différenciation myogénique dans la lignée cellulaire musculaire. CTCF est une protéine régulatrice épigénétique multifonctionnelle, qui a d'abord été identifiée comme un répresseur transcriptionnel. En parallèle à la régulation de la transcription, CTCF joue également un rôle essentiel dans le maintien de l'architecture génomique. Des études récentes indiquent que CTCF est impliqué dans les maladies musculaires. Cependant, le rôle de CTCF dans l'homéostasie *in vivo* du muscle squelettique n'a pas été exploré. Notre nouvelle étude a examiné si CTCF joue un rôle dans la formation et la fonction des muscles squelettiques en utilisant une souris *HSA^{Cre/+};Ctcf^{fl/fl}*. Dans ce modèle, l'expression de *Ctcf* est spécifiquement réduite dans les myonucléi du muscle squelettique, à partir de 9.5 jours après le coït. Nous avons constaté que ces souris commençaient à perdre progressivement du poids et de la masse musculaire 8 semaines après la naissance et présentaient une fonte musculaire spectaculaire après 13 semaines. De plus, les souris déficientes en CTCF présentent également de graves défauts dans leur fonction et contraction musculaire. Aussi, la perte de CTCF dans les muscles squelettiques a entraîné des signes de régénération à 13 semaines, même si ces muscles n'avaient plus que quelques myofibres dégénératives. Cela suggère que les muscles déficients en CTCF peuvent souffrir de lésions musculaires continues qui engendrent une forte et constante régénération musculaire. À la suite de l'analyse des changements transcriptionnels engendrés par la perte de CTCF dans le tissu musculaire, la répression des gènes impliqués dans la contraction musculaire et l'homéostasie

semble jouer un rôle important dans la fonte musculaire observé dans les souris déficientes en CTCF.

Acknowledgement

First, I would like to thank Dr. Colin Crist and Dr. Michael Witcher for their invaluable guidance in research, for being my backup in the completion of experiments, and for their advice in my life and future career.

Further, I would like to thank Solène Jamet for all her assistance and patience. And I also would like to thank all the past and present members in two labs for their friendly support: Benjamin Lebeau, Cheng Kit Wong, Xiaoting You, Tiejun Zhao, Harry Cheng, Charlotte Sénéchal, Emmanuel Asante, Antoine Meant, Meredyth Elisseou, Mariam Hany Mohamed Anwar, Jie Su.

Moreover, I would like to thank our collaborators, Dr. Sonia Del Rincon from McGill University and Dr. Tom Cheung from Hong Kong University of Science and Technology. I would also like to thank my committee members, Dr. Elham Rahme, Dr. Natasha Chang, and Dr. Anastasia Nijnik for their feedback and suggestions. And I would like to acknowledge employees in the Lady Davis Institute for their assistance.

Lastly, I am grateful for the encouragement and support of my family and friends.

Contribution of Authors

Solene Jamet assisted with the start of all muscle-related experiments. Margarita Bartish from Dr. Sonia Del Rincon's laboratory assisted with immunophenotyping. RNA-seq was carried out by the collaborator Dr. Tom Cheung from Hong Kong University of Science and Technology, and processed to reveal differentially expressed genes by Benjamin Lebeau in Dr. Witcher's laboratory. And I completed all other experimental work.

Dr. Colin Crist and Dr. Michael Witcher provided suggestions for the thesis writing. And Benjamin checked the grammar of the French version's abstract.

1 Introduction

1.1 Skeletal muscle

There are three distinct types of muscle tissue in mammals: smooth muscle, cardiac muscle, and skeletal muscle. And the latter two are both striated muscles which generate force and contract. As one of the most plastic and dynamic tissues in humans, more than 600 skeletal muscles account for approximately 40 to 50 percentage of total body weight. Skeletal muscle is mainly composed of around 75 percent of water, 20 percent of protein, and other substances (e.g., mineral salts, lipid, and glycogen) (Frontera and Ochala, 2015). In the human body, there are 14 major muscle groups widely spread in the upper limb, lower limb, anterior and posterior side of the trunk, and other subgroups which do not coordinate with the skeleton for movement, usually in the hands, eyes, tongue, etc.

1.1.1 Muscle architecture

The function of tissue always determines its structure. One role of skeletal muscle in the body is to generate force, produce power, and provide movement. Based on muscle distribution, they are responsible for various movements, including walking, breathing, chewing, swallowing, and eye rotating. It is achieved by the contractions of muscles with voluntary control of the motor unit, and it is supported by another role of skeletal muscle, a metabolic organ that provides muscle glycogen fuel. Moreover, different types of muscle have various sizes because of the diverse size and number of the individual types of muscle fibers (Frontera and Ochala, 2015). For example, in humans, medial *gastrocnemius* muscle contains over 1 million muscle fibers, while the number of fibers in the *tibialis anterior* muscle is around 270 thousand. The shape of muscles also varies, involving fusiform muscle, parallel muscle, convergent muscle, circular muscle, bipennate muscle, unipennate muscle, and multipennate muscle.

Uniformly, the architecture of skeletal muscle is characterized by its well-organized and well-shaped structure, along with a particular arrangement of groups of skeletal muscle fibers, and connective tissue components. Specifically, each muscle is enclosed by epimysium, an irregular connective tissue. And bundles of fibers (fascicles) are surrounded by a second layer of connective tissue, called perimysium. Inside a fascicle, the third layer around a single muscle fiber is known as epimysium (Figure 1.1-1). These three layers of connective tissue play a role in separating muscle for an independent contraction, activating subsets of muscle fibers for a specific movement, and transferring muscle force, respectively (Gillies and Lieber, 2011). And the pathological change in the deposition of connective tissue may alter the muscle structure and influence muscle function (Berria et al., 2006; Lieber and Ward, 2013).

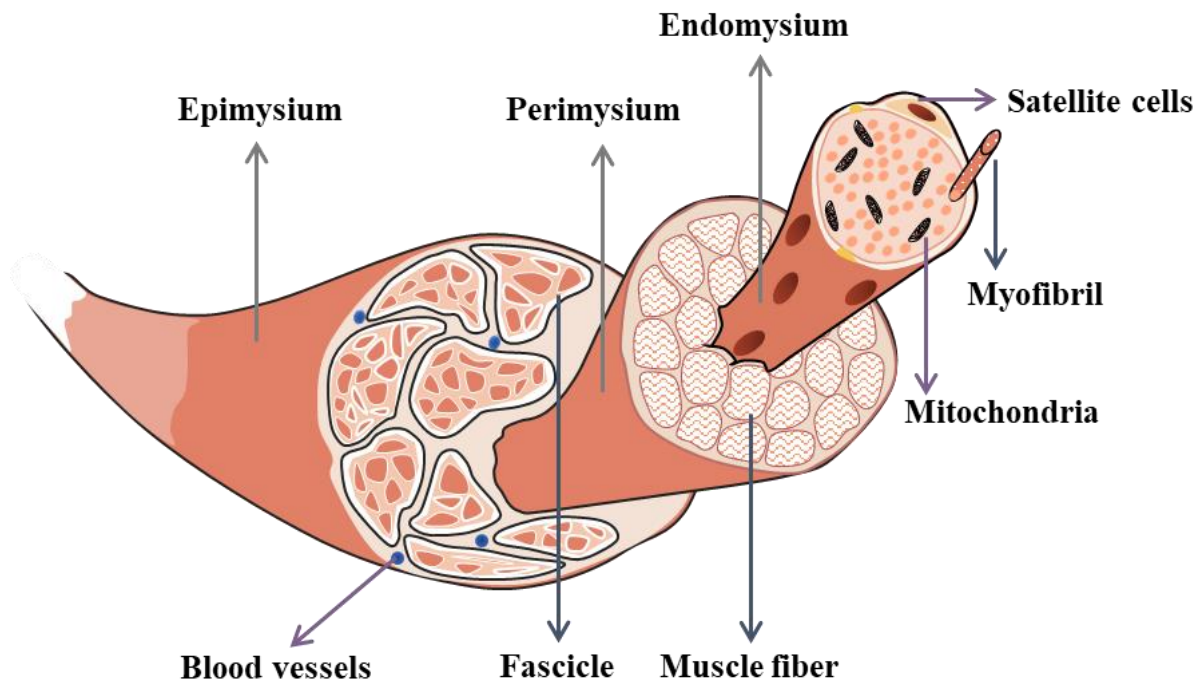


Figure 1.1-1 Illustration of skeletal muscle hierarchical structure.

Skeletal muscle tissue is surrounded by a layer of connective tissue (epimysium), and fascicles and blood vessels are underneath the epimysium. Fascicles are composed of bundles of myofibers and the outer perimysium. And each muscle fiber is encased in another connective tissue, endomysium, and holds an in-parallel array of myofibrils and critical

organelles, for instance, mitochondria. Satellite cells locate between endomysium and cell membrane.

1.1.2 Muscle fiber

Since skeletal muscle cells have long and cylindrical shapes with polynucleate nature, they are commonly named muscle fibers or myofibers. An individual muscle fiber is surrounded by a cell membrane (sarcolemma) and organized into thousands of myofibrils, which run the length of the muscle fiber and contain sarcomeres. And billions of myofilaments assembled in the myofiber form sarcomeres. As the basic unit of muscle contractile, the sarcomere is defined as a cytoskeleton structure between two Z-discs, with the middle H zone (Figure 1.1-2). And sarcomeres have a delicate arrangement of both thick and thin myofilaments that form the striated appearance of myofibers (Frontera and Ochala, 2015; Gillies and Lieber, 2011).

Specifically, the thick filaments constitute the dark A band of cytoskeleton structures and are anchored at the M-line in the middle of the sarcomere by Myosin protein, while the light I band is composed of thin filaments and anchored at the Z-discs by α -actin and other regulatory proteins (Figure 1.1-2) (Frontera and Ochala, 2015; Gillies and Lieber, 2011). Actin and myosin are two abundant proteins in the myofibers (Fujita et al., 1999), accounting for 70 to 80 percent of the total proteins. Myosin protein complexes contain heavy chain and light chain regions; the former one interacts with actin and regulate force generation, while the latter one has a binding site with adenosine triphosphate (ATP). Moreover, titin and nebulin also contribute to the properties of sarcomeres. Although they are not directly involved in producing force, titin and nebulin both help to stabilize the attachment, respectively for the thick filament and the thin filaments (Monroy et al., 2012; Ottenheijm and Granzier, 2010).

The heterogeneity of skeletal muscle is due to the diverse phenotypes of muscle fibers. The same type of muscle tissue in different mammalian species or different sorts of muscle tissue in the same species has various proportions of myofiber types because of the adaptation to physics and metabolic activities. There are multiple ways to classify the types of muscle

fibers, for instance, the red or white color of muscle fibers, fast or slow-twitch speed of contraction, oxidative or glycolytic metabolism as a predominance, the levels of protein isoform expression (Galpin et al., 2012; Needham, 1926; Schiaffino and Reggiani, 2011). One widely-used method in mice is to divide myofibers into four types with diverse representative myosin expression: type 1 fiber with slow-twitch and oxidative metabolic type, type 2A fiber with fast-twitch and oxidative metabolic type, type 2X and 2B fiber with fast-twitch and glycolysis metabolic type (Chemello et al., 2011; Schiaffino and Reggiani, 2011; Spangenburg and Booth, 2003) (Table 1.1-1).

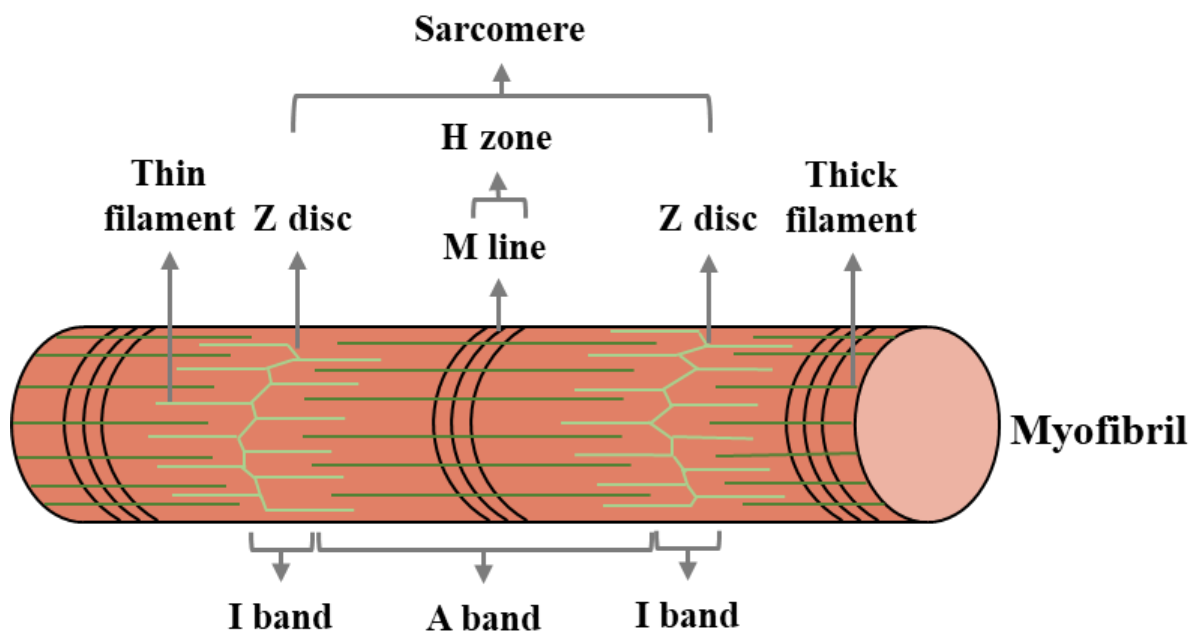


Figure 1.1-2 Schematic diagram of myofibril structure in a relaxed state.

Thin and thick filaments constitute sarcomeres between two Z discs, and sarcomeres further constitute a single myofibril. Based on the distribution of these two filaments, myofibrils are organized into I band and A band. Myofibrils enable muscle contraction through a sliding filament mechanism.

Fiber type	Type 1	Type 2A	Type 2X	Type 2B
Color type	Red	Red/White	White	White
Contraction type	Slow	Fast	Fast	Fast
Metabolic type	Oxidative	Oxidative	Glycolytic	Glycolytic
Representative myosin	MYH7	MYH2	MYH1	MYH4

Table 1.1-1 The common classifications of muscle fibers in mice.

Muscle fibers can be divided by representative myosin expression into four types: type 1 slow-twitch myofibers and type 2A, type 2X, and type 2B fast-twitch myofibers. Specifically, oxidative metabolism is predominant in type 1 and type 2A myofibers, while type 2X and type 2B muscle fibers depend on glycolysis metabolism. Because the myoglobin abundance is tightly linked to the metabolic type of fibers, type 1 myofibers are white, type 2A fibers are mixed red and white, while type 2X and 2B are red.

1.1.3 Muscle contraction

Muscle tissue is initially activated by the signal of motor neurons from the brain in the myoneural junction and exhibits excitation-contraction coupling in physiology, and then muscle contracts. The mechanism of muscle contraction is known as the sliding filament theory. The thick and thin myofilaments in myofibers do not change their lengths, but instead, the thin myofilaments slide across the thick myofilaments (Horowitz and Podolsky, 1987). As a result, sarcomere shortens. The H zone and the I band regions both shrink, but the length of the A band keeps constant. The molecular event beneath this model is termed cross-bridge cycling, which is a process of the interactions between ATP and the actin-myosin cross-bridge (Geeves et al., 2005).

Based on the muscle actions, contraction can be grouped into two basic types: static and dynamic muscle contractions. Statics contraction, also referred to as isometric muscle contraction, is employed when generating force, the muscle is kept in a fixed length and the attached joint or limb does not move (Gordon et al., 1966). Dynamic contractions are divided

into concentric and eccentric muscle contractions, and these two are often simultaneous with each other in a movement (Douglas et al., 2017). The difference is that the former happens when the muscle is shortened, while the latter occurs in the lengthened muscle.

Moreover, depending on the length and frequency of contraction, muscle contraction can be classified into three actions: twitch, tetanus and summation (van Zandwijk et al., 1998). A twitch is a single contraction. It starts from the latent period, which incorporates the beginning of a single stimulation, a transport of motor neurons, and a chemical transmission at the myoneural junction. Then muscle contracts and the tension of contraction reaches its maximum. After the contraction period, the muscle steps into the relaxation period and in the final returns to its resting tension. If an additional twitch contraction occurs before the end of the relaxation period in the previous twitch, it increases the peak amount of muscle tension, and summation is produced. One way to form summation is by recruiting additional muscle fibers within a muscle. When a weak signal activates muscle to contract, the smaller motor units are more excitable to be stimulated, but with the increased strength of the signal, the larger motor units are also gradually activated. Another way to achieve the summation is to increase the frequency of stimulation. The signal for activation is sometimes ineffective to arrive at the myoneural junction synchronously, so during the process of signal transmission, the frequency varies and results in summation. Furthermore, tetanus occurs when the force of tension is generated to the maximum point but then plateaus without relaxation.

1.1.4 Muscle metabolism

Muscle metabolism is driven by the energy demand of muscle contractions, and in the human body, muscle activities occupy an important part of the total energy consumption. The disorder of muscle metabolism may result in myopathies, termed metabolic myopathies, generally exhibiting genetic defects, for example, the lack of enzymes and disruption of ATP production (Adler and Shieh, 2015). Based on the specific defect, there are three categories: glycogen storage diseases, lipid storage disorder, and mitochondrial myopathy. Specifically,

glycogen storage diseases could be caused by either an autosomal recessive inheritance (e.g., *PYGM*, *PFKM* or *PHKA1* gene mutation), or a random genetic mutation (e.g., *ALDOA*, *ENO3* and *PGMI* gene).

All muscle fibers are capable to produce ATP. The energy is supplied by adenosine diphosphate (ADP) through cleaving the third phosphate group of ATP. To maintain a muscle contraction, an intrinsic supply of ATP is not sufficient. It also requires the replenish of ATP from phosphocreatine carbohydrates, lipids, and even amino acids, with a source order starting from ones inside muscle fibers and then elsewhere in the body, like the liver (Egan and Zierath, 2013).

The main intrinsic source of metabolic energy is the glycogen in myofibers, and skeletal muscle is the largest glycogen storage organ, even 4-fold of the liver (Egan and Zierath, 2013). Glycogen is a carbohydrate polymer and it can be broken down into individual subunits and produce simple sugar glucose through enzymatic hydrolysis. Generally, aerobic respiration sustains muscular activity, and a molecule of glucose is decomposed into CO₂ and H₂O with the generation of 36 ATP molecules. But in the absence of oxygen, anaerobic respiration occurs. One glucose is broken down into lactic acid and generates 2 ATP molecules. Compared to the aerobic pathways, although anaerobic glycolysis has a smaller production of ATP molecular and accumulates lactic acid, its rapid rate of ATP production can be effectual in some cases (Hargreaves and Spriet, 2020).

As mentioned in 1.1.2 muscle fiber, the muscle fibers can be grouped into four types with different representative myosin expressions. This difference is closely connected with the abundance of the oxygen transport protein (myoglobin), mitochondrial density, and the contribution of oxidative metabolism. The slow-twitch type 1 and fast-twitch type 2A myofibers are characterized by a high level of myoglobin expression and mitochondria content. And aerobic metabolism is predominant in their activities with a rich vascular supply. The fast-twitch type 2X and type 2B myofibers have less myoglobin and mitochondria, but anaerobic pathway and glycolysis metabolism are more effectively involved (Needham, 1926; Schiaffino and Reggiani, 2011; Zierath and Hawley, 2004).

Mitochondria are critical organelles in skeletal muscle as a key regulator of the metabolic status in myofibers (Hargreaves and Spriet, 2020; Hood et al., 2019). Different from other types of tissue, the mitochondria in skeletal muscle are usually shaped as a reticulum structure. And they are subdivided into two groups (Cogswell et al., 1993; Picard et al., 2013). The ones, called reside the subsarcolemmal (SS) mitochondria, provide energy for membrane transport and gene transcription, while the other ones, termed intermyofibrillar (IMF) mitochondria, facilitate contraction by providing ATP to myofilaments. Despite the difference, the two types of mitochondria networks together maintain a dynamic interplay in skeletal muscle. During exercise and muscle differentiation, the mitochondria undergo the fusion and biogenesis to expand sharing network and facilitate metabolism. Conversely, under aging or disuse of muscle, the fission and mitophagy in mitochondria are enhanced (Egan and Zierath, 2013; Loson et al., 2013; Mishra and Chan, 2016).

1.2 Muscle regeneration

Muscle regeneration is essential for maintaining the homeostatic process of the adult skeletal muscle. After prenatal and postnatal muscle development, adult skeletal muscle retains the capacity to regenerate in response to trauma, which is achieved by activating muscle stem cells. Due to aging or diseases (e.g., cancer cachexia and sarcopenia), the ability of muscle stem cells can be affected. And the specific responding cells in the muscle stem cell niches vary from the type of stimulus. The responses are usually coordinated by degeneration, inflammation, regeneration, and remodeling.

1.2.1 Satellite cells

Muscle stem cells (MuSCs), also named satellite cells, lie between the basement membrane and the sarcolemma of myofibers (Mauro, 1961). In undamaged muscles, they are mitotically quiescent, but they can respond to muscle injury and they have the myogenic potential. Quiescent MuSCs are labeled by the paired domain transcription factor PAX7 and cluster of

differentiation protein CD34 (Beauchamp et al., 2000; Uezumi et al., 2010). And *Pax7* is specifically expressed in satellite cells (Kuang et al., 2006; Seale et al., 2000). After the trauma, the PAX7 positive satellite cells are activated and start to express myoblast determination protein 1 *MyoD* and myogenic factor 5 *Myf5* (Crist et al., 2012; Fujita and Crist, 2018; Rudnicki et al., 1993; Sabourin et al., 1999). Normally, the number of satellite cells keeps stable before and after their contribution to muscle regeneration under a precise regulation (Crist, 2017). Meanwhile, some of the activated satellite cells undergo self-renewal to maintain the stem cell pool. A multipotent cell can process symmetric division into two daughter cells in the same state, or they can be asymmetrically divided into two types of daughter cells, activated and quiescent cells (Kawabe et al., 2012; Kuang et al., 2007)

Then activated muscle stem cells can proliferate into myoblasts that continue expressing *MyoD* and *Myf5* (Megoney et al., 1996; Rudnicki et al., 1993). The myoblasts further differentiate into central-nucleated myocytes with *Myog* and *Myf6* expression (encodes Myogenin and MRF4), which are muscle-specific basic-helix-loop-helix transcription factors (Charge and Rudnicki, 2004; Dumont et al., 2015). Then myocytes fusion into multinucleated myotubes where human α -skeletal actin (*HSA*) starts to express, as well as Myogenin and MRF4 proteins (Iwata et al., 2018; Nicole et al., 2003). Finally, myotubes become newly mature myofibers expressing embryonic myosin heavy chain protein, which is encoded by *Myh3* gene (Davie et al., 2007; Olguin et al., 2007; Rawls et al., 1998) (Figure 1.2-1).

However, the regenerative capacity of satellite cells may decline along with the age-associated or cell-intrinsic changes. In aged mice, the ability of activation and proliferation is impaired in the MuSCs (Grounds, 1998; Sadeh, 1988; Welle, 2002), while it remains controversial whether there is a difference in the number of the muscle stem cells compared to the young ones (Roth et al., 2000; van der Meer et al., 2011; Wagers and Conboy, 2005). The acceleration of senescence or apoptosis in MuSCs is also linked to aging (Jejurikar et al., 2006), and the weakened function of MuSCs leads to the loss of nuclei in the large fibers (Brack et al., 2005). Diseases could also induce the symptom of muscle wasting and impact on MuSCs. Patients suffering from cancer cachexia exhibit severe muscle atrophy (Powers et al., 2016). Even though MuSCs can be activated in response to muscle injury, the activated cells are not

capable to undergo the subsequent differentiation because of persistent PAX7 protein expression (Olguin et al., 2007; Oustanina et al., 2004). But it is noticeable that the contribution of MuSCs in muscle loss diseases is still debatable, like in sarcopenia, although it is accompanied by the reduced numbers of myofibers and more infiltration of fibrotic cells, the MuSCs function is normal (Fry et al., 2015; Verdijk et al., 2014).

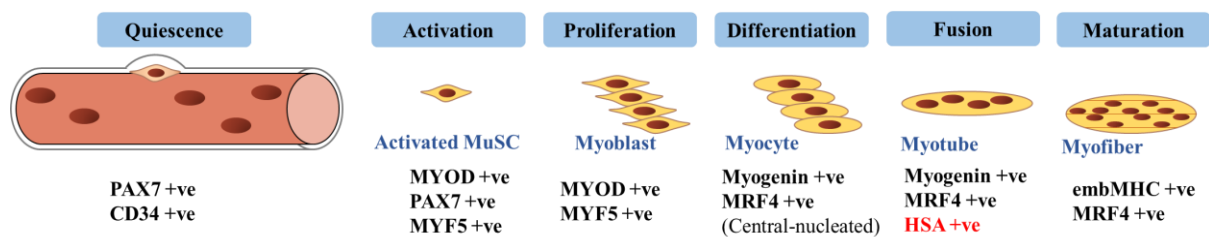


Figure 1.2-1 The progression and expression profile of myogenic lineage.

In muscle stem cell niches, quiescent satellite cells are activated and proliferate to generate myoblasts. Then these myogenic progenitor cells undergo differentiation into central-nucleated myocytes, fusion into multi-nucleated myotubes, and maturation into newly-formed myofibers. And there exist unique representative protein expressions for each stage. And key modulators of myogenic lineage progression are also shown at the bottom. Transcription factor PAX7 is necessary for the maintenance and activation of satellite cells but is lost after proliferation. The four myogenic regulatory factors, MYF5, MYOD, Myogenin, and MRF4, are sequentially induced in the following process. Human α -skeletal actin (*HSA*) starts to express in multinucleate myotubes. And the terminally differentiated myofibers also express embryonic myosin heavy chain protein (embMHC).

1.2.2 Minor trauma

One of the most common traumatic events is muscle injuries that could happen at any time in daily life. Minor muscle traumas more frequently occur in the human body, for example, muscle strains (Crisco et al., 1994; Garrett, 1990). Following this kind of damage to the muscle

fiber, the quiescent muscle stem cells in the muscle stem cell niches are prompted to activate, proliferate into myoblast, and differentiate into new myofibers. The resulting myofibers fuse with the damaged and degenerated myofiber and restore muscle integrity (Garrett, 1990; Jarvinen et al., 2005).

However, Roman, William, et al. discovered a new myofiber repair process that is independent of muscle stem cells (Roman et al., 2021). Adult mice were subjected to a mild musculoskeletal injury and myonuclei are attracted to this injured location through a signaling cascade involving calcium, Cdc42, and phosphokinase C. The movements of myonuclei are closely related to microtubules and dynein. These repositioned nuclei also participate in the transportation of messenger RNA for cellular restoration on a local level.

1.2.3 Major trauma

Massive injury, such as a toxic snakebite, is accounted into major traumas to the muscle. Although extensive damage happens, the skeletal muscle still has small groups of healthy cells. In the remaining viable cell, different types of cells all take part in the regeneration process. There are three stages starting from the stimulation of injury to the full recovery, including inflammatory phase, regenerative phase, and restorative phase, while three key events are also time-overlaid with each other (Baghdadi and Tajbakhsh, 2018; Chazaud, 2020).

First, molecules containing damage-associated molecular patterns (DAMPs) are released upon major trauma, for example, high mobility group protein B1 (Giordano et al., 2015). Because of these signals, neutrophils and monocytes are activated (Baghdadi and Tajbakhsh, 2018; Wosczyzna and Rando, 2018). Then neutrophils undergo apoptosis and monocytes further become macrophages (Fadok et al., 2001), followed by a shift from M1 macrophages to M2 macrophages (Deng et al., 2012). Plenty of pro-inflammatory cytokines (TNF- α , IL-6), chemokine (CCL17, CCL2), and growth factors (FGF, IGF-I, TGF- β 1) are secreted by the inflammatory cells (Brigitte et al., 2010; Collins and Grounds, 2001; Wang et al., 2014), and T cells start to take part in (Zhang et al., 2014). Meanwhile, when immune cells invade the injured area, these inflammatory molecules stimulate the proliferation of satellite cells. Transforming

growth factor $\beta 1$ (TGF- $\beta 1$) induces the proliferation of fibroblasts and results in the deposition of connective tissue (Lemos et al., 2015). Stimulated by TGF- $\beta 1$ and other signals, the myoblasts are differentiated into the newly-formed myofibers within the extracellular matrix (Li and Huard, 2002). Along with the apoptosis of inflammatory cells and fibroblasts (Lemos et al., 2015), inflammation and collagen infiltration are lowered. In the end, the injured muscle exhibits its original appearance.

1.2.4 Chronic regeneration

A range of myopathies can lead to a state of chronic regeneration as the repeated injury of myofibers. As a result, muscle stem cells are frequently activated and undergo myogenesis to form new muscle fibers that will repair the ongoing damage (Baghdadi and Tajbakhsh, 2018; Robson et al., 2011). One example is Duchenne muscular dystrophy. In the muscular dystrophy X-linked (MDX) mouse model, the skeletal muscle experience continuous cycles of degeneration and regeneration (Chemello et al., 2020; Haddix et al., 2018).

1.3 CTCF function

CCCTC-binding factor (CTCF) locates to the nucleus and is a ubiquitously expressed protein in eukaryotes (Filippova et al., 1996). Because it was first found that it can bind to three regularly spaced repeats of the core sequence CCCTC, it was named CCCTC binding factor (Lobanenkov et al., 1990). CTCF plays an indispensable role in vertebrates, which can be inferred from its conserved characteristics and its lethality. Specifically, CTCF is highly conserved in coding and non-coding regions, but especially its zinc-finger domain which shows strong conservation from humans to nematodes (Filippova et al., 1996; Moon et al., 2005). Complete CTCF deficiency in mice leads to early implantation lethality (Moore et al., 2012). And de novo mutations in CTCF are identified in human individuals with intellectual disability (Gregor et al., 2013).

The structure of CTCF protein is composed of three separate domains: an unstructured N-terminal domain, a central zinc-finger domain with 11 zinc fingers, and a C-terminal domain (Arzate-Mejia et al., 2018) (Figure 1.3-1). Various combinations of zinc fingers are used to interact with a cognate response element, which shows great DNA sequence diversity (Hashimoto et al., 2017). Moreover, the three domains of CTCF can individually or collectively interact with other proteins. These interacting partners include basal transcription proteins, DNA binding proteins, chromatin architectural protein, and so on (Battistelli et al., 2014; Chernukhin et al., 2007b; Klenova et al., 2001; Xiao et al., 2011b; Xiao et al., 2015; Yin et al., 2017).

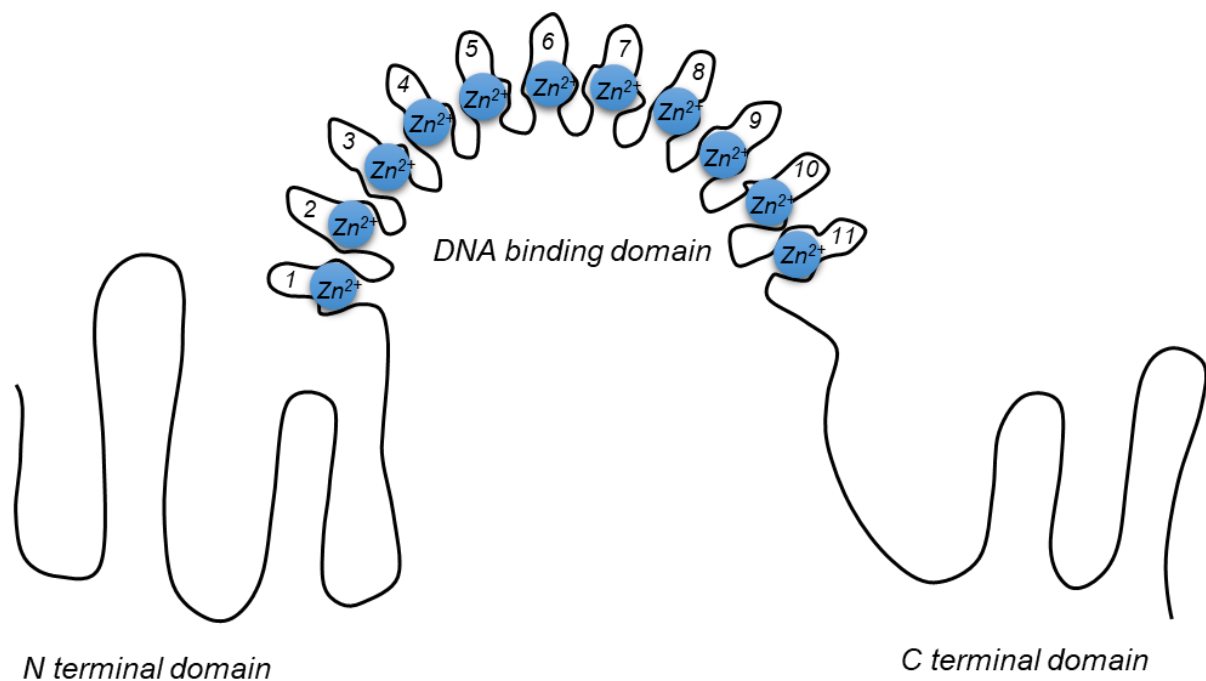


Figure 1.3-1 Domain structure of CTCF protein

CTCF protein is composed of three domains: N-terminal domain, C-terminal domain, and DNA-binding domain with 11 Zn-finger subdomains.

1.3.1 Role in transcription

Initially, CTCF was discovered as a negative regulator of the chicken *C-myc* gene

(Filippova et al., 1996; Klenova et al., 1993; Lobanenkov et al., 1990). Genome analysis finds that 55,000 -65,000 CTCF binding sites exist in the mammalian genome (Chen et al., 2012). Specifically, approximately 50 percent of these sites are present in intergenic regions, around 15 percent at proximal promoter regions, and about 35 percent of them at two sorts of intragenic regions, the introns, or exons (Chen et al., 2012; Chen et al., 2008). Plenty of studies have proved that CTCF broadly impacts on gene expressions for both repression and activation, although more as a repressor (Filippova et al., 1996; Filippova et al., 2002; Ren et al., 2017; Vostrov and Quitschke, 1997; Wan et al., 2008). Therefore, CTCF is capable to play a diverse role in the transcription process.

On the one hand, CTCF directly participates in regulating transcription. The C-terminal domain of CTCF protein can interact with RNA polymerase II (Pol II) and thus CTCF-Pol II complex is formed. It suggests that CTCF may recruit Pol II to its target genes in the preinitiation stage of transcription (Chernukhin et al., 2007a). Moreover, our lab previously discovered that CTCF is directed by transcription factor general transcription factor II-I (TFII-I) to bind to its target genes, and they together recruit cyclin-dependent kinase 8 to facilitate the initiation stage of transcription (Pena-Hernandez et al., 2015).

On the other hand, CTCF is the first identified insulator protein in vertebrates and regulates gene expression. In general, the mutual interaction between the promoter and its corresponding enhancer is accomplished through spatial proximity leading to gene activation. A key aspect of insulator function is to prohibit promoter-enhancer contacts and conduct the enhancer blocking action through the structural impediment in the chromatin loop (Chepelev et al., 2012; Dekker et al., 2002; Fudenberg et al., 2016; Kadauke and Blobel, 2009). Due to this function, CTCF is capable of blocking the inappropriate communication between enhancer and promoter and preventing unnecessary gene activation (Moon et al., 2005).

As an insulator, a classical example is represented by the chicken *β -globin* locus where CTCF blocks the enhancer activity (Splinter et al., 2006; Tolhuis et al., 2002). In the 20th century, CTCF was identified to bind to a 42-bp fragment in the chicken *β -globin* locus, and this binding site is responsible for the enhancer blocking. Following this, chromosome

conformation capture technology provided additional information that CTCF facilitates the formation of a chromatin loop that contains the *β-globin* gene and its corresponding locus control region (LCR) in the erythroid cells. Because of its formation, the *β-globin* site is repositioned, the communication with enhancer is prevented, and the target gene is repressively transcribed. However, CTCF binding to LCR is absent in fetal brain cells (Figure 1.3-2 A). Another example is the *H19/Igf2* locus. Genomic imprinting is an epigenetic phenomenon where the imprinted gene expression depends on whether it is inherited maternally or paternally (Pidsley et al., 2012). *Igf2* is an imprinted gene and its expression favors the allele inherited from the father. The *H19* and *Igf2* genes are separated from each other by the imprinting control region (ICR). CTCF cannot bind the methylated imprinting control region on the paternal chromosome but can bind the unmethylated one from the maternal allele. So, in the maternal allele, with CTCF binding and the insulator activity, the signal between the *H19*-proximal enhancer and the *Igf2* promoter is blocked and thus the *Igf2* gene is inactivated. Conversely, in the paternal allele, without blocking, the *H19* enhancer contacts with the *Igf2* promoter and activates *Igf2* transcription (Hark et al., 2000; Pidsley et al., 2012; Yoon et al., 2007) (Figure 1.3-2 B).

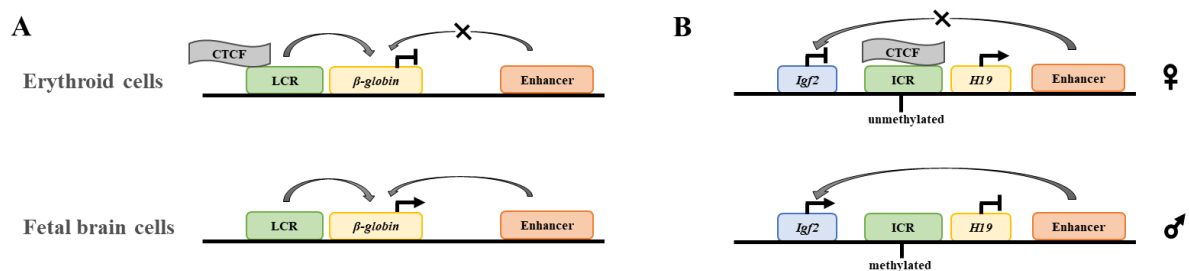


Figure 1.3-2 Transcriptional regulation by CTCF at model gene loci

(A) The regulatory mechanism of CTCF on *β-globin* locus is tissue-specific. CTCF binding to the locus control region of *β-globin* gene is available in erythroid cells and aids to form the chromatin loop to isolate the *β-globin* gene from the enhancer and inactivate *β-globin*.

However, the binding is prevented in fetal brain cells and *β-globin* is actively expressed.

(B) Genomic imprinting in the *H19/Igf2* locus has different interactions of CTCF depending on the maternal or paternal allele. The unmethylation of the maternal imprinting control

region allows CTCF binding, blocks the interactions between *H19* enhancer and *Igf2* promoter, and inhibits *Igf2* expression. But in the paternal chromosome, the methylated imprinting control region is prevented from CTCF binding.

1.3.2 Role in genome organization

In the current model for the mammalian 3D genomic organization, chromosomes occupy distinct territories within the nucleus. Compartments are divided into Compartment A, the transcriptionally active DNA, and Compartment B, less active DNA. Usually, the denser and less active DNA cluster along the nuclear periphery and around the nucleolus, while more accessible and active DNA cluster around nuclear speckles. This phenomenon is termed compartmentalization. The genome is organized into a series of large chromatin loops, over 700 kb in length, called topologically associating domains (TADs). These are contiguous regions of the genome, that may form DNA-DNA contacts with itself, but not with other regions (outside the TAD). Thus, TADS are insulated from regions outside the TAD, and has been referred to as insulated neighborhoods. In the insulated neighborhood, a TAD is almost always defined by CTCF anchors at the base. Intra-TAD microarchitecture consists of a diverse array of promoter-promoter links, enhancer-promoter linkages and other small domains that may also be mediated by CTCF or cohesion (Dixon et al., 2012; Fudenberg et al., 2016; Hsieh et al., 2020; Lieberman-Aiden et al., 2009; Nora et al., 2012; Rao et al., 2014; Sanborn et al., 2015). These intra-TAD contacts are referred to as subTADs.

One widely-recognized theory for loop formation is loop extrusion (Davidson et al., 2019; Fudenberg et al., 2016; Ganji et al., 2018; Nuebler et al., 2018). It is primarily driven by cohesin-mediated extrusion until it is stopped by convergent CTCF sites (Fudenberg et al., 2016; Sanborn et al., 2015). The cohesin protein complex is composed of three core subunits, SMC3, SMC1A, and RAD21, and shaped like a ring (Nasmyth and Haering, 2009; Stedman et al., 2008). CTCF-guided chromatin loops can function to isolate the elements inside loops from the outer ones. They also can facilitate the contact between gene and their promoters. To a large extent. the formation process depends on the exact interactions between CTCF and cohesion.

CTCF deficiency, loss of N terminals of CTCF, or the depletion of the cohesin subunit, all remove some of the original genome loops (Li et al., 2020; Nora et al., 2017; Pugacheva et al., 2020).

As a genome organizer, CTCF aids the existence of chromosomal interactomes. The appearance of a new technique, chromatin interaction analysis with paired-end tag sequencing (Li et al., 2014), analyzed the long-range chromatin interactions orchestrated by CTCF. This analysis identified approximately 1500 intra-chromosomal interactions and 300 inter-chromosomal contacts (Handoko et al., 2011). And from the map of chromosomal interactions, CTCF plays a role in chromatin boundaries for compartments and the isolation and facilitation of gene elements in mouse embryonic stem cells (Handoko et al., 2011). And it was also found that the activity of genes is related to the distance to CTCF-binding sites, the more proximal ones are more active (Yaffe and Tanay, 2011). Moreover, at the boundaries of TADs, the sites bound by CTCF have an enrichment of housekeeping genes (Dixon et al., 2012). Together, these findings provide powerful evidence for CTCF's role in genome organization.

1.3.3 Role in muscular diseases

Myotonic dystrophy type 1 (DM1) is caused by a type of dynamic mutation, the expansion of gene-specific trinucleotide repeats. It is most common that a CTG repeat expands in the 3' noncoding region of *DMPK* on chromosome 19q13.3 (Brook et al., 1992; Mahadevan et al., 1992). The original tract length is typically below 20 repeats, while in DM1, the expanded ones are more than 34 repeats and tend to experience continuous mutations, thus increasing the length even up to thousands of repeats. Filippova, Galina N., et al. discovered that CTCF is involved in the regulation of gene expression in this disease (Filippova et al., 2001). They identified the sequence area that *cis*-elements can act with contains five genes, such as *DMPK* and *SIX5*. And CTG repeats localize in the center of this area between the two CTCF binding sites. CTCF can function as an insulator to inhibit the contact between the enhancer of *SIX5* and the *DMPK* promoter. Because the locus of congenital myopathy is methylated at CpG dinucleotides and the combination by CTCF is sensitive to the methylation, it suggests that the

binding activity of the CTCF insulator may be lost, which leads to the high level of *DMPK* expression (Figure 1.3-3 A). And the abnormal hypermethylation at the DM1 locus with CTG expansions was further confirmed (Castel et al., 2011; Cleary et al., 2010).

Furthermore, in the 4q35 chromosome, CTCF and A-Type Lamins (Lamin A and Lamin C) can interact in D4Z4 repeats to repress some of the downstream gene expression, including *Ascl1*, *Pdlim3*, *Sorbs2*, and *Wwc2* (Ottaviani et al., 2009). Therefore, D4Z4 repeats facilitate the insulator role of CTCF. Facio-scapulo-humeral dystrophy (FSHD) is the third most common myopathy and causes the symptom of irreversible muscle weakness. It is related to the shortened D4Z4 array (van der Maarel et al., 2012). And due to a different interaction between D4Z4 repeats and CTCF, there exists a change of chromatin organization where CTCF-binding sites are hidden, as a result, the long-distance chromatin interactions are modified and some of the repressed 4q35 genes are induced to express (Gaillard et al., 2019) (Figure 1.3-3 B).

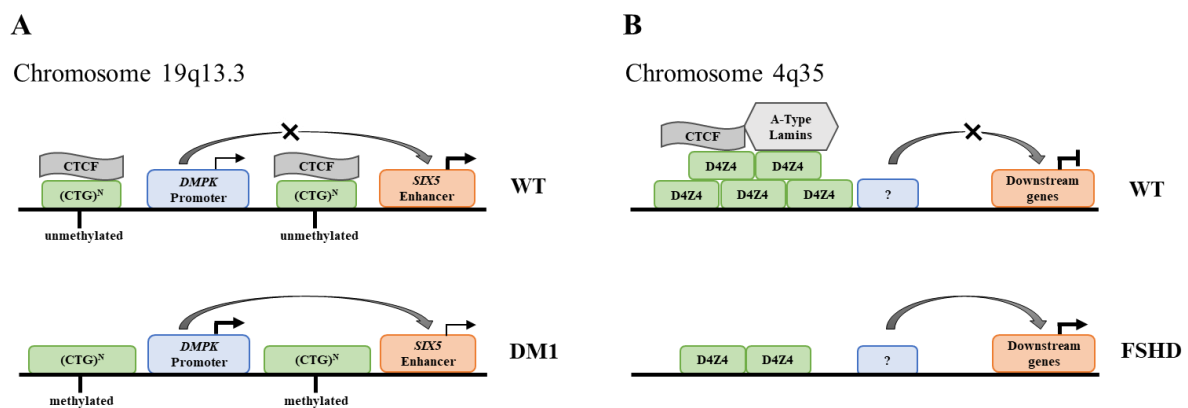


Figure 1.3-3 Current model for the role of CTCF in muscular diseases.

(A) In DM1 disease, the methylated CTG expansions prevent the binding with CTCF and its function as an insulator, thus influencing the gene expression of *DMPK* and *SIX5*.

(B) In FSHD disease, the shortened D4Z4 repeats hide the binding site for CTCF and promote the expression of originally repressed genes.

2 The role of CTCF in skeletal muscle homeostasis

2.1 Introduction

There is evidence that supports the role of CTCF in the myogenic regulation. In zebrafish embryos, CTCF may activate the expression of *Wnt11* and then stimulate the expression of myogenic differentiation regulatory factors *MyoD* and *Myog*. Upon the absence of CTCF, the contribution to myogenic regulatory factors on the expression of muscle-specific genes is repressed and these genes are downregulated (Delgado-Olguin et al., 2011). In another study, they found that myogenic regulatory factor MYOD directs fibroblast to trans-differentiate into skeletal muscle myoblast. There exists an enriched change in the interaction strength of MYOD binding at insulated neighborhood boundaries. And DNA motif analysis discovered the enrichment of CTCF- and MYOD-binding motifs in these altered MYOD-bound insulated neighborhood boundaries. It suggests that MYOD binds at CTCF-anchored boundaries in fibroblasts and alters the structure of insulated neighborhoods and the interactions inside them. Thus, MYOD-mediated myogenic commitment and differentiation are achieved (Dall'Agnesse et al., 2019).

Moreover, during the myogenic differentiation process, CTCF recruits MYOD in the C2C12 muscle cell line. They bind to the core promoter of terminal differentiation marker α -*SG* together, activate muscle-specific genes expression, and induce myogenic differentiation (Delgado-Olguin et al., 2011). A recent study also reveals that CTCF is involved in AUF1-mediated muscle development and regeneration. CTCF activates *Auf1* transcription through binding to its promoter and silencing of CTCF strongly decreases *Auf1* expression during myoblast differentiation. AUF1 regulates a stage-specific degradation of downstream micro RNAs (mRNAs). Specifically, AUF1 disrupts *Twist1* mRNA stability for initial myoblast differentiation, *CyclinD1* mRNA for blocking muscle stem cell proliferation, and *RGS5* mRNA for terminal myotube maturation (Abbadì et al., 2019).

It is believed that CTCF regulates the transcription in myogenic cells or the cells that have the potential to form myogenic cells. In addition to the transcriptional role, CTCF also mediates

genome architecture in the myogenic program. *P57* is a paternally imprinted gene and encodes for a cyclin-dependent kinase inhibitor that plays a crucial role in maintaining and promoting cell cycle arrest. Its promoter is controlled by the distant regulatory region KvDMR1 and CTCF mediates the formation of the repressive chromatin loop that constrains *p57* expression. However, during skeletal muscle differentiation, this CTCF-directed constraint is relieved by a functional interaction between MYOD and CTCF at KvDMR1. Thus, *p57* is induced in differentiating muscle cells (Battistelli et al., 2014).

2.2 Hypothesis

According to the previous study, it is already known that CTCF takes part in regulating muscle-specific gene expressions and the differentiation of muscle cells (Abbadi et al., 2019; Battistelli et al., 2014; Dall'Agnese et al., 2019; Delgado-Olguin et al., 2011). However, the study about the role of CTCF in cell lines provides us with limited information. It is due to the fact that the results and conclusions based on *ex vivo* culture do not equally match the situation in alive animals, where muscle cells are members of the muscle microenvironment and they influence each other.

Because CTCF plays a critical role in the transcriptional programming of muscle stem cell differentiation *in vitro* and in the maintenance of 3D genome structure, we hypothesize that CTCF plays an indispensable role in skeletal muscle homeostasis.

2.3 Objectives

Our goal is to define the role of CTCF in skeletal muscle *in vivo*, using a mouse model where *Ctcf* is specifically ablated in skeletal muscle. We chose to engineer a mouse where Cre recombinase is driven by the HSA promoter to delete floxed *Ctcf* gene in skeletal muscle. Human α -skeletal actin (*HSA*) is specifically expressed in skeletal muscle, starting at 9.5 days *post coitum* (Miniou et al., 1999). It is a time when a small proportion of the embryonic

myogenic progenitors fuse to form primary myofibers (Kelly and Zacks, 1969). And during the myogenic differentiation program, *HSA* is first expressed in the multinucleated myotubes (Iwata et al., 2018; Nicole et al., 2003).

By using the mouse model, we will further define whether the loss of CTCF leads to skeletal muscle defects, explore how skeletal muscle responds to the CTCF deficiency (e.g., triggering muscle regeneration process), and probe for the mechanisms via RNA-seq analysis.

In addition, as mentioned, CTCF is involved in muscle-related diseases, (e.g., facio-scapulo-humeral dystrophy, Duchenne muscular dystrophy, and myotonic dystrophy) (Castel et al., 2011; Cleary et al., 2010; Gaillard et al., 2019; Ottaviani et al., 2009; Peterson et al., 2018; Weiss et al., 2018). It suggests that the study of CTCF in skeletal muscle may show us more mechanism explanations of muscle diseases and novel ideas for the drug treatment of clinical application.

2.4 Results

2.4.1 *HSA*^{Cre/+}; *Ctcf*^{fl/+} mice exhibit muscle defects

To investigate the role of CTCF in skeletal muscle *in vivo*, *HSA*^{Cre/+}; *Ctcf*^{fl/+} mice were crossed with *Ctcf*^{fl/+} mice and thus generating a new conditional knockout mouse model (*HSA*^{Cre/+}; *Ctcf*^{fl/fl}) (referred to as *Ctcf* mKO) with a deficiency of *Ctcf* in skeletal muscle cells. Depletion of endogenous *Ctcf* is driven by *HSA*-Cre through deleting exon 8 (Figure 2.4-1 A). Quantitative RT-PCR and western blotting were performed and separately targeted for *Ctcf* gene and CTCF protein. Compared to the liver tissue, *tibialis anterior* muscles of 7-week-old *Ctcf* mKO mice had significantly decreased *Ctcf* expression in both transcript and protein levels (Figure 2.4-1 B-C). Immunofluorescence staining against CTCF was also implemented. We focused on the CTCF signals that were located inside myofibers and overlaid with DAPI signals. It proved that *Ctcf* expression in myonuclei was also significantly reduced in 7-week-old *tibialis anterior* (TA) muscles of *Ctcf* mKO mice (Figure 2.4-1 D-E).

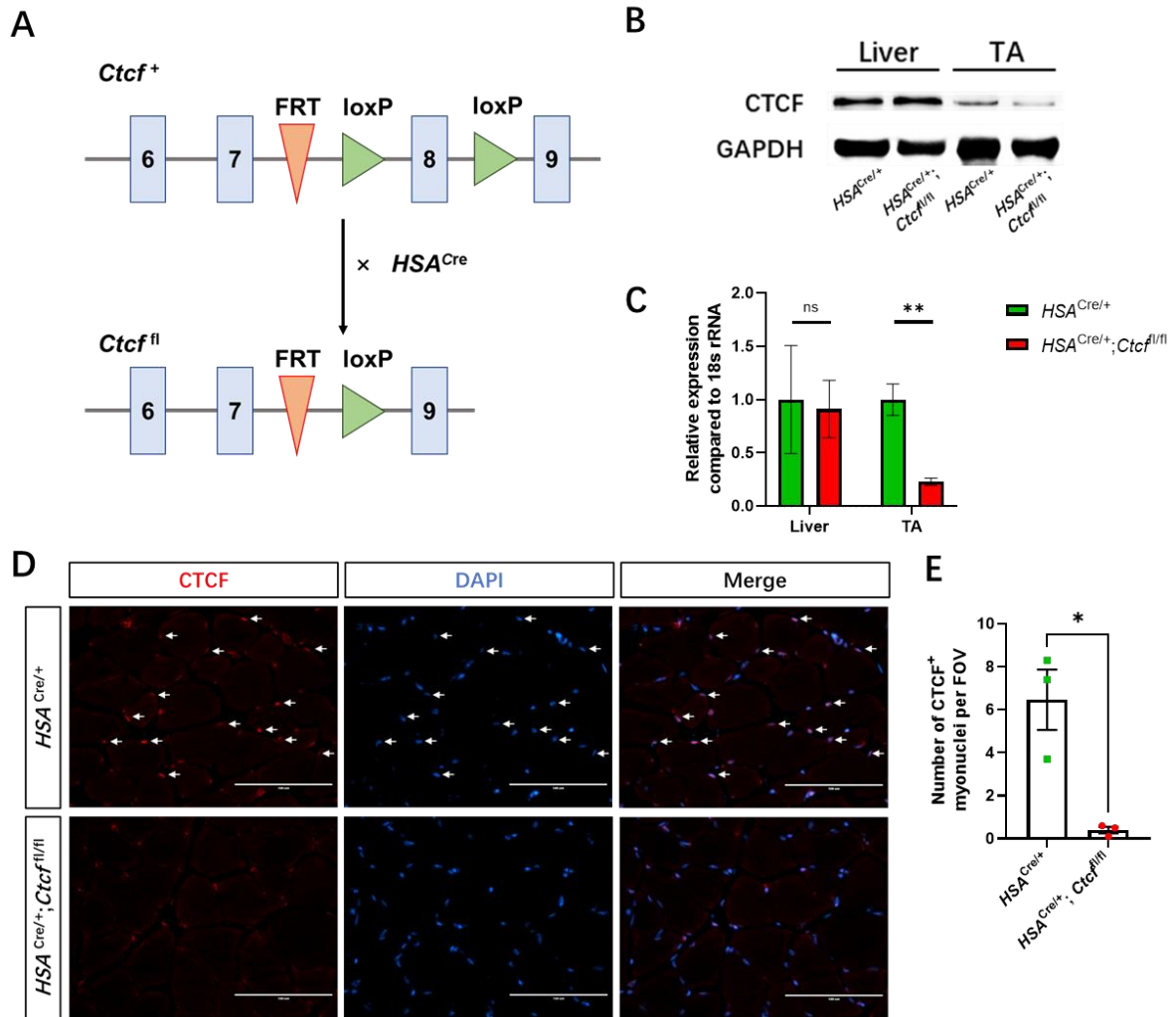


Figure 2.4-1 *Ctcf* expression is reduced in *Ctcf* mKO mice.

(A) Schematic diagram of *Ctcf*^{fl/fl} mouse model construction.

(B) Western blotting image of immunoblotting against CTCF in the liver and *tibialis anterior* (TA) muscle at 7 weeks. GAPDH served as a loading control.

(C) Relative *Ctcf* transcript levels in the liver and TA muscle at 7 weeks, determined by RT-qPCR (n = 3 in each group). Levels were normalized to 18S ribosomal RNA.

(D) Immunofluorescence staining of TA muscle cross-sections from control and *Ctcf* mKO mice using the antibody against CTCF (n = 3 in each group). Scale bar: 100 μm.

(E) The number of CTCF positive myonuclei per field of view (FOV) observed in Figure D.

To understand the effect of CTCF deletion in skeletal muscle, we observed mice morphology starting from 5 weeks. Through monitoring weight over time, CTCF-deficient mice exhibited progressive weight loss since around 8 weeks, and they were obviously different from control mice at 10 weeks (Figure 2.4-2 A). And we also noted a significant decrease in their weight at 13 weeks (Figure 2.4-2 A-B), which was up to approximately 20 percentage of maximum weight. Meanwhile, the dramatic muscle wasting (*tibialis anterior* muscle, diaphragm muscle, and *gastrocnemius* muscle) was also found in 13-week-old *Ctcf* mKO mice (Figure 2.4-2 B-C), instead of in 7 and 9-week-old mice (Figure 2.4-2 D-E).

To evaluate whether the loss of CTCF causes muscle functional defects, the muscle abilities were tested both *in vivo* and *ex vivo*. Four-limb hanging test is an efficient and non-invasive method to evaluate muscle strength and it was first performed at 7 weeks to avoid muscle strain for younger mice. Under a fixed maximum testing time as 10 minutes, the decrease in maximum four-limb hanging time was apparent from 10 weeks to 13 weeks (Figure 2.4-2 F), which suggests global physical function was weakened due to the loss of CTCF. We also dissected *extensor digitorum longus* muscle from 13-week-old mice to assess the contractile properties. And decreases in the force-frequency curves for both absolute force (mN) and specific force (N/cm²) were observed in *Ctcf* mKO mice (Figure 2.4-2 G-H). Together, it shows that skeletal muscles that lost CTCF had weight, strength, and contractile defects.

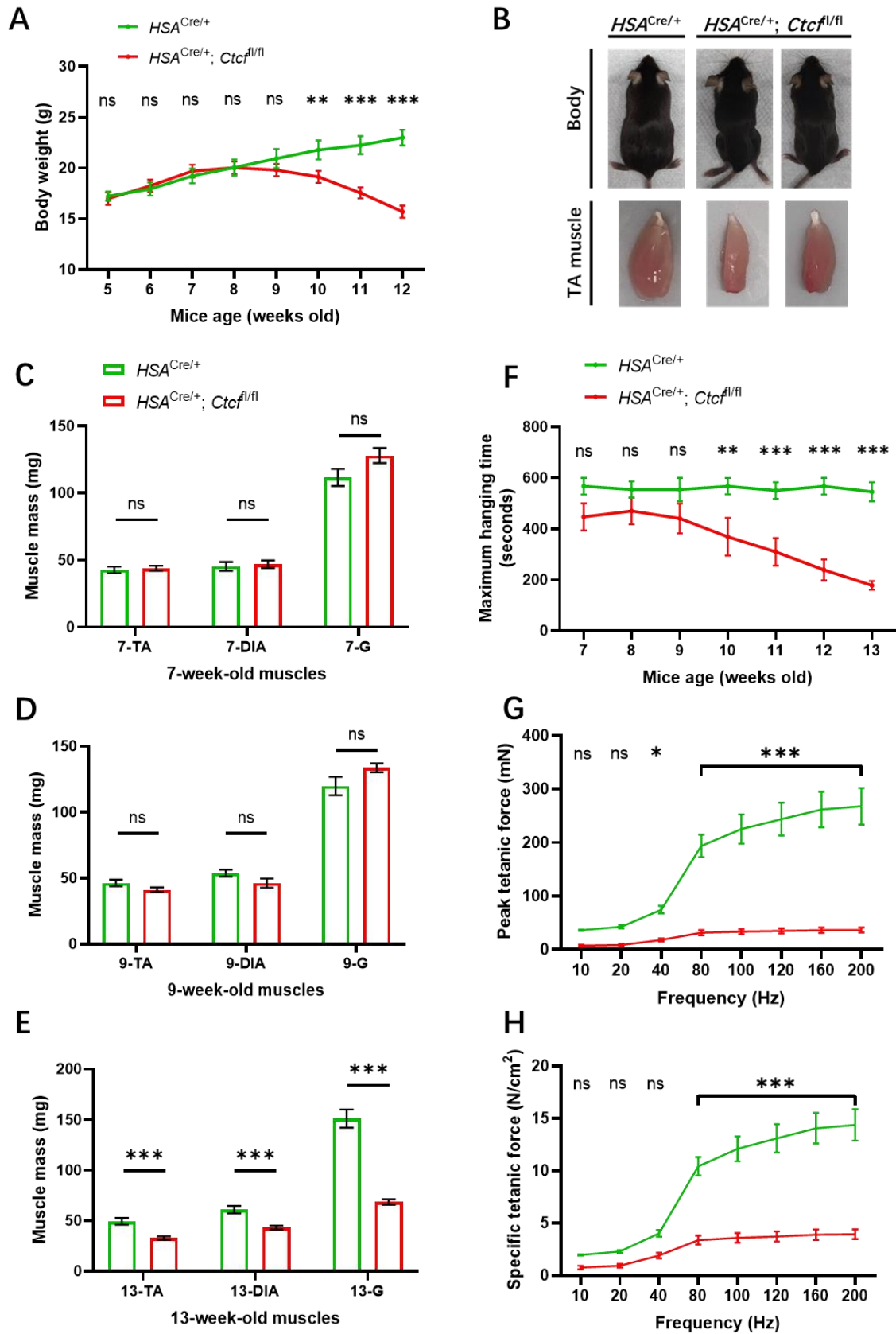


Figure 2.4-2 CTCF-deficient mice exhibit weight loss and muscle functional defects.

(A) The weights of *Ctcf*-deficient mice differed from the ones of control mice (n = 8 in each group).

(B) *HSA^{Cre/+}; Ctcf^{f/f}* mice were significantly smaller than the control mice at 13 weeks, as well as the TA muscle sizes.

(C-E) Muscle mass data was collected from 7-week-old (C), 9-week-old (D) and 13-week-old (E) of control and *Ctcf* mKO mice, including *tibialis anterior* muscles (TA), diaphragm muscles (DIA), and *gastrocnemius* muscles (G) (for Figure C and D, n = 6 in the TA and DIA groups and n = 4 in G groups; for Figure E, n = 10 in the TA and DIA groups and n = 5 in G groups).

(F) The measurements of muscle strength were tested through the peak time of the four-limb hanging test (n = 8 in each group).

(G-H) The summation contraction of *extensor digitorum longus* muscles was shown in the way of force-frequency curves for both absolute force (G) and specific force (H) (n = 3 in each group).

2.4.2 CTCF-deficient mice exhibit signs of muscle regeneration

To explore whether this muscle wasting is accompanied by muscle injury and regeneration, we performed immunofluorescence for muscle regeneration markers at 13 weeks (Fujita et al., 2021). PAX7 was used to count muscle stem cells, which can further proliferate into myogenic progenitor cells. And myogenic progenitor cells can differentiate into myocytes, which were marked by Myogenin. Then myocytes fuse to form myotubes, and mature to be newly formed myofibers, which were marked by embryonic myosin heavy chain (embMHC) and central nucleus.

Tibialis anterior muscle of 13-week-old *Ctcf* mKO mice was characterized by more embMHC positive myofibers (Figure 2.4-3 D, F), Myogenin positive myofibers (Figure 2.4-3 E, F), and centrally nucleated myofibers (Figure 2.4-3 A, C, G), indicating more newly formed

myofibers. CTCF-deficient tissue was also characterized by more PAX7 positive cells (Figure 2.4-3 A-B, G). It presented the existence of more satellite cells in the TA muscles of *Ctcf* mKO mice, suggesting the possible activation process of satellite cells. Moreover, though the number of myofibers was not obviously increased in *Ctcf* mKO mice (Figure 2.4-3 H), the average cross-sectional area of myofibers in 13-week-old TA muscle was decreased (Figure 2.4-3 A, G, I). Because smaller fibers could also indicate the newly-formed myofibers (Dalbis et al., 1988; Knappe et al., 2015; Skuk et al., 2006), the distribution of myofiber sizes was further analyzed. The distribution was shifted towards smaller myofibers. And *Ctcf* mKO mice had more myofibers with sizes less than 1200 μm^2 and fewer myofibers with sizes over 1500 μm^2 (Figure 2.4-3 J). It can be inferred from these results that loss of CTCF caused muscle damage in TA muscles, thus producing more activated satellite cells and increased muscle regeneration to repair the spontaneous injury.

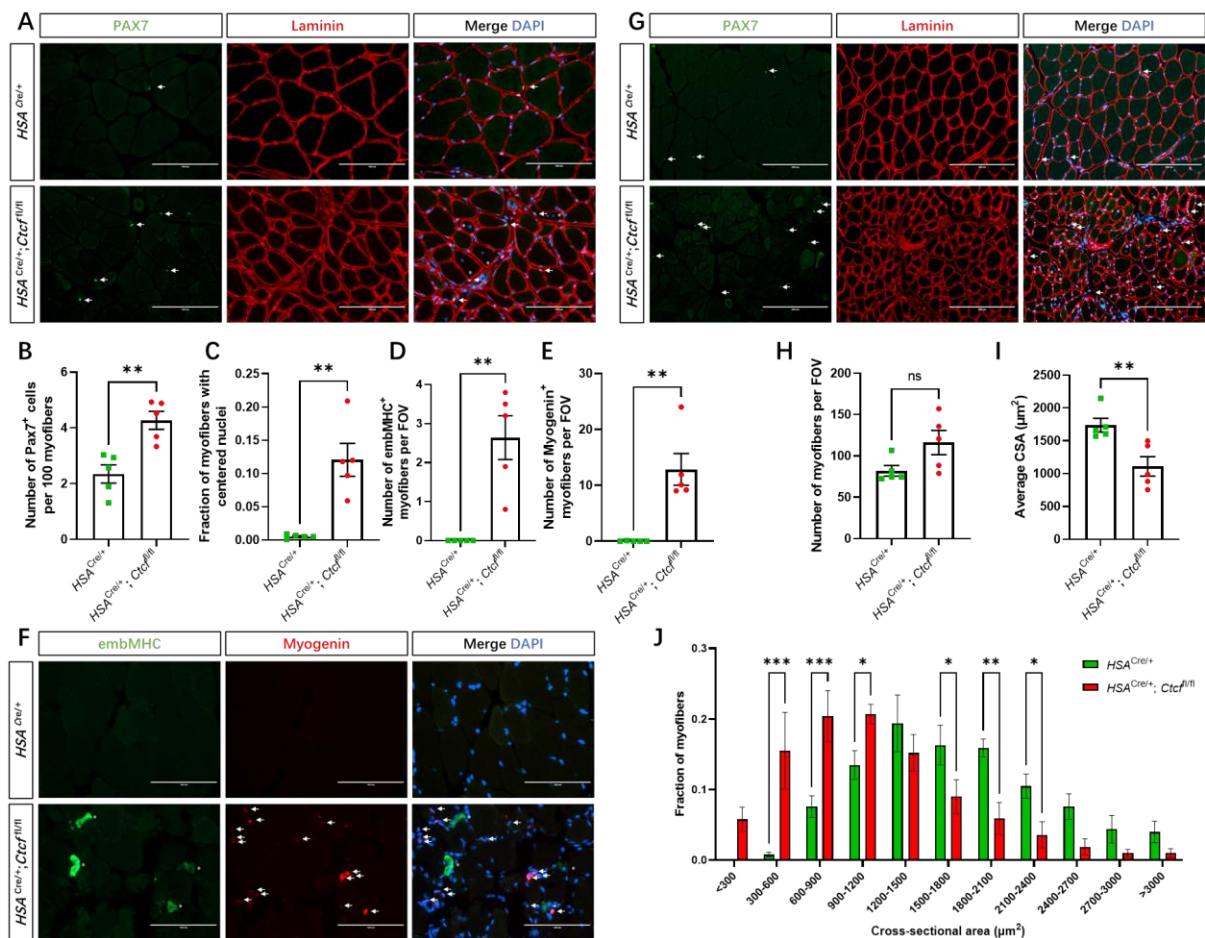


Figure 2.4-3 CTCF-deficient *tibialis anterior* (TA) muscle exhibit signs of regeneration at 13 weeks.

(A) Immunofluorescence staining of TA muscle cross-sections from the control and *Ctcf* mKO mice using antibodies against Pax7 (green), Laminin (red), and DAPI (blue). Scale bars: 100 μm . White arrows indicate the presence of PAX7 positive satellite cells and white asterisks denote the central nucleated myofibers.

(B) Quantification of the number of PAX7 positive satellite cells per 100 myofibers identified in Figure G (n = 5 in each group).

(C) Quantification of the fraction of central-nucleated myofibers identified in Figure G (n = 5 in each group).

(D-E) Quantification of the number of embMHC positive myofibers (D) and Myogenin positive myofibers (E) identified under scale bars 200 μm (n = 5 in each group).

(F) Immunostaining for embMHC (green), Myogenin (red) and DAPI (blue) on the transverse sections of the TA muscles. Scale bars: 100 μm . White asterisks denote the embMHC positive myofibers and white arrows indicate the presence of Myogenin positive myofibers.

(G) Same immunofluorescence staining panels in TA muscle cross-sections as figure A, but with scale bars, 200 μm .

(H-I) Quantification of the number of myofibers (H) and mean cross-sectional areas (I) identified in Figure G (n = 5 in each group).

(J) The distribution of myofiber cross-sectional areas identified in Figure G (n = 5 in each group).

Next, the same immunofluorescence panels were labeled in the diaphragm muscle. It also demonstrates that there were an increased number of embMHC positive cells (Figure 2.4-4 D, F), Myogenin positive cells (Figure 2.4-4 E, F), centrally nucleated myofibers (Figure 2.4-4 A, C, G), and activated satellite cells (Figure 2.4-4 A-B, G), which were all apparent compared to

control mice. Different from the result in the TA muscle, diaphragm muscle had decreased number of myofibers (Figure 2.4-4 H), but it was possibly caused by the smaller cross-sectional width in diaphragm muscle (Figure 2.4-4 G, I). The reduction of diaphragm muscle thickness also provided evidence for the diaphragm muscle defects in *Ctcf* mKO mice (Figure 2.4-4 G, I). Moreover, although there was no big change in the average cross-sectional area of myofibers (Figure 2.4-4 G, J), in CTCF-deficient mice, more myofibers were distributed to the ones under $200 \mu\text{m}^2$ instead of the ones between 300 to $500 \mu\text{m}^2$ (Figure 2.4-4 K). These results in the diaphragm muscle also support that skeletal muscle in *Ctcf* mKO mice displayed signs of muscle regeneration.

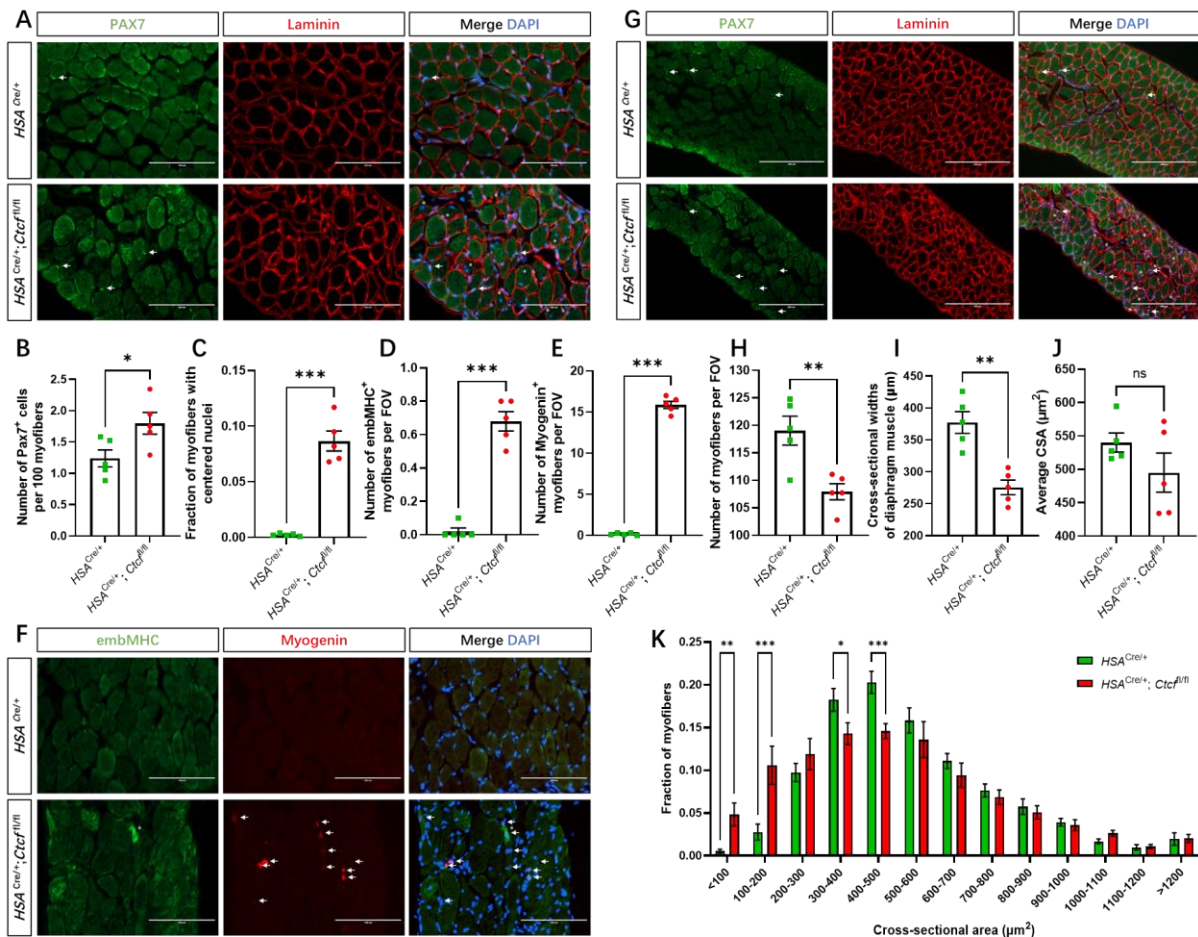


Figure 2.4-4 The loss of CTCF in diaphragm (DIA) muscles leads to increased muscle regeneration at 13 weeks.

(A) Immunostaining for PAX7 (green), Laminin (red), and DAPI (blue) on the transverse

sections of the DIA muscles from the control and *Ctcf* mKO mice. Scale bars: 100 μ m. White arrows indicate the presence of PAX7 positive satellite cells and white asterisks denote the central nucleated myofibers.

(B) The number of PAX7 positive satellite cells per 100 myofibers identified in Figure G (n = 5 in each group).

(C) Fraction of central-nucleated myofibers identified in Figure G (n = 5 in each group).

(D-E) The number of embMHC positive myofibers (D) and Myogenin positive myofibers (E) identified under scale bars 200 μ m (n = 5 in each group).

(F) Immunofluorescence analysis with antibodies against embMHC (green), Myogenin (red) and DAPI (blue) in DIA muscle cross-sections. Scale bars: 100 μ m. White asterisks denote the embMHC positive myofibers and white arrows indicate the presence of Myogenin positive myofibers.

(G) Immunostaining for PAX7, Laminin, and DAPI in DIA muscle cross-sections. Scale bars: 200 μ m.

(H-J) Quantification of the number of myofibers (H), cross-sectional width (I) and mean cross-sectional areas (J) identified in Figure G (n = 5 in each group).

(K) The distribution of myofiber cross-sectional areas identified in Figure G (n = 5 in each group).

2.4.3 The loss of CTCF in muscle causes collagen deposition

Next, we explored histological characteristics of *Ctcf* mKO mice. In normal muscles in response to injury, the satellite cells are activated to form new myofibers, accompanying with transient extracellular matrix deposition (Gillies and Lieber, 2011). Since fibrosis participates in skeletal muscle regeneration and the *Ctcf* mKO mouse model exhibits muscle regeneration, we wondered whether there exists a fibrosis change in this model. In order to evaluate this,

Sirius red was used to detect collagen (Calvi et al., 2012). After qualification, it shows that collagen deposition existed in the 12-week-old TA and diaphragm muscles of *Ctcf* mKO mice (Figure 2.4-5 A-B).

2.4.4 CTCF-deficient muscles do not exhibit signs of apoptosis

Apoptosis is one of the programmed cell death ways in muscle when the first response to injury, and the intrinsic and extrinsic pathways are both naturally occurring processes (Carraro and Franceschi, 1997; Tidball et al., 1995). Here we explored whether there exists DNA breakage through the TUNEL assay. Compared to the result of technical positive control with DNase I treatment, there was no apoptosis change in the TA and diaphragm muscle of 12-week-old *Ctcf* mKO mice (Figure 2.4-5 C-D). Cleaved caspase 3 is also involved in the apoptosis signaling pathway (Brentnall et al., 2013), of which antibody was used to detect signals in muscle sections in our laboratory. Via detection of cleaved caspase 3, it also proves that two types of muscles in 12-week-old *Ctcf* mKO mice did not have apoptosis alterations (Figure 2.4-5 E-F).

2.4.5 Muscles that lost CTCF exhibit weak signs of degeneration

Muscle regeneration includes several interrelated and time-dependent phases and one of them is the degeneration of myofibers (Forcina et al., 2020). Degenerating muscle fibers usually have an increase in membrane permeability, whose changes can be detected by Evans blue dye (Hamer et al., 2002). In order to explore the existence of muscle degeneration and evaluate membrane permeability in skeletal muscle of *Ctcf* mKO mice, Evans blue dye injection was performed at 13 weeks. It shows that there existed a few damaged myofibers in the TA and diaphragm muscles of 13-week-old *Ctcf* mKO mice (Figure 2.4-5 G-H).

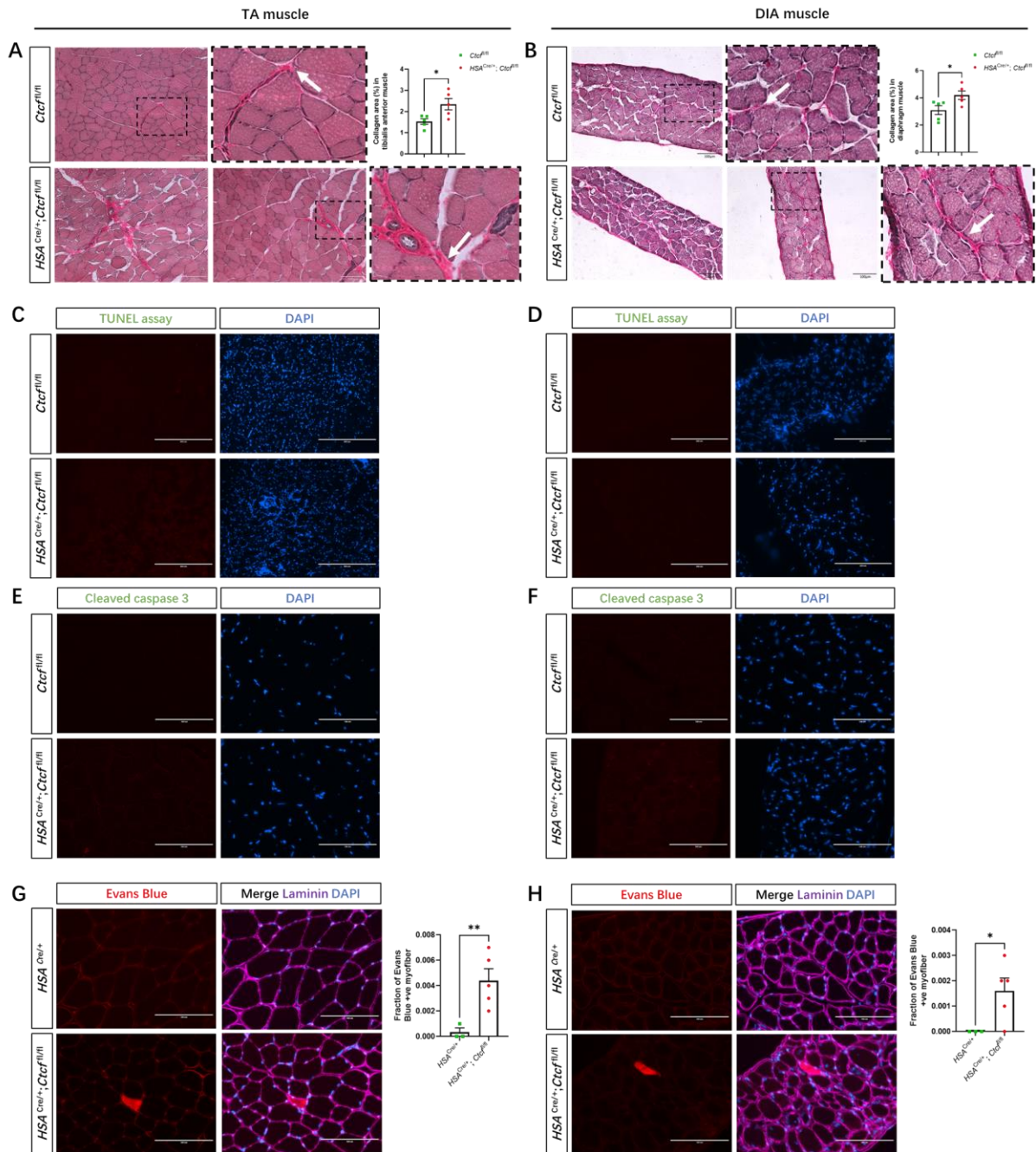


Figure 2.4-5 The detections of fibrosis, apoptosis, and muscle degeneration in CTCF-deficient muscles.

(A-B) Representative images and qualifications of Sirius red staining on transverse sections of TA (A) and DIA muscles (B) at 12 weeks (n = 5 in each group). White arrows indicate the collagen depositions.

(C-D) TUNEL assay staining with DAPI immunostaining at 12 weeks in TA (C) and DIA

muscles (D) to detect DNA fragmentation (n = 3 in each group).

(E-F) Immunostaining for cleaved caspase 3 and DAPI in 12-week-old TA (E) and DIA (F) muscles to detect apoptosis. (n = 3 in each group)

(G-H) Representative images of Evans blue positive myofibers merged with Laminin and DAPI in 13-week-old TA (G) and DIA (H) muscles to detect muscle degeneration. And the qualifications of the number of damaged myofibers (n = 3 in control mice group and n = 5 in *Ctcf* mKO mice group).

2.4.6 The loss of CTCF in muscle leads to weak signs of inflammation

Upon muscle injury, neutrophils and monocytes are activated. And they secrete signals which stimulate the proliferation of satellite cells. After immune cells invade the injured area, M1 macrophages shift to M2 macrophages, along with the differentiation process of muscle stem cells and muscle repair (Chazaud, 2020; Tidball, 2017). In brief, inflammation is related to muscle regeneration and skeletal muscle regeneration partly requires inflammatory responses. And our previous data shows the muscle regeneration phenomenon in *Ctcf* mKO mice. We wondered whether there exist differences in inflammatory cells proportions in *Ctcf* mKO mice, so the immunophenotyping was performed in the TA and diaphragm muscles of 13-week-old *Ctcf* mKO mice.

Since CD45 is a major transmembrane glycoprotein expressed on all nucleated hematopoietic cells, CD45 was used to define the immune cells' population in general (Figure 2.4-6 A). Total T cells, T helper cells, and T cytotoxic cells were respectively labeled by CD3, CD4, and CD8 (Figure 2.4-6 B). CD11b positive cells represented myeloid cells (Figure 2.4-6 C), and its four subcell lineages, Ly6G⁺ neutrophils, Ly6C⁺ monocytes, CD11c⁺ and MHCII⁺ dendritic cells, and F4/80⁺ macrophages were further detected (Figure 2.4-6 D-E). In terms of the subtypes of macrophages, CD11c⁺, MHCII⁺, and CD86⁺ cells were regarded as M1 macrophages cells (Figure 2.4-6 F), and Arg⁺ cells as M2 macrophages (Figure 2.4-6 G).

Through the statistical analysis, a significant increase of T cytotoxic cells was found in diaphragm muscles of *Ctcf* mKO mice (Figure 2.4-6 B). However, it cannot be ignored that there exists a limited number of inflammatory cells in muscle tissues (around 10 percent) and the variation is relatively large among biological samples. These reasons could lead to either ignoring the change because of no statistical difference or amplifying the small change. The immunophenotyping results in muscles will be firmly substantiated by adding more replicates in each group. Overall, the trends seem different between TA muscles and DIA muscles of *Ctcf* mKO mice: more myeloid cells in TA muscles (Figure 2.4-6 C-E), while more T cells in DIA muscles (Figure 2.4-6 B). Moreover, because there were two-fold CD11c⁺ and MHCII⁺ M1 macrophages cells in the TA muscles of *Ctcf* mKO mice (Figure 2.4-6 F), there may exist an M1 to M2 macrophages shift in CTCF-loss TA muscle.

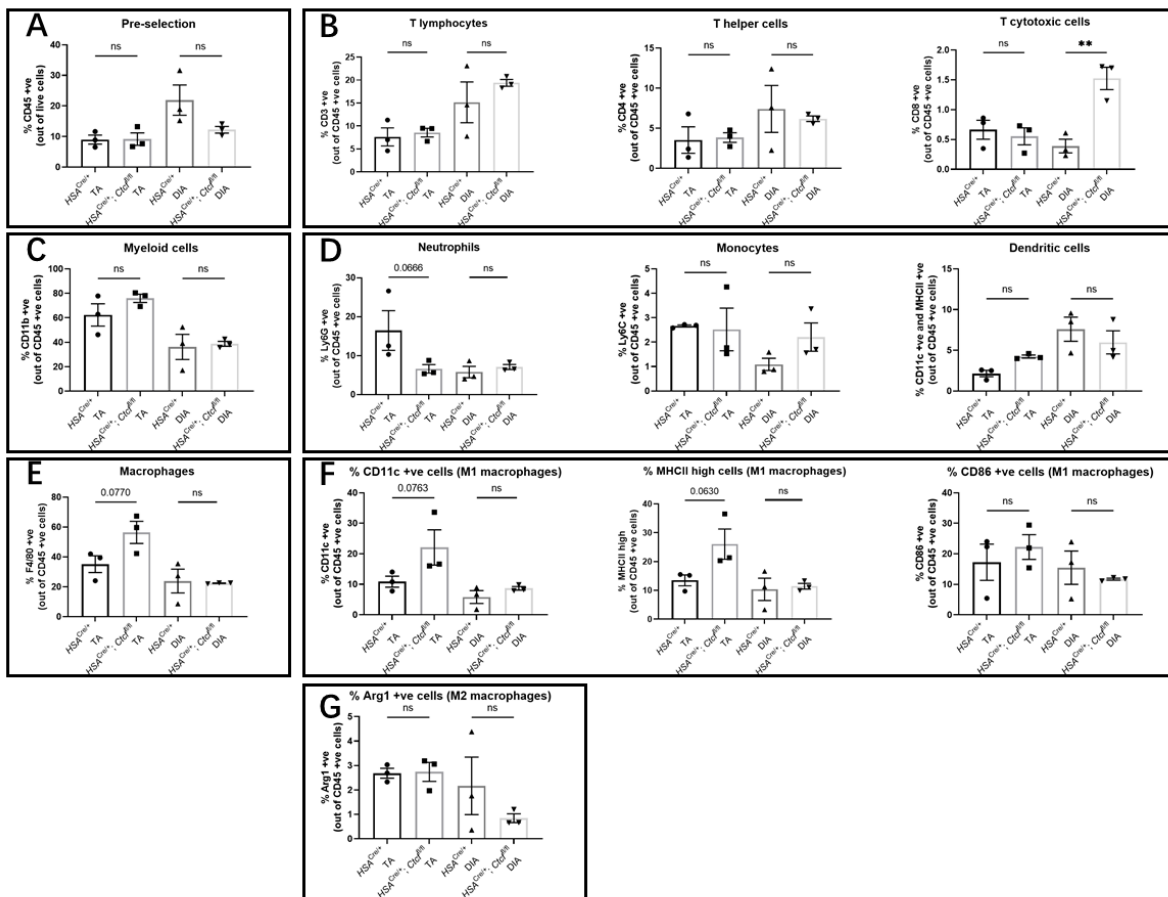


Figure 2.4-6 Immunophenotyping in the TA muscles and diaphragm muscles of control and knockout mice.

- (A) Flow cytometry analysis of immune cell population through CD45⁺ cells.
- (B) Fractions of T cell lineages demonstrated by CD3⁺ T lymphocytes, CD4⁺ T helper cells, and CD8⁺ T cytotoxic cells in CD45⁺ immune cells.
- (C) Percentage of myeloid cells which stain positively for CD11b in CD45⁺ immune cells.
- (D-E) The four subtypes of myeloid cells are indicated through the staining intensity of Ly6G⁺ neutrophils, Ly6C⁺ monocytes, CD11c⁺ and MHCII⁺ dendritic cells (D), and F4/80⁺ macrophages (E) in CD45⁺ immune cells.
- (F) Fraction of M1 macrophages represented by CD11c⁺, MHCII⁺, and CD86⁺ cells in CD45⁺ immune cells.
- (G) Percentage of Arg⁺ M2 macrophages in CD45⁺ immune cells. Data in (A-G) is presented as mean ± SEM and n = 3 in each group.

2.4.7 Transcriptome analysis in *HSA*^{Cre/+}; *Ctcf*^{fl/fl} mice

To further explore the mechanism of muscle wasting in *Ctcf* mKO mice, RNA-seq was performed on *gastrocnemius* muscles from three timepoints, and each group contained three biological replicates. A principal component analysis was used to observe the similarity among samples. And it shows that the samples of *HSA*^{Cre/+} mice (Ctrl) and CTCF-deficient mice (KO) were basically separated into four distinct clusters: all control mice from three timepoints, 7-week-old, 9-week-old, and 13-week-old *Ctcf* mKO mice (Figure 2.4-7 A). Specifically, the loss of CTCF in 13-week-old mice led to 50% variance with control mice and 23% variance with 7-week-old *Ctcf* mKO mice (Figure 2.4-7 A). And there may be a general tendency of time-related transcriptome change in *Ctcf* mKO mice, gradually from 7 weeks to 9 weeks and to 13 weeks (Figure 2.4-7 A).

Then the differentially expressed genes (DEGs) from two types of mice were compared at the same timepoint. There was a strong effect on the transcriptome due to CTCF deletion in skeletal muscle, and the number of both upregulated and downregulated DEGs were increased

along with the time (391 versus 429 at 7 weeks, 378 versus 362 at 9 weeks, and 781 versus 858 at 13 weeks) (Figure 2.4-7 B).

DEGs were further analyzed and DEGs of *Ctcf* mKO mice samples were compared to the ones of *HSA*^{Cre/+} mice. First gene set enrichment analysis was based on Gene Ontology Biological Process 2021 database. In terms of the upregulation of enrichments, ‘response to unfolded protein’ pathway, ‘response to stress’-related pathway, and ‘response to insulin’-related pathway were positively regulated at both 9 and 13 weeks (Figure 2.4-7 C, E, G). However, the top ten enriched pathways at 7 weeks were completely different from the ones at 9 or 13 weeks and there were only two or three DEGs involved in each of these ten pathways. It may indicate there exists a transcriptome difference of upregulated genes between 7-week-old and 9/13-week-old *Ctcf* mKO mice. And it may explain why the phenotype (body weight loss and muscle mass reduction) is not obvious in 7-week-old CTCF-deficient mice.

For the downregulated biological process, the top three pathways, ‘muscle contraction’, ‘muscle filament sliding’, and ‘actin-myosin filament sliding’, contained the enrichments of DEGs at all three timepoints (Figure 2.4-7 D, F, H). But at 7-week-old, skeletal muscle of *Ctcf* mKO mice also had unique downregulated transcriptome enrichments, which are related to inflammation, including ‘cellular response to cytokine stimulus’, ‘macrophage activation’, and ‘negative regulation of myeloid leukocyte mediated immunity’. It may indicate that 7-week-old mice has inflammatory response to the loss of CTCF, and this could be the reason why *Ctcf* mKO mice do not have muscle defects at 7 weeks.

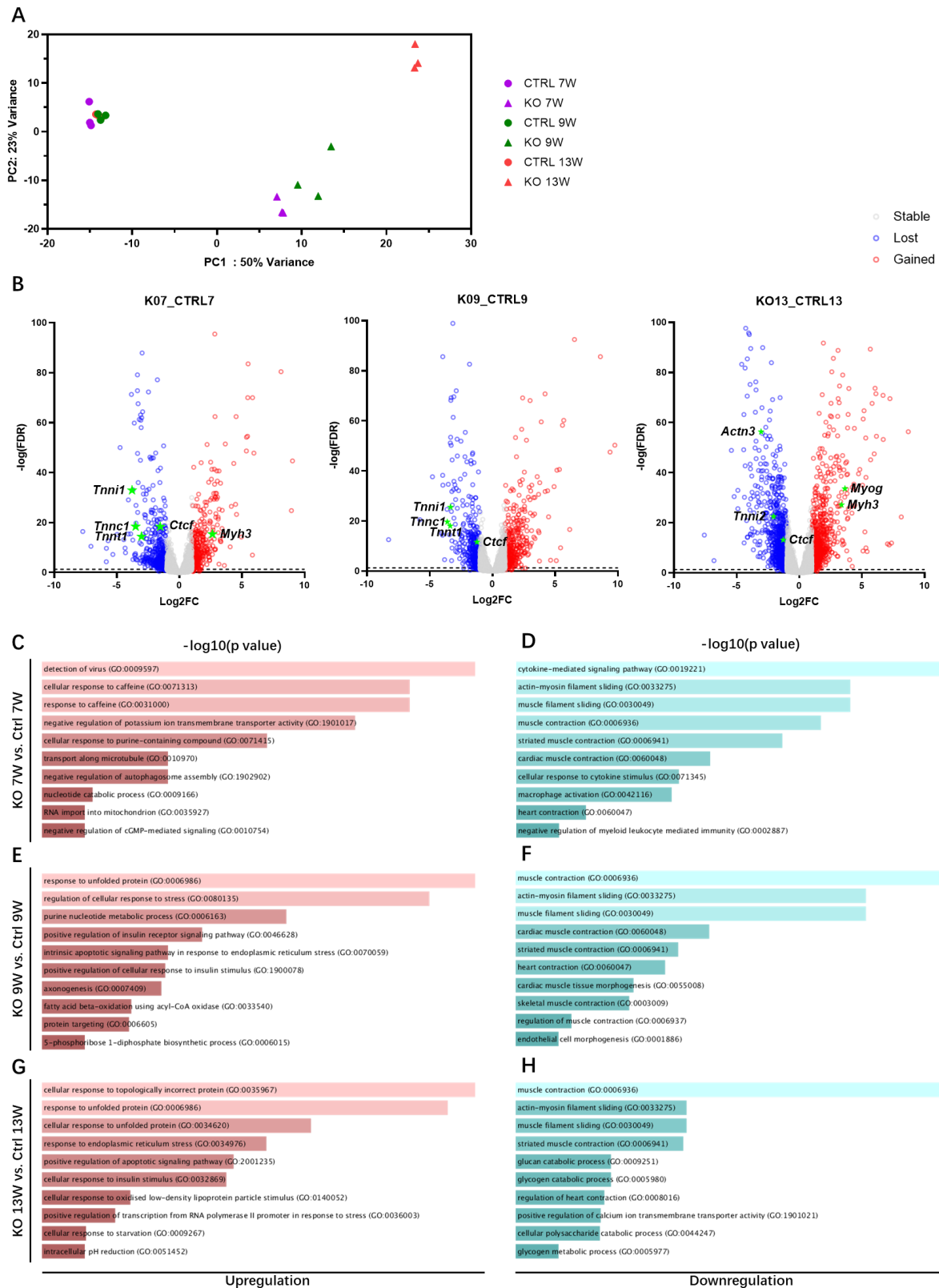


Figure 2.4-7 Transcriptome analysis of *gastrocnemius* muscles in 7, 9, and 13-week-old *Ctcf* mKO mice.

(A) A plot of principle component analysis derived from RNA sequencing profiling of control mice (circle label) and CTCF-deficient mice (triangle label) at 7 weeks (purple), 9 weeks (green), and 13 weeks (red) (n = 3 in each group).

(B) Volcano plots depicting differentially expressed genes between the control and knockout mice at 7, 9 and 13 weeks. The threshold of P-value is indicated by a dot line and the differentially expressed genes are defined as the changes of expression greater than 2-fold. All genes are classified into the gained genes (red), the lost genes (blue), and the stable genes (grey). The muscle contraction-related genes (*Tnni1*, *Tnnc1*, *Tnnt1*, *Tnnt2* and *Actn3*), muscle regeneration-related genes (*Myh3* and *Myog*), and *Ctcf* gene are indicated in each timepoint.

(C-H) Analysis of upregulated genes (C, E, G) and downregulated genes (D, F, H) was performed by the gene set enrichment analysis of Gene Ontology Biological Process 2021 database. The color and length of bars present the significance calculated by $-\log_{10}$ (p value). The top 10 enriched pathways are shown in each comparison.

In the following, the muscle-related DEGs information from the gene set analysis in Gene Ontology Biological Process 2021 database was specifically analyzed. First, the Venn diagrams and heatmaps of the DEGs that are involved in ‘muscle contraction’ and ‘muscle filament sliding’ pathways were analyzed. The data show that, along with the age, most of the contraction-related gene expressions were steadily decreasing (Figure 2.4-8 B, D) and the number of influenced genes were increased in *Ctcf* mKO mice (Figure 2.4-8 A, C). These downregulated DEGs involve *Acta1*, *Actn3*, *Tpm3*, *Tnnt1*, *Tnnc1*, and *Tnni2*. It confirms the conclusion that muscle defects in global physical function and muscle contractile properties were triggered by the loss of CTCF (Figure 2.4-2 F-H).

Muscle contractile properties in a muscle are closely related to the distribution of its myofiber in slow or fast muscle (Zierath and Hawley, 2004). In order to explore whether CTCF-deficient mice have changes in muscle fiber types, from RNA-seq data, we collected six representative myosin gene expressions to distinguish the types of muscle fibers (Figure 2.4-8 E). These genes include MYH7 and MYL3 labeling slow muscle type 1 myofibers, fast muscle

marker MYL1, type 2A fast-twitch muscle fiber marker MYH2, type 2X fast-twitch muscle fiber marker MYH1, and type 2B muscle fiber marker MYH4. Specifically, slow myofiber markers, *Myh7* and *Myl3*, were downregulated at 7 and 9 weeks of *Ctcf* mKO mice but recovered at 13 weeks (Figure 2.4-8 E). Conversely, the fast muscle markers, *Myll* and *Myh4*, are decreased at 13 weeks instead of 7 and 9 weeks (Figure 2.4-8 E). It suggests that there may exist muscle fiber type conversion due to the loss of CTCF and the proportion of myofiber types varies from the age of *Ctcf* mKO mice.

To date, it was found that CTCF is involved in several muscular diseases, for example, myotonic dystrophy type 1 and facio-scapulo-humeral dystrophy (Castel et al., 2011; van der Maarel et al., 2012). Congenital myopathies are a group of rare muscle diseases that usually present from birth accompanying with the disorders of muscle contraction. Since contraction disorder is also a phenotype in *Ctcf* mKO mice, the genes implicated in congenital myopathies (Jungbluth et al., 2018) are further explored according to RNA-seq data. These selected genes were downregulated in *Ctcf* mKO mice with a differential expression (Figure 2.4-8 F).

Moreover, the neuromuscular junction is essential to muscle contraction and the defects in the neuromuscular junction can result in impaired muscle contraction (Li et al., 2018). When the produced acetylcholine binds to the acetylcholine receptor in the neuromuscular junction, muscle receives this signal and subsequently contracts. The gene expression from the RNA-seq data shows the upregulation of genes related to muscle-type acetylcholine receptors in 13-week-old *Ctcf* mKO mice (Figure 2.4-8 G), which may react to the decreased muscle contraction in order to rescue it.

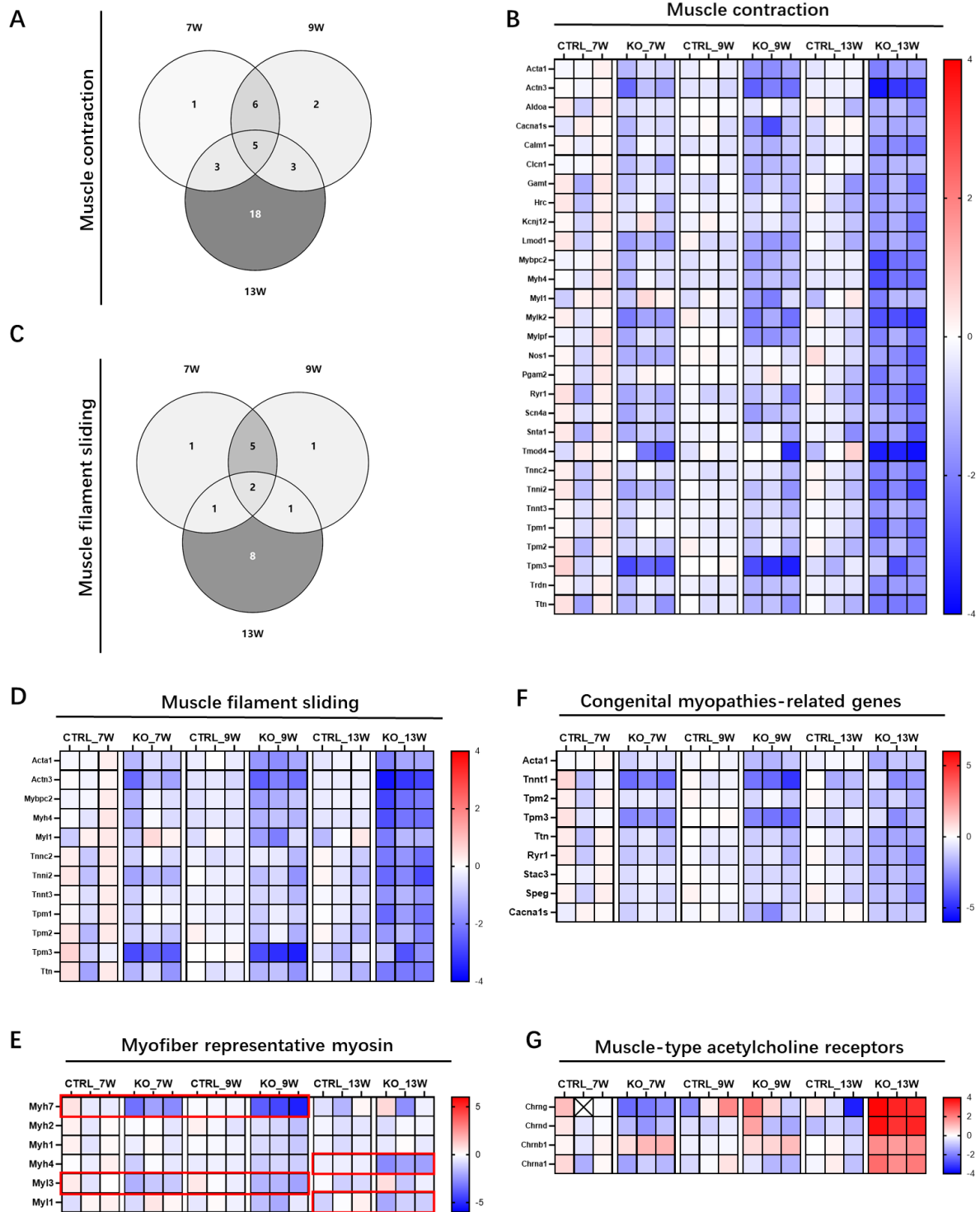


Figure 2.4-8 The Venn diagrams and heatmaps of selected differentially expressed genes (DEGs) in *Ctcf* mKO mice and control mice at 7, 9, and 13 weeks.

(A-B) The enrichment of muscle contraction was analyzed at three timepoints through comparing the number of related DEGs (A) and their gene expressions (B).

(C-D) The Venn diagram about the number of associated genes from muscle filament sliding (C) and the corresponding z-score heatmap (D) in 7, 9, and 13-week-old mice.

(E) The expression of six genes related to muscle fiber type is shown in a heatmap form. Red boxes indicate the differentially expressed genes in specific timepoints.

(F) The z-score heatmap of nine genes involved in congenital myopathies, which have muscle contraction disorders.

(G) A heatmap of four genes related to muscle-type acetylcholine receptors.

Slow muscle and fast muscle respectively display oxidative and glycolytic metabolism (Zierath and Hawley, 2004). Thus, the alteration of myofiber type disproportion indicates that *Ctcf*mKO mice may have different energy use strategies compared to the control mice. Muscle metabolism is supported by the robust activity of mitochondria. Therefore, the transcript level of five complexes that are involved in the mitochondrial respiratory chain (Alston et al., 2017) was further explored through RNA-seq data. There was not an obvious overall change, however, it existed abnormal regulation of related genes in five complexes of muscle tissue, *Ndufb7*, *Ndufaf5* and *Ndufaf3* genes in complex I, *Uqcrrh* gene in complex III, *Cox8a* and *Scol1* genes in complex IV, and *Atp5k* gene in complex V (Figure 2.4-9 A-E). It may be also related to the upregulated enrichment 'RNA import into mitochondrion' (Figure 2.4-7 C). Meanwhile, the transcript levels of mitochondrial DNA were basically increased at three timepoints (Figure 2.4-9 F). It indicates that mitochondria in *Ctcf*mKO mice may undergo reproduction and fusion in response to the energy change with an increased mitochondrial turnover.

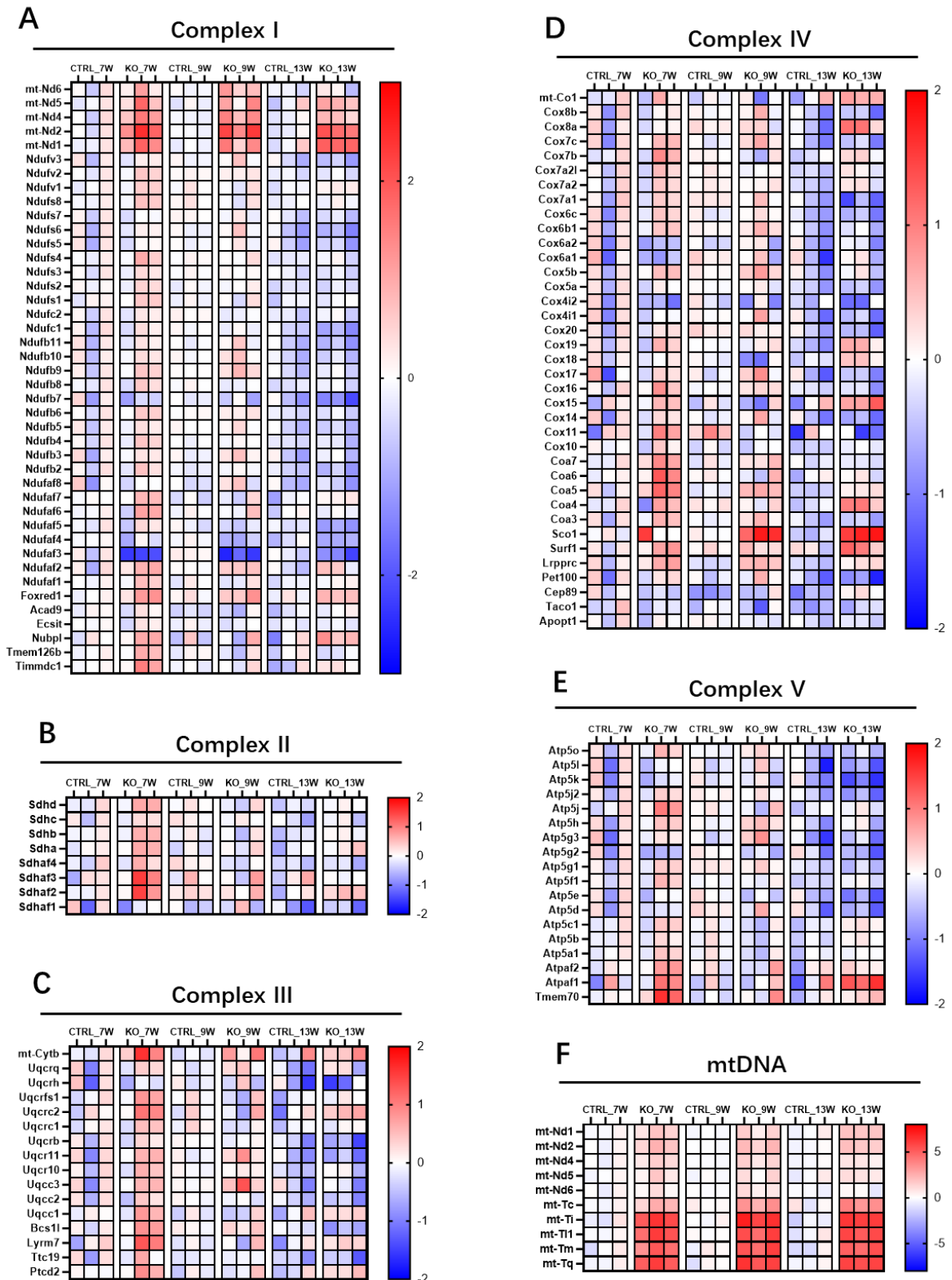


Figure 2.4-9 The summary of the gene expression related to mitochondria.

(A-E) A z-score heatmap of mitochondrial respiratory chain-related genes respectively in complex I (A), complex II (B), complex III (C), complex IV (D), and complex V (E).

(F) The increased transcript levels of mitochondrial DNA in *Ctcf* mKO mice from RNA-seq data.

Another gene set enrichment analysis based on MSigDB Hallmark 2020 also provides more ideas for the possible mechanisms about the role of CTCF in skeletal muscle. Regarding the upregulated gene sets, there were strong enrichments related to ‘fatty acid metabolism’ in all three ages of CTCF-loss muscle samples (Figure 2.4-10 A, C, E). There was also a strong enrichment related to ‘mTORC1 signaling’ at three ages (Figure 2.4-10 A, C, E). And the number of associated genes was greatly increased at 13 weeks (Figure 2.4-11 A). The genes include *Acr3*, *Cdkn1a*, *Ddit3*, *Slc2a1*, *Dapp1*, and *Trib3*, which are involved in PI3K/Akt/mTOR signaling (Figure 2.4-11 E).

Furthermore, the upregulated enrichment of ‘unfolded protein response’ was also obvious at 9 and 13 weeks (Figure 2.4-10 C, E). The number of its related genes was increased along with time (Figure 2.4-11 B). Specifically, it involves genes that encodes the 70 kDa heat shock protein (Hsp70/HSPA) family: *HSPA2*, *HSPA5*, *HSPA9*, and *HSPA14*, eukaryotic initiation factor 4F complexes: *eIF4a1* and *eIF4ebp1*, and the stress sensor, activated transcription factor 6 *Atf6* (Figure 2.4-11 F).

In addition, it shows that there were upregulated enrichments of apoptosis at 7, 9 and 13 weeks (Figure 2.4-10 A, C, E), along with the increased account of related DEGs (Figure 2.4-11 C). However, there was no apoptosis change be detected in the muscles of 13-week-old *Ctcf* mKO mice (Figure 2.4-5 C-F). Recent evidence shows that myonuclei may be protected from apoptosis because mature skeletal muscle upregulates the expression of potent survival proteins and experiences autophagy, also a way of programmed cell death (Bruusgaard et al., 2012; Masiero et al., 2009; Xiao et al., 2011a). And the apoptotic nuclei detected within the muscle tissue in the published study may be the mononuclear cells that reside outside the myofibers instead of the myonuclei (Tedesco et al., 2010). In addition, because our samples used for RNA-

seq are the whole muscle tissue, the upregulation of apoptosis signaling could also be caused by other cell types. Moreover, in *Ctcf* mKO mice, most of these selected DEGs involved in apoptosis are also related to autophagy pathway, which plays a role in muscle homeostasis and involves in muscle atrophy. For example, these DEGs include *Gadd45a*, *Hmgb2*, *Dap*, *Casp6*, and *Hmox1* (Figure 2.4-11 G) (An et al., 2015; Levin-Salomon et al., 2014; Meyer et al., 2018; Zhang et al., 2015).

With respect to the downregulation in *Ctcf* mKO mice, ‘myogenesis’ enrichment was negatively regulated at three timepoints (Figure 2.4-10 B, D, F), It is similar to result from Gene Ontology Biological Process 2021 database that the enriched ‘muscle contraction’ pathway was downregulated. However, except for the genes related to muscle contraction (e.g., *Actn3*, *Tpm3*, and *Tnni2*), this ‘myogenesis’ gene set enrichment also contains the genes involved in ‘extracellular structure organization’, for instance, *Colla1*, *Coll5a1*, *Sparc*, *Itgb4*, *Col6a2*, and *Fgf2* (Kashyap et al., 2010).

It can also be found that ‘epithelial mesenchymal transition’ at 9 and 13 weeks (Figure 2.4-10 D, F). The epithelial-mesenchymal transition is a process when epithelial cells differentiate into fibroblasts or myofibroblasts. These fibroblasts can contribute to the excessive accumulation of connective tissue, so epithelial-mesenchymal transition is involved in tissue fibrosis (Thiery et al., 2009). In the downregulated enrichment of ‘epithelial mesenchymal transition’ (Figure 2.4-11 D), the number of associated genes was raised a lot at 13 weeks (Figure 2.4-11 H). Hultström M, Leh S, Paliege A, et al. found that the accumulation of interstitial fibrous collagen is related to significant downregulation of collagen I mRNA and other extracellular matrix components (Hultstrom et al., 2012). And it was also found that amino acid depletion causes significantly decreased mRNA level of collagen I in human lung fibroblasts (Krupsky et al., 1997). Together, it provides a justification for the findings in 13-week-old *Ctcf* mKO mice that the collagen diffuse was accumulated, but the enrichment of fibrosis-related gene sets was downregulated to rescue collagen deposition.

Moreover, the ‘inflammatory response’ pathway was only highlighted in a downregulated way in 7-week-old *Ctcf* mKO mice (Figure 2.4-10 B). This 7-week-old downregulation of

inflammatory response also matches the analysis from Gene Ontology Biological Process 2021 database (Figure 2.4-7 D). It means that the 7-week-old mice may have decreased or increased inflammatory signaling. In addition, the inflammation-associated genes were basically not changed between control and knockout mice at 9 and 13 weeks. It is possible because the low proportions of inflammatory cells in the muscle sample, the slight change could be hid in the whole sample transcriptome analysis of 9 and 13 weeks. Based on the slight increase of immunity response in 13-week-old CTCF-deficient mice through immunophenotyping (Figure 2.4-6), the trend of immunity situation in *Ctcf* mKO mice still needs to be further investigated.

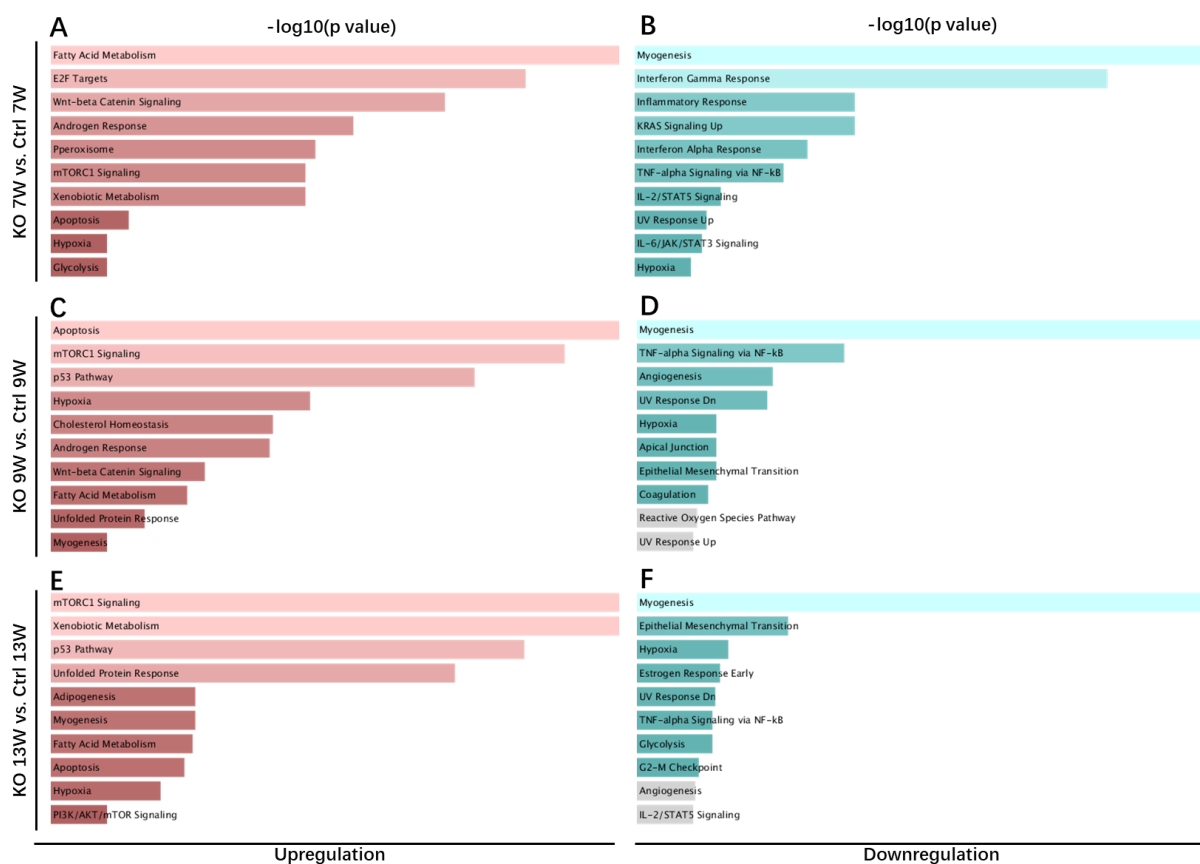


Figure 2.4-10 The gene set enrichment analysis of differentially expressed genes based on MSigDB Hallmark 2020.

(A-F) The top ten upregulations (A, C, E) and downregulations (B, D, F) in the enriched pathways of DEGs were shown, respectively for 7-week-old (A-B), 9-week-old (C-D), and 13-week-old (E-F) muscle samples. The color and length of bars present the significance (calculated by $-\log_{10}(p \text{ value})$).

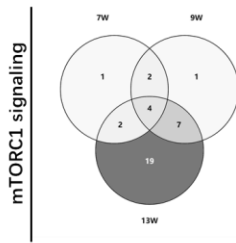
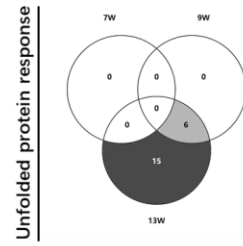
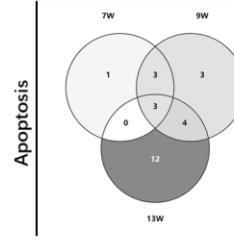
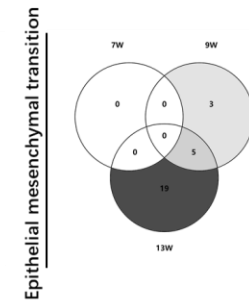
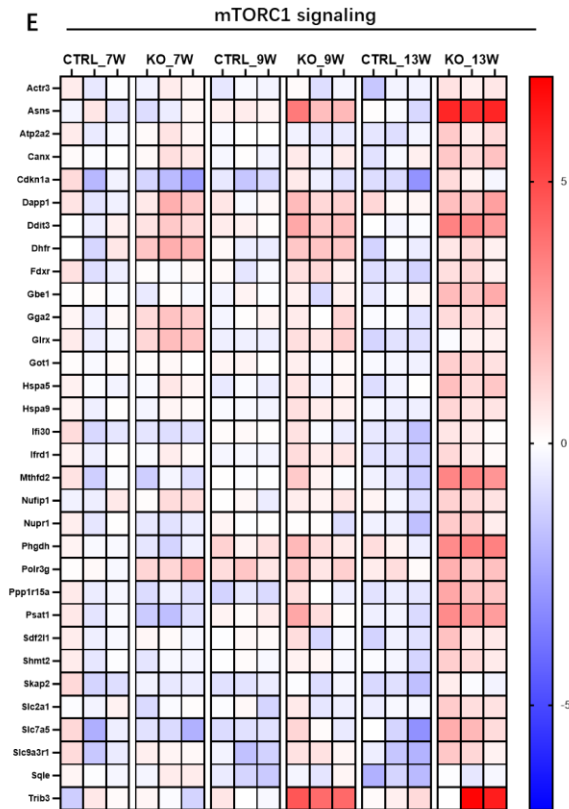
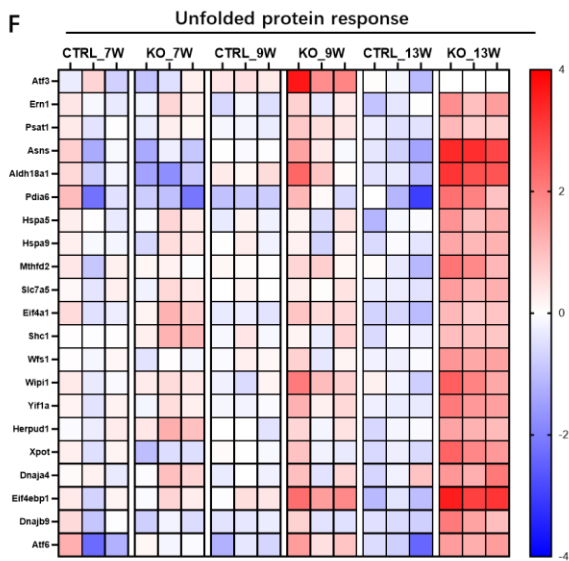
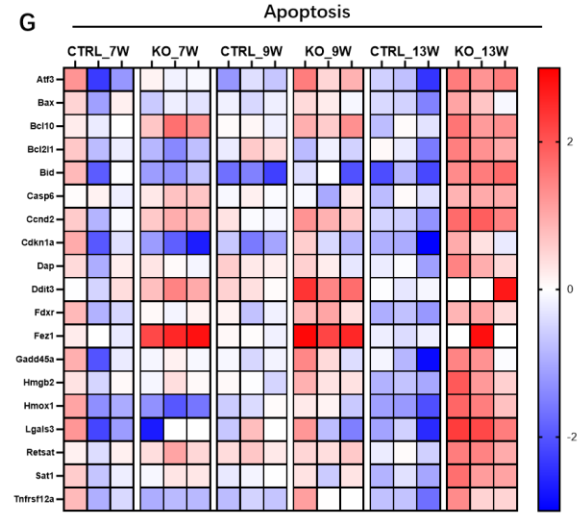
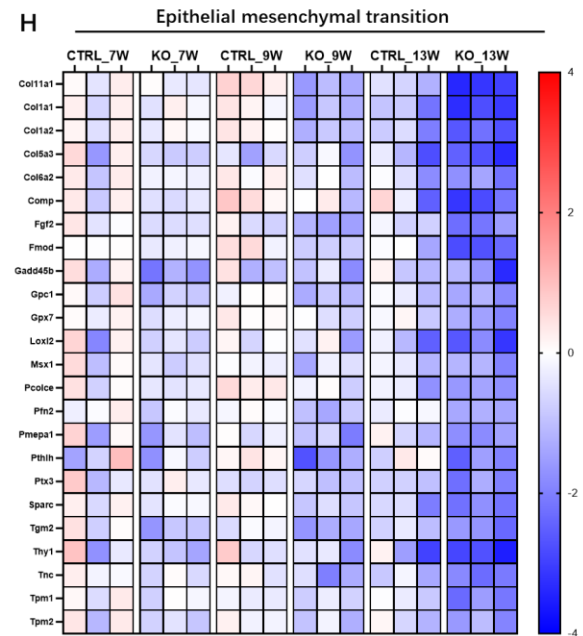
A**B****C****D****E****F****G****H**

Figure 2.4-11 The Venn diagrams and heatmaps of differentially expressed genes (DEGs) selected from the enriched pathways based on MSigDB Hallmark 2020.

(A-D) The number of related DEGs in the enrichment of signaling pathways are compared at three timepoints shown as Venn diagrams, separately focusing on mTORC1 signaling (A), unfolded protein response (B), epithelial mesenchymal transition (C), and apoptosis (D).

(E-H) The z-score heatmaps of associated genes from enriched gene sets in 7, 9, and 13-week-old mice, respectively about mTORC1 signaling (A), unfolded protein response (B), epithelial mesenchymal transition (C), and apoptosis (D). (n = 3 in each group).

The last gene set enrichment analysis is based on the ENCODE and ChEA Consensus TFs from ChIP-X databases. The databases utilize the libraries of gene sets from published ChIP-chip, ChIP-seq, ChIP-PET, and DamID experiments (Lachmann et al., 2010). From this analysis, it can be inferred whether the DEGs of *Ctcf* mKO mice are enriched in a specific gene set that are putative targets of transcription factors. Specifically, the downregulated genes caused by the loss of CTCF more possibly match to CTCF and MYOD1 targeted gene sets (Figure 2.4-12 B, D, F), while upregulated genes may be not related to CTCF or MYOD motifs (Figure 2.4-12 A, C, E). In addition, these upregulated enrichments are linked to the transcription factors mediating chromatin organization, for example, ESR1, GATA2, and E2F family of transcription factors: E2F1, E2F4, and E2F6 (Figure 2.4-12 A, C, E) (Jeselson et al., 2018; Jing et al., 2008; Lu et al., 2007; Magri et al., 2014). It suggests that the upregulated genes in *Ctcf* mKO mice could be influenced by the change of chromatin structure that is indirectly caused by the loss of CTCF. And in both upregulation and downregulation, there existed enrichment about Cohesin protein, such as the subunits SMC3 and RAD21 (Figure 2.4-12 A-F) (Nasmyth and Haering, 2009). Furthermore, the number of these downregulated genes potentially caused by the loss of CTCF was increased along with the time (Figure 2.4-12 G). Moreover, the gene ontology biological process analysis shows that downregulated genes linked by CTCF were more likely related to mitochondrial pathways (Figure 2.4-12 H). Because mitochondria play an indispensable role in the maintenance of muscle metabolism

(Hood et al., 2019), reduced *Ctcf* expression in muscle may also influence muscle metabolism.

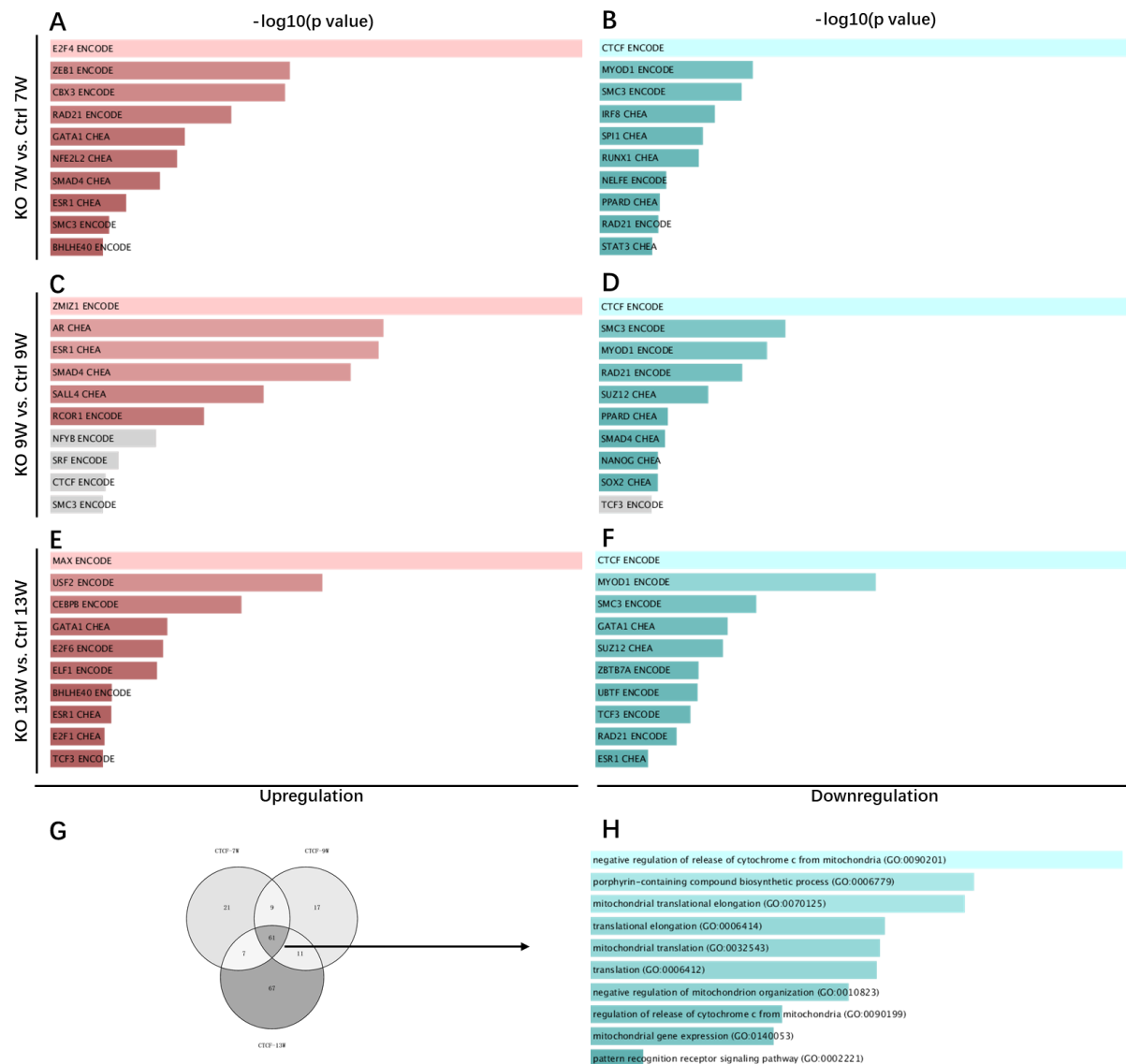


Figure 2.4-12 The gene set enrichment analysis of differentially expressed genes based on ENCODE and ChEA Consensus TFs from ChIP-X databases.

(A-F) The top 10 enriched pathways of upregulated genes (A, C, E) and downregulated genes (B, D, F) were ordered according to their significance, $-\log_{10}(p \text{ value})$.

(G) Venn diagram showing the number of genes possibly mediated by CTCF from the analysis in ENCODE and ChEA Consensus TFs from ChIP-X databases.

(H) GO Biological Process analysis of overlaid *Ctcf*-related genes in Figure A. Intensity and length of bars indicate significance.

2.5 Materials and Methods

2.5.1 Mice

Ctcf^{fl/+} mice, carrying flox sites flanking exon 8, belonged to Dr. Witcher's laboratory and *HSA*^{Cre/+} mice were obtained from The Jackson Laboratory (Miniou et al., 1999). *Ctcf*^{fl/+} were bred with *HSA*^{Cre/+} mice to obtain *HSA*^{Cre/+}; *Ctcf*^{fl/+} mice. And these offspring were crossed with *Ctcf*^{fl/+} mice again to generate CTCF knockout mice (*HSA*^{Cre/+}; *Ctcf*^{fl/fl}). Recombination was achieved by crossing *Ctcf* exon-flanked loxP mice with the Cre recombinase for HSA promoter. *HSA*^{Cre/+} mice or *Ctcf*^{fl/fl} mice were used as controls and the mouse strains were maintained based on a C57BL/6 background. Standard caring and euthanasia were approved and operated under the regulations of McGill University and the Lady Davis Institute.

2.5.2 Four limb hanging test

Global physical function can be evaluated by this non-invasive method (Klein et al., 2012). Briefly, the test was started when mice were 7-week-old. Each time only one mouse was placed in the center of a wire mesh screen (1.5 × 1.5cm) with a 35cm distance from the soft bedding. And we set a fixed maximum time as 600 seconds, then if mice fall off within this time, two more tries were be given, and the longest hanging time out of three results was taken into final calculation. The rest time between each trial for one mouse was as least five minutes.

2.5.3 *Ex vivo* muscle contractility assay

13-week-old mice were successively anesthetized to isolate *extensor digitorum longus* muscles of the right side. 300C: Dual-Mode Lever System and Dynamic Muscle Control and Analysis Software (Aurora Scientific) were used for the following procedures. The tissues were placed in Ringer's buffer at 30 °C with 95% O₂ and 5% CO₂ and the two-side tendons were attached to the equipment. Optimal muscle length (L₀) was first measured and the force was

gradually adjusted to achieve the maximum twitch force. After stimulating the muscles under the frequencies from 10 Hz to 200 Hz, a force-frequency curve was formed as the measurement of absolute force (P_0), also called as peak tetanic force. The data of muscle weight (W_0) was also collected to estimate cross-sectional area, and specific muscle force (P_1) was normalized by the approximate cross-sectional area and calculated by this formula:

Specific muscle force = Absolute force \times Fiber length \times Muscle density

$$P_1 \text{ (N/cm}^2\text{)} = P_0 \text{ (N)} \times (0.44 \times L_0) \text{ (cm)} \times (1.06 \text{ (g/cm}^3\text{)} / W_0 \text{ (g))}$$

2.5.4 Immunofluorescence

The *tibialis anterior* muscle and diaphragm muscle were extracted from $HSA^{Cre/+}$ mice and $HSA^{Cre/+}; Ctef^{fl/fl}$ mice at 7, 12 or 13 weeks. Tissues were washed in phosphate-buffered saline, fixed in 0.5% paraformaldehyde for 2 hours, and suffused in 20% sucrose overnight at 4 °C. Tissues were then washed, placed into foil molds, and completely frozen in the optimal cutting medium through methylbutane bath in liquid nitrogen. After preparations of cryosections by the cryostat, 10 μ m thick sections were made, washed, and then probed by indicated antibodies. It included anti-rabbit CTCF antibody, anti-rabbit cleaved caspase 3 antibody, anti-mouse Pax7 antibody, anti-rabbit Laminin antibody, anti-mouse embryonic myosin heavy chain (embMHC) antibody, and anti-rabbit Myogenin antibody. Images were captured and analyzed by EVOS® FL Cell Imaging System and/or ImageJ. The data were expressed as means \pm SEM (standard error of the mean). And for biological replicates, each group had more than three samples. And for technical replicates, five or ten sections were processed and counted. All statistical analysis was performed by GraphPad Prism software. Moreover, an unpaired t-test is used to evaluate statistical significance, and a significant difference is indicated by two-paired p values with $p < 0.05$.

2.5.5 Histological staining

Sirius red staining was performed for the histological characterization of collagen in tissue sections (Calvi et al., 2012). Briefly, tissues were sectioned into 10 μ m thick sections in advance. Frozen sections were thawed at room temperature and fixed with 4% paraformaldehyde in a glass chamber. Next, Slides were incubated with Weigert's hematoxylin solution for 10 minutes, and washed under running tap water for at least 5 minutes. And sections were immersed in 0.2% phosphomolybdic acid solution for 5 minutes, following two-time washing. After the incubation in the Sirius red dye solution for 1 hour, slides were rinsed twice in acetic acid solution. Finally, sequential ethanol incubations (70% ethanol, 90% ethanol, and 100% ethanol) were performed, and coverslips were mounted onto slides using xylene. The measurement of area stained in red, which is collagen deposition, was quantified by the ImageJ software.

Evans blue dye is widely used to assess the cellular membrane permeability (Hamer et al., 2002). 10 mg/mL of Evans blue dye solution was prepared and sterilized. Intraperitoneal injection of this solution was performed based on mice body weight. Next day after injection, 13-week-old mice were sacrificed. And the *tibialis anterior* muscles and diaphragm muscles were resected and processed by the procedure in 2.5.4 Immunofluorescence. For this experiment, the labels of Laminin protein and DAPI were performed in these slides.

DNA fragmentation is the sign of the late stage of apoptosis, which can be detected by nick-end labeling of DNA through the TUNEL assay (Mohan et al., 2015). ApopTag Red *In Situ* Apoptosis Detection Kit (Sigma-Aldrich) was used for the detection of apoptosis in tissue sections. In brief, the starting procedures in 2.5.4 Immunofluorescence were followed to first make fresh sections. Next, all sections were pretreated in proteinase K. As a positive control, each time one slide was treated by DNase I, while the rest were kept in PBS. Then all slides were subsequently covered by equilibration buffer, working strength TdT enzyme mixture, working/stop wash buffer, and working strength rhodamine antibody solution. In final, before coverslips were mounted, DAPI incubation was last for 15 minutes.

2.5.6 Real-time qPCR

RNA was extracted from the *tibialis anterior* muscle or *gastrocnemius* muscle with GenElute™ Mammalian Total RNA Miniprep Kit (Sigma-Aldrich). 500 ng of RNA was used to synthesize cDNA in reverse transcription PCR (RT-PCR) and 1 µL of the diluted cDNA was used for quantitative PCR (qPCR). 18S ribosomal RNA was used as an endogenous control for normalization. Primer sequences are listed in Table 2.5-1.

Name	Forward Sequence	Reverse Sequence
18S rRNA	GTAACCCGTTGAACCCATT	CCATCCAATCGGTAGTAGCG
<i>Ctcf</i>	ACACTGTCATAGCCCGAAAA	CAGCATCACAGTAGCGACATT

Table 2.5-1 The primers information contains target gene names, forward sequences, and reverse sequences.

The primers targets for housekeeping gene 18S ribosomal RNA and the target gene *Ctcf*.

2.5.7 Western blotting

The *tibialis anterior* muscles and liver tissues were collected and ground into powder. The samples were disrupted by the whole cell lysis buffer (20 mM Tris pH 7.5, 420 mM NaCl, 2 mM MgCl₂, 1 mM EDTA, 10% glycerol, 0.5% NP-40, 0.5% Triton, 200 mM P8340, 1 M DTT, 1 M NaF, 1 M BGP) on ice. The lysates were centrifuged at maximum speed at 4 °C for 15 min, and then the supernatants were collected. For quantifying the protein concentration, 1 µL sample was mixed with 1mL Bradford reagent. The absorbance was detected by spectrophotometer and thus the concentration was speculated. The same number of proteins was used for the detection of the same types of tissues in the control and experimental group. Following the standard SDS-PAGE technique, different sizes of proteins in the same sample were separated by 10% resolving gel and 5% stacking gel. The gels were transferred to nitrocellulose membranes. And the membranes were blocked by 5% skim milk in tris-buffered

saline with Tween and probed by the primary antibody overnight at 4 °C with rocking. After several times washing, secondary antibody was added, and the blot was exposed under the machine with fresh enhanced chemiluminescence mixture.

2.5.8 Immunophenotyping

Tibialis anterior muscles and diaphragm muscles were resected from sacrificed mice at 13 weeks. The tissues were mechanically minced following the protocol of Skeletal Muscle Dissociation Kit (Miltenyi Biotec). Single-cell suspension in PBS was counted, blocked, and then stained with indicated antibodies (Table 2.5-2). Immunophenotyping data was subsequently acquired with BD LSRFortessa flow cytometer (BD Biosciences). The gating strategies used for analysis are shown in Figure 2.4-6.

Sample	Marker	Conjugate	Identifier	Dilution
Ctrl	Water			1:100
1	CD45	BUV395	UV1	1:400
2	CD11b	e450	U2	1:1000
3	MHCII	BV650	V3	1:500
4	CD11c	BV786	Y1	1:100
5	Ly6G	FITC	J8	1:1000
6	F4/80	PE	PE	1:100
7	Ly6C	pe-cf594	C4	1:400
8	CD86	PeCy7	D8	1:100
9	CD3	BV711	VA1	1:50
10	CD8	Percp cy55	N2	1:50
11	CD4	APC Cy7	I1	1:200
12	Arg1	AF700	G3	1:100

Table 2.5-2 The experimental design for immunophenotyping is listed.

It contains the control sample with water and 12 samples incubated with other antibodies in a certain concentration in each group.

2.5.9 RNA-seq and analysis

The *gastrocnemius* muscles were isolated from 7-week-old, 9-week-old and 13-week-old control mice and *Ctcf* mKO mice. RNA extraction was performed via GenElute™ Mammalian Total RNA Miniprep Kit (Sigma-Aldrich) all with the DNase I treatment. 5 µL RNA samples by three replicates each group, total 18 samples were sent to our collaborator, Dr. Tom Cheung from Hong Kong University of Science and Technology for RNA sequencing. The RNA-seq libraries were prepared using Tn5 transposases with adaptors and PCR amplification and it was followed by a BGISEQ-500RS (2 x 100) sequencing. And 40 million reads per sample was provided (Yue et al., 2020). The quality control and preprocessing of reads were carried out on the original sequencing BAM files via Trimmomatic v0.32 and paired sequences were aligned to a reference mouse genome through STAR v2.3.0e. After UCSC hg19 annotation, “FeatureCount” files were obtained and used for differential expression analysis through DESeq2 (Shorstova et al., 2019). The selection of differentially expressed genes was based on fold change > 2 and FDR < 0.05. Gene ontology (GO) analysis was performed through Enrichr based on GO Biological Process 2021, MSigDB Hallmark 2020 and ENCODE and ChEA Consensus TFs from CHIP-X databases. The heatmaps and volcano plots were generated by GraphPad Prism 9.

3 Discussion

3.1 CTCF is necessary for muscle contraction

So far, we know that 13-week-old *Ctcf* mKO mice lost muscle weight and had muscle functional defects (Figure 2.4-2). And downregulated DEGs in knockout mice enriched in the ‘muscle contraction’ and ‘muscle filament sliding’ gene sets at 7, 9, and 13 weeks (Figure 2.4-7 D, F, H). It indicates that the loss of CTCF disrupts the muscle contraction activity of skeletal muscles in mice.

Moreover, the analysis of representative myosin gene expressions provides us with the possible change of myofiber type distribution in *Ctcf* mKO mice. It shows that there exists downregulated expressions of slow type I myofiber markers, *Myh7* and *Myl3* at 7 and 9 weeks, but in 13-week-old CTCF-loss muscles, the type 2X and type 2B fast-twitch muscle fiber markers *Myll* and *Myh4* are downregulated (Figure 2.4-8 E). It raises a possibility that CTCF deficiency causes the muscle fiber type disproportion, thus leading to defects in muscle contraction. The difference in representative myosin expressions may also explain why the knockout mice exhibit serious muscle defects at 13 weeks instead of 7 or 9 weeks. But it still requires further demonstration of the sequential relationship between myofiber type disproportion and contractile defect. It can be detected via immunostaining targeted for both myofiber type markers and contractile markers at the same timepoint.

Dysfunctional nerve-muscle communication also underlies muscle weakness disorders, which are termed congenital myasthenic syndrome in a genetic form (Nicole et al., 2017). Specifically, nicotinic acetylcholine receptors (nAChR) are responsible for transferring the signaling in the neuromuscular junction. And thus, they play an indispensable role in maintaining the communication to trigger muscle contraction. For instance, the mutations of *Chrnd* and *Chrng* lead to the inefficient neuromuscular transmission and further muscle developmental abnormalities (Mueller et al., 2006; Seo et al., 2015). In the muscles of 13-week-old *Ctcf* mKO mice, muscle-type nAChR subunits $\alpha 1$, $\beta 1$, δ , and γ were all downregulated, which are respectively encoded by *Chrna1*, *Chrnb1*, *Chrnd*, and *Chrng* (Figure 2.4-8 G). Therefore, it is possible that the muscle contractile defect in 13-week-old *Ctcf* mKO

mice is also related to the downregulation of nAChR-related genes, except for the relationship with the accumulation of the downregulation of muscle contraction-related genes.

Furthermore, we linked the DEGs from *Ctcf* mKO mice to the genes involved in congenital myopathies, which are characterized by muscle weakness. These DEGs include *Acta1*, *Tnnt1*, *Tpm2*, *Tpm3*, *Ttn*, *Ryr1*, *Stac3*, *Speg*, and *Cacna1s* (Figure 2.4-8 F). They are involved in the ‘muscle contraction’, ‘muscle filament sliding’, and ‘actin-myosin filament sliding’ pathways. And their mutations can cause central core disease, multi-minicore disease, centronuclear myopathy, congenital fiber type disproportion, and nemaline myopathy (Jungbluth et al., 2018). With further study on the relationship of CTCF and muscle contraction, our study of CTCF in skeletal muscle homeostasis can also provide more ideas in studying the mechanism and clinical treatment of congenital myopathies.

3.2 CTCF deficiency may influence muscle metabolism

Muscle metabolism is closely related to muscle contraction activity and its disorder could also cause muscle functional defects (Hood et al., 2019). In addition, the previous studies show that the loss of CTCF in different cell types leads to changes in mitochondrial signaling. ChIP-qPCR analyses proved that CTCF was recruited to the transcription start sites of the tested mitochondrial genes, which were downregulated in limb development due to the loss of CTCF (Soshnikova et al., 2010). Roy et al. found that Frataxin (*Fxn*) gene, encoding a mitochondrial protein, was most dramatically downregulated in CTCF-deficient placental endothelial cells. And it was further demonstrated that CTCF activates the promoter of the *Fxn* gene and limits reactive oxygen species accumulation in endothelial cells (Roy et al., 2018). In *Ctcf* mutant embryonic hearts, genes related to mitochondrial function were upregulated. And mitochondria from mutant cardiomyocytes are not capable of maturing properly (Gomez-Velazquez et al., 2017).

In *Ctcf* mKO mice, the gene set analysis based on ENCODE and ChEA Consensus TFs from ChIP-X databases, shows that the downregulated genes caused by the loss of CTCF tend to be the targets of transcription factor, CTCF and MYOD1 (Figure 2.4-12 B, D, F). And there

was an increasing trend in the number of downregulated genes linked by CTCF (Figure 2.4-12 G). Moreover, the gene ontology biological process analysis shows that the overlaid genes of the three timepoints' CTCF-related genes tend to be involved in mitochondria-related pathways (Figure 2.4-12 H). For example, the downregulated *Fxn* gene encodes a mitochondria protein and regulates cell iron metabolism (Du et al., 2020). And the downregulated genes, *Gfm1*, *Mrpl23*, and *Mrps2* take part in the mitochondrial translation (Molina-Berenguer et al., 2022; Sylvester et al., 2004). Therefore, reduced *Ctcf* expression in muscle may also influence muscle metabolism.

In addition, the transcript levels of mitochondrial DNA were increased at three timepoints of *Ctcf* mKO mice. It includes the genes of the mitochondrial genome coding for the NADH-ubiquinone oxidoreductase (*mt-Nd1*, *mt-Nd2*, *mt-Nd4*, *mt-Nd5*, and *mt-Nd6*) and coding for transfer RNA (*mt-Tc*, *mt-Ti*, *mt-Tll*, *mt-Tm*, and *mt-Tq*). This change raises the possibility that the loss of CTCF in muscles promotes the mitochondria reproduction (Figure 2.4-9 F).

However, it still needs further investigation whether mitochondria biogenesis occurs at the protein level in *Ctcf* mKO mice. In order to evaluate muscle physiology, we can test the comprehensive mitochondrial phenotyping in muscle tissue, in terms of oxygen consumption, chemical energy production, and reactive oxygen species production. The use of transmission electron microscopy will also provide a morphological examination of mitochondria in muscle tissue. Our study on the relationship between CTCF and mitochondria will deepen the understanding of muscle metabolism and mitochondrial myopathy.

3.3 The loss of CTCF may trigger unfolded protein response and mTORC1 signaling

mTOR which is an atypical serine/threonine kinase regulates cell growth and metabolism. And it comes in two forms, mTORC1 and mTORC2, which have different subunit compositions and performs different cellular functions (Magnuson et al., 2012). mTORC1 core complex is composed of the PI3K-related protein kinase family member mTOR, Raptor, and mLST8 (Saxton and Sabatini, 2017). There are four downstream pathways in the mTOR1 signaling. After phosphorylation by mTORC1, 4E-BP1 suppresses translation while S6K1

positively affects mRNA translation and ribosome biosynthesis (Batoool et al., 2019; Dowling et al., 2010). mTORC1 also phosphorylates ATG13 and ULK1 and inhibits their protein expressions, thus preventing autophagosome assembly (Chan, 2009; Hosokawa et al., 2009). Moreover, mTORC1 can inhibit Lipin 1 to prevent lipid synthesis (Peterson et al., 2011). Glycolytic gene expression and angiogenesis can also be increased by the activation of mTORC1 (Ding et al., 2018). Furthermore, there exists complex bidirectional crosstalk between mTORC1 and unfolded protein response (UPR) and the results of their cooperation might be synergistic (Hotamisligil, 2010; Peterson et al., 2011; Thomas et al., 2006; Um et al., 2004) or antagonistic (Hoyer-Hansen and Jaattela, 2007; Hsieh et al., 2010; Zoncu et al., 2011).

In *Ctcf* mKO mice, the gene set enrichment analysis based on MSigDB Hallmark 2020 reveals that the upregulated enrichment related to ‘mTORC1 signaling’ was strong at three ages (Figure 2.4-10 A, C, E). And the enrichment in ‘unfolded protein response’ was also obvious at the upregulated gene sets of 9 and 13 weeks (Figure 2.4-10 C, E). Moreover, the number of these two pathway-associated genes was greatly increased at 13 weeks (Figure 2.4-11 A-B). Moreover, rodent studies clearly show that mTORC1 signaling can be activated by the increased mechanical loading and it induces protein synthesis (Jacobs et al., 2014). However, there is also evidence that a severe form of myopathy that begins in the late stages of life is caused by continuous activation of mTORC1 in skeletal muscle (Castets et al., 2013). Therefore, one possibility in *Ctcf* mKO mice is that the loss of CTCF may trigger unfolded protein response and mTORC1 signaling, which are secondary responses to the difficult support for muscle contraction and massive muscle-relative protein loss. Another possibility could be that CTCF deficiency directly activates mTORC1 signaling and then instigate muscle defects.

Furthermore, mTORC1 can be activated through heterodimer TSC1/TSC2 (tuberous sclerosis complex 1 and 2) in response to insulin signaling (Saxton and Sabatini, 2017). Regulator-Rag complex can also be the activator of mTORC1 and recruits mTORC1 to the lysosomal membrane when sensing amino acids (Sancak et al., 2010). In *Ctcf* mKO mice, *Tsc1* and *Tsc2* were not differentially expressed. However, the genes encoding the subunits of the Regulator-Rag complex, *Lamtor3*, and *Rragc* were upregulated at 13 weeks. And 13-week-old CTCF-deficient muscle also has an increased expression of *Lamp2* gene (lysosomal-associated

membrane protein 2). Although they are not included in the ‘mTORC1 signaling’ gene set enrichment, the change in their transcript level suggests that there may exist a mTORC1 activation by amino acids.

So far, the activation of unfolded protein response and mTORC1 signaling in CTCF-deficient mice was only predicted from the DEGs pathway analysis. In the future, we can test the mRNA and protein levels of UPR target genes and mTORC1 target genes. If these activations are confirmed, mTOR inhibitor treatment can be further performed in mice. We will explore whether the muscle contraction defects or the possible muscle metabolism change can be rescued. And this discovery can demonstrate the sequential mechanism between muscle atrophy and UPR or mTORC1 signaling in *Ctcf* mKO mice, as well as CTCF function in skeletal muscle homeostasis.

3.4 The potential mechanism of *Ctcf* mKO mice

In summary, based on the increased muscle regeneration and decreased muscle contraction, it can be predicted that the loss of CTCF may lead to chronic and continuous injuries in skeletal muscle. Along with time, even though maintaining the potential of muscle regeneration, the CTCF-deficient muscle may not be capable of complete self-repair, so the *Ctcf* mKO mice begin to progressively exhibit reduced muscle mass and decreased muscle physical function (Figure 3-1). And the phenotype is especially most severe at 13 weeks due to the accumulation of injuries.

From the gene set enrichment analysis of RNA-seq data at 7, 9, and 13 weeks, the influenced pathway can be inferred. Noticeably, the mTORC1 signaling is potentially upregulated since 7-week-old muscle, along with the downregulation of muscle contraction-related pathways. Moreover, the upregulation of unfolded protein response is obvious at 9 and 13 weeks. Because abnormal activation of mTORC1 signaling can cause dysfunctional protein synthesis and protein degradation, unfolded protein response could be triggered in response to the stress caused by muscle defects of metabolism.

Moreover, CTCF plays an indispensable role in the genome structure, especially in maintaining the chromatin loop as an insulator. And the gene set enrichment analysis shows that downregulated genes are putative targets of CTCF and are closely linked to muscle contraction. It indicates that the muscle contraction may be directly regulated by the related genes inside the chromatin loop directed by CTCF (Figure 3-1).

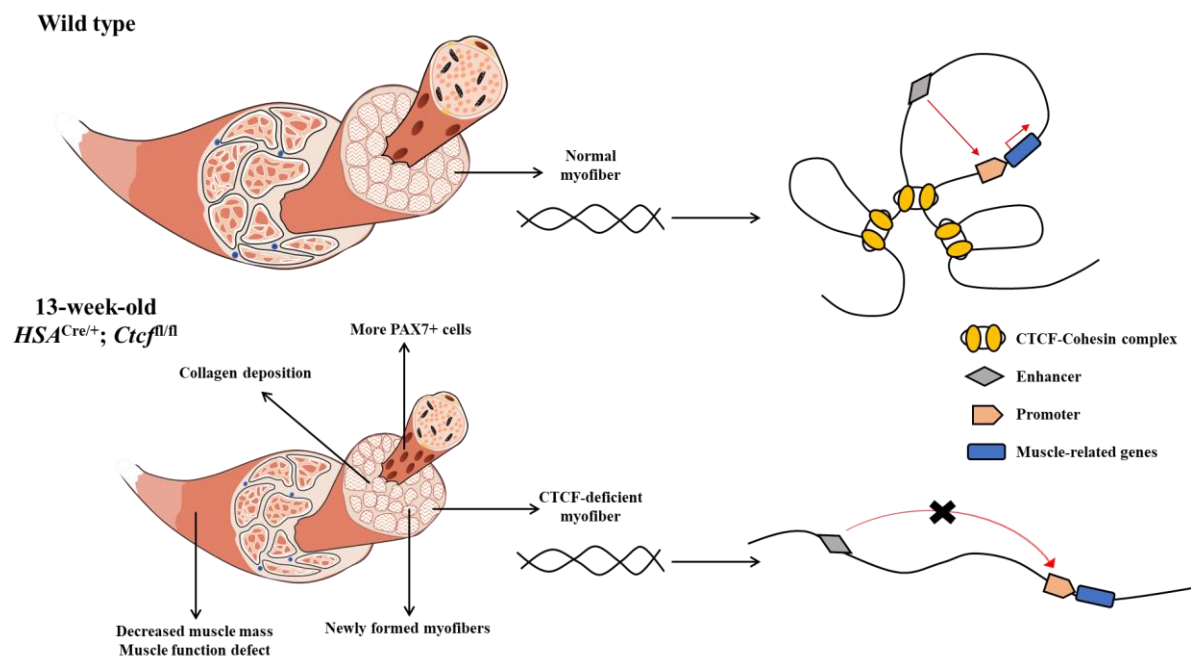


Figure 3-1 The schematic model of skeletal muscles in 13-week-old *Ctf* mKO mice.

Compared to the *HSA*^{Cre/+} mice, 13-week-old *Ctf* mKO mice exhibit body weight loss and muscle mass reduction, along with muscle contraction defect. In their skeletal muscles, there exist the signs of regeneration, including more PAX7 positive cells (satellite cells) and the appearance of newly formed myofibers. Meanwhile, collagen deposition is induced, as one stage in muscle regeneration. From RNA-seq data, the muscle contraction-related genes are downregulated. It may be caused by the disruption of chromatin loop, which blocks the interaction of enhancers and promoters and thus inhibits the originally active muscle-linked genes. Therefore, there may exist a change of spatial chromatin structure due to the absence of CTCF, which influences the expression of muscle-related genes and leads to muscle defects.

4 Conclusion

This work presents evidence to support the indispensable role of CTCF in skeletal muscle homeostasis. The loss of CTCF in muscles leads to serious muscle defects and shortens the mice's life expectancy. Muscle regeneration also occurs in both the *tibialis anterior* muscles and the diaphragm muscles in response to the nature injury brought by CTCF deficiency. Moreover, due to the regulator function in both gene transcription and chromosome structure, CTCF loss also triggers dramatic transcriptome changes, and the effect is expanded along with age.

We will continue to work on the identification of CTCF functional pathways in skeletal muscle. And based on the phenotypes of the mouse model, we believe that this study will provide insights for the treatment of skeletal muscle wasting diseases.

5 References

- Abbadi, D., Yang, M., Chenette, D.M., Andrews, J.J., and Schneider, R.J. (2019). Muscle development and regeneration controlled by AUF1-mediated stage-specific degradation of fate-determining checkpoint mRNAs. *Proceedings of the National Academy of Sciences of the United States of America* *116*, 11285-11290.
- Adler, M., and Shieh, P.B. (2015). Metabolic Myopathies. *Seminars in Neurology* *35*, 385-397.
- Alston, C.L., Rocha, M.C., Lax, N.Z., Turnbull, D.M., and Taylor, R.W. (2017). The genetics and pathology of mitochondrial disease. *Journal of Pathology* *241*, 236-250.
- An, Y., Zhang, Z., Shang, Y., Jiang, X., Dong, J., Yu, P., Nie, Y., and Zhao, Q. (2015). miR-23b-3p regulates the chemoresistance of gastric cancer cells by targeting ATG12 and HMGB2. *Cell Death & Disease* *6*.
- Arzate-Mejia, R.G., Recillas-Targa, F., and Corces, V.G. (2018). Developing in 3D: the role of CTCF in cell differentiation. *Development* *145*.
- Baghdadi, M.B., and Tajbakhsh, S. (2018). Regulation and phylogeny of skeletal muscle regeneration. *Developmental Biology* *433*, 200-209.
- Batool, A., Majeed, S.T., Aashaq, S., Majeed, R., Shah, G., Nazir, N., and Andrabi, K.I. (2019). Eukaryotic Initiation Factor 4E (eIF4E) sequestration mediates 4E-BP1 response to rapamycin. *International Journal of Biological Macromolecules* *125*, 651-659.
- Battistelli, C., Busanello, A., and Maione, R. (2014). Functional interplay between MyoD and CTCF in regulating long-range chromatin interactions during differentiation. *Journal of Cell Science* *127*, 3757-3767.
- Beauchamp, J.R., Heslop, L., Yu, D.S.W., Tajbakhsh, S., Kelly, R.G., Wernig, A., Buckingham, M.E., Partridge, T.A., and Zammit, P.S. (2000). Expression of CD34 and Myf5 defines the majority of quiescent adult skeletal muscle satellite cells. *Journal of Cell Biology* *151*, 1221-1233.
- Berria, R., Wang, L.S., Richardson, D.K., Finlayson, J., Belfort, R., Pratipanawatr, T., De

Filippis, E.A., Kashyap, S., and Mandarino, L.J. (2006). Increased collagen content in insulin-resistant skeletal muscle. *American Journal of Physiology-Endocrinology and Metabolism* 290, E560-E565.

Brack, A.S., Bildsoe, H., and Hughes, S.M. (2005). Evidence that satellite cell decrement contributes to preferential decline in nuclear number from large fibres during murine age-related muscle atrophy. *Journal of Cell Science* 118, 4813-4821.

Brentnall, M., Rodriguez-Menocal, L., De Guevara, R.L., Cepero, E., and Boise, L.H. (2013). Caspase-9, caspase-3 and caspase-7 have distinct roles during intrinsic apoptosis. *Bmc Cell Biology* 14.

Brigitte, M., Schilte, C., Plonquet, A., Baba-Amer, Y., Henri, A., Charlier, C., Tajbakhsh, S., Albert, M., Gherardi, R.K., and Chretien, F. (2010). Muscle Resident Macrophages Control the Immune Cell Reaction in a Mouse Model of Notexin-Induced Myoinjury. *Arthritis and Rheumatism* 62, 268-279.

Brook, J.D., McCurrach, M.E., Harley, H.G., Buckler, A.J., Church, D., Aburatani, H., Hunter, K., Stanton, V.P., Thirion, J.P., Hudson, T., *et al.* (1992). MOLECULAR-BASIS OF MYOTONIC-DYSTROPHY - EXPANSION OF A TRINUCLEOTIDE (CTG) REPEAT AT THE 3' END OF A TRANSCRIPT ENCODING A PROTEIN-KINASE FAMILY MEMBER. *Cell* 68, 799-808.

Bruusgaard, J.C., Egner, I.M., Larsen, T.K., Dupre-Aucouturier, S., Desplanches, D., and Gundersen, K. (2012). No change in myonuclear number during muscle unloading and reloading. *Journal of Applied Physiology* 113, 290-296.

Calvi, E.N.D., Nahas, F.X., Barbosa, M.V., Calil, J.A., Ihara, S.S.M., Silva, M.D., de Franco, M.F., and Ferreira, L.M. (2012). An experimental model for the study of collagen fibers in skeletal muscle. *Acta Cirurgica Brasileira* 27, 681-686.

Carraro, U., and Franceschi, C. (1997). Apoptosis of skeletal and cardiac muscles and physical exercise. *Aging Clinical and Experimental Research* 9, 19-34.

Castel, A.L., Nakamori, M., Tome, S., Chitayat, D., Gourdon, G., Thornton, C.A., and Pearson,

C.E. (2011). Expanded CTG repeat demarcates a boundary for abnormal CpG methylation in myotonic dystrophy patient tissues. *Human Molecular Genetics* 20, 1-15.

Castets, P., Lin, S., Rion, N., Di Fulvio, S., Romanino, K., Guridi, M., Frank, S., Tintignac, L.A., Sinnreich, M., and Ruegg, M.A. (2013). Sustained Activation of mTORC1 in Skeletal Muscle Inhibits Constitutive and Starvation-Induced Autophagy and Causes a Severe, Late-Onset Myopathy. *Cell Metabolism* 17, 731-744.

Chan, E.Y. (2009). mTORC1 Phosphorylates the ULK1-mAtg13-FIP200 Autophagy Regulatory Complex. *Science Signaling* 2.

Charge, S.B.P., and Rudnicki, M.A. (2004). Cellular and molecular regulation of muscle regeneration. *Physiological Reviews* 84, 209-238.

Chazaud, B. (2020). Inflammation and Skeletal Muscle Regeneration: Leave It to the Macrophages! *Trends in Immunology* 41, 481-492.

Chemello, F., Bean, C., Cancellara, P., Laveder, P., Reggiani, C., and Lanfranchi, G. (2011). Microgenomic Analysis in Skeletal Muscle: Expression Signatures of Individual Fast and Slow Myofibers. *Plos One* 6.

Chemello, F., Wang, Z., Li, H., McAnally, J.R., Liu, N., Bassel-Duby, R., and Olson, E.N. (2020). Degenerative and regenerative pathways underlying Duchenne muscular dystrophy revealed by single-nucleus RNA sequencing. *Proceedings of the National Academy of Sciences of the United States of America* 117, 29691-29701.

Chen, H., Tian, Y., Shu, W., Bo, X., and Wang, S. (2012). Comprehensive Identification and Annotation of Cell Type-Specific and Ubiquitous CTCF-Binding Sites in the Human Genome. *Plos One* 7.

Chen, X., Xu, H., Yuan, P., Fang, F., Huss, M., Vega, V.B., Wong, E., Orlov, Y.L., Zhang, W., Jiang, J., *et al.* (2008). Integration of external signaling pathways with the core transcriptional network in embryonic stem cells. *Cell* 133, 1106-1117.

Chepelev, I., Wei, G., Wangsa, D., Tang, Q.S., and Zhao, K.J. (2012). Characterization of

genome-wide enhancer-promoter interactions reveals co-expression of interacting genes and modes of higher order chromatin organization. *Cell Research* 22, 490-503.

Chernukhin, I., Shamsuddin, S., Kang, S.Y., Bergstrom, R., Kwon, Y.-W., Yu, W., Whitehead, J., Mukhopadhyay, R., Docquier, F., Farrar, D., *et al.* (2007a). CTCF interacts with and recruits the largest subunit of RNA polymerase II to CTCF target sites genome-wide. *Molecular and Cellular Biology* 27, 1631-1648.

Chernukhin, I., Shamsuddin, S., Kang, S.Y., Bergstrom, R., Kwon, Y.W., Yu, W.Q., Whitehead, J., Mukhopadhyay, R., Docquier, F., Farrar, D., *et al.* (2007b). CTCF interacts with and recruits the largest subunit of RNA polymerase II to CTCF target sites genome-wide. *Molecular and Cellular Biology* 27, 1631-1648.

Cleary, J.D., Tome, S., Castel, A.L., Panigrahi, G.B., Foiry, L., Hagerman, K.A., Sroka, H., Chitayat, D., Gourdon, G., and Pearson, C.E. (2010). Tissue- and age-specific DNA replication patterns at the CTG/CAG-expanded human myotonic dystrophy type 1 locus. *Nature Structural & Molecular Biology* 17, 1079-U1077.

Cogswell, A.M., Stevens, R.J., and Hood, D.A. (1993). PROPERTIES OF SKELETAL-MUSCLE MITOCHONDRIA ISOLATED FROM SUBSARCOLEMMAL AND INTERMYOFIBRILLAR REGIONS. *American Journal of Physiology* 264, C383-C389.

Collins, R.A., and Grounds, M.D. (2001). The role of tumor necrosis factor-alpha (TNF-alpha) in skeletal muscle regeneration: Studies in TNF-alpha(-/-) and TNF-alpha(-/-)/LT-alpha(-/-) mice. *Journal of Histochemistry & Cytochemistry* 49, 989-1001.

Crisco, J.J., Jokl, P., Heinen, G.T., Connell, M.D., and Panjabi, M.M. (1994). A MUSCLE CONTUSION INJURY MODEL - BIOMECHANICS, PHYSIOLOGY, AND HISTOLOGY. *American Journal of Sports Medicine* 22, 702-710.

Crist, C. (2017). Emerging new tools to study and treat muscle pathologies: genetics and molecular mechanisms underlying skeletal muscle development, regeneration, and disease. *Journal of Pathology* 241, 264-272.

Crist, C.G., Montarras, D., and Buckingham, M. (2012). Muscle Satellite Cells Are Primed for

Myogenesis but Maintain Quiescence with Sequestration of Myf5 mRNA Targeted by microRNA-31 in mRNP Granules. *Cell Stem Cell* *11*, 118-126.

Dalbis, A., Couteaux, R., Janmot, C., Roulet, A., and Mira, J.C. (1988). REGENERATION AFTER CARDIOTOXIN INJURY OF INNERVATED AND DENERVATED SLOW AND FAST MUSCLES OF MAMMALS - MYOSIN ISOFORM ANALYSIS. *European Journal of Biochemistry* *174*, 103-110.

Dall'Agnesse, A., Caputo, L., Nicoletti, C., di Iulio, J., Schmitt, A., Gatto, S., Diao, Y.R., Ye, Z., Forcato, M., Perera, R., *et al.* (2019). Transcription Factor-Directed Re-wiring of Chromatin Architecture for Somatic Cell Nuclear Reprogramming toward trans-Differentiation. *Molecular Cell* *76*, 453-+.

Davidson, I.F., Bauer, B., Goetz, D., Tang, W., Wutz, G., and Peters, J.M. (2019). DNA loop extrusion by human cohesin. *Science* *366*, 1338-+.

Davie, J.K., Cho, J.-H., Meadows, E., Flynn, J.M., Knapp, J.R., and Klein, W.H. (2007). Target gene selectivity of the myogenic basic helix-loop-helix transcription factor myogenin in embryonic muscle. *Developmental Biology* *311*, 650-664.

Dekker, J., Rippe, K., Dekker, M., and Kleckner, N. (2002). Capturing chromosome conformation. *Science* *295*, 1306-1311.

Delgado-Olguin, P., Brand-Arzamendi, K., Scott, I.C., Jungblut, B., Stainier, D.Y., Bruneau, B.G., and Recillas-Targa, F. (2011). CTCF Promotes Muscle Differentiation by Modulating the Activity of Myogenic Regulatory Factors. *Journal of Biological Chemistry* *286*.

Deng, B., Wehling-Henricks, M., Villalta, S.A., Wang, Y., and Tidball, J.G. (2012). IL-10 Triggers Changes in Macrophage Phenotype That Promote Muscle Growth and Regeneration. *Journal of Immunology* *189*, 3669-3680.

Ding, Y., Shan, L., Nai, W., Lin, X., Zhou, L., Dong, X., Wu, H., Xiao, M., Zhou, X., Wang, L., *et al.* (2018). DEPTOR Deficiency-Mediated mTORc1 Hyperactivation in Vascular Endothelial Cells Promotes Angiogenesis. *Cellular Physiology and Biochemistry* *46*, 520-531.

Dixon, J.R., Selvaraj, S., Yue, F., Kim, A., Li, Y., Shen, Y., Hu, M., Liu, J.S., and Ren, B. (2012). Topological domains in mammalian genomes identified by analysis of chromatin interactions. *Nature* 485, 376-380.

Douglas, J., Pearson, S., Ross, A., and McGuigan, M. (2017). Eccentric Exercise: Physiological Characteristics and Acute Responses. *Sports Medicine* 47, 663-675.

Dowling, R.J.O., Topisirovic, I., Alain, T., Bidinosti, M., Fonseca, B.D., Petroulakis, E., Wang, X., Larsson, O., Selvaraj, A., Liu, Y., *et al.* (2010). mTORC1-Mediated Cell Proliferation, But Not Cell Growth, Controlled by the 4E-BPs. *Science* 328, 1172-1176.

Du, J., Zhou, Y., Li, Y.C., Xia, J., Chen, Y.J., Chen, S.F., Wang, X., Sun, W.D., Wang, T.T., Ren, X.Y., *et al.* (2020). Identification of Frataxin as a regulator of ferroptosis. *Redox Biology* 32.

Dumont, N.A., Bentzinger, C.F., Sincennes, M.C., and Rudnicki, M.A. (2015). Satellite Cells and Skeletal Muscle Regeneration. *Comprehensive Physiology* 5, 1027-1059.

Egan, B., and Zierath, J.R. (2013). Exercise Metabolism and the Molecular Regulation of Skeletal Muscle Adaptation. *Cell Metabolism* 17, 162-184.

Fadok, V.A., Bratton, D.L., Guthrie, L., and Henson, P.M. (2001). Differential effects of apoptotic versus lysed cells on macrophage production of cytokines: Role of proteases. *Journal of Immunology* 166, 6847-6854.

Filippova, G.N., Fagerlie, S., Klenova, E.M., Myers, C., Dehner, Y., Goodwin, G., Neiman, P.E., Collins, S.J., and Lobanenko, V.V. (1996). An exceptionally conserved transcriptional repressor, CTCF, employs different combinations of zinc fingers to bind diverged promoter sequences of avian and mammalian c-myc oncogenes. *Molecular and Cellular Biology* 16, 2802-2813.

Filippova, G.N., Qi, C.F., Ulmer, J.E., Moore, J.M., Ward, M.D., Hu, Y.J., Loukinov, D.I., Pugacheva, E.M., Klenova, E.M., Grundy, P.E., *et al.* (2002). Tumor-associated zinc finger mutations in the CTCF transcription factor selectively alter its DNA-binding specificity. *Cancer Research* 62, 48-52.

Filippova, G.N., Thienes, C.P., Penn, B.H., Cho, D.H., Hu, Y.J., Moore, J.M., Klesert, T., Lobanenkov, V.V., and Tapscott, S.J. (2001). CTCF-binding sites flank CTG/CAG repeats and form a methylation-sensitive insulator at the DM1 locus. *Nature Genetics* 28, 335-343.

Forcina, L., Cosentino, M., and Musaro, A. (2020). Mechanisms Regulating Muscle Regeneration: Insights into the Interrelated and Time-Dependent Phases of Tissue Healing. *Cells* 9.

Frontera, W.R., and Ochala, J. (2015). Skeletal Muscle: A Brief Review of Structure and Function. *Calcified Tissue International* 96, 183-195.

Fry, C.S., Lee, J.D., Mula, J., Kirby, T.J., Jackson, J.R., Liu, F.J., Yang, L., Mendias, C.L., Dupont-Versteegden, E.E., McCarthy, J.J., *et al.* (2015). Inducible depletion of satellite cells in adult, sedentary mice impairs muscle regenerative capacity without affecting sarcopenia. *Nature Medicine* 21, 76-80.

Fudenberg, G., Imakaev, M., Lu, C., Goloborodko, A., Abdennur, N., and Mirny, L.A. (2016). Formation of Chromosomal Domains by Loop Extrusion. *Cell Reports* 15, 2038-2049.

Fujita, K., Ye, L.H., Sato, M., Okagaki, T., Nagamachi, Y., and Kohama, K. (1999). Myosin light chain kinase from skeletal muscle regulates an ATP-dependent interaction between actin and myosin by binding to actin. *Molecular and Cellular Biochemistry* 190, 85-90.

Fujita, R., and Crist, C. (2018). Translational Control of the Myogenic Program in Developing, Regenerating, and Diseased Skeletal Muscle. In *Myogenesis in Development and Disease*, D. Sassoon, ed., pp. 67-98.

Fujita, R., Jamet, S., Lean, G., Cheng, H.C.M., Hebert, S., Kleinman, C.L., and Crist, C. (2021). Satellite cell expansion is mediated by P-eIF2 alpha-dependent Tacc3 translation. *Development* 148.

Gaillard, M.C., Broucqsault, N., Morere, J., Laberthonniere, C., Dion, C., Badja, C., Roche, S., Nguyen, K., Magdinier, F., and Robin, J.D. (2019). Analysis of the 4q35 chromatin organization reveals distinct long-range interactions in patients affected with Facio-Scapulo-Humeral Dystrophy. *Scientific Reports* 9.

Galpin, A.J., Raue, U., Jemiolo, B., Trappe, T.A., Harber, M.P., Minchev, K., and Trappe, S. (2012). Human skeletal muscle fiber type specific protein content. *Analytical Biochemistry* 425, 175-182.

Ganji, M., Shaltiel, I.A., Bisht, S., Kim, E., Kalichava, A., Haering, C.H., and Dekker, C. (2018). Real-time imaging of DNA loop extrusion by condensin. *Science* 360, 102-105.

Garrett, W.E. (1990). MUSCLE STRAIN INJURIES - CLINICAL AND BASIC ASPECTS. *Medicine and Science in Sports and Exercise* 22, 436-443.

Geeves, M.A., Fedorov, R., and Manstein, D.J. (2005). Molecular mechanism of actomyosin-based motility. *Cellular and Molecular Life Sciences* 62, 1462-1477.

Gillies, A.R., and Lieber, R.L. (2011). STRUCTURE AND FUNCTION OF THE SKELETAL MUSCLE EXTRACELLULAR MATRIX. *Muscle & Nerve* 44, 318-331.

Giordano, C., Mojumdar, K., Liang, F., Lemaire, C., Li, T., Richardson, J., Divangahi, M., Qureshi, S., and Petrof, B.J. (2015). Toll-like receptor 4 ablation in mdx mice reveals innate immunity as a therapeutic target in Duchenne muscular dystrophy. *Human Molecular Genetics* 24, 2147-2162.

Gomez-Velazquez, M., Badia-Careaga, C., Lechuga-Vieco, A.V., Nieto-Arellano, R., Tena, J.J., Rollan, I., Alvarez, A., Torroja, C., Caceres, E.F., Roy, A., *et al.* (2017). CTCF counter-regulates cardiomyocyte development and maturation programs in the embryonic heart. *Plos Genetics* 13.

Gordon, A.M., Huxley, A.F., and Julian, F.J. (1966). VARIATION IN ISOMETRIC TENSION WITH SARCOMERE LENGTH IN VERTEBRATE MUSCLE FIBRES. *Journal of Physiology-London* 184, 170-+.

Gregor, A., Oti, M., Kouwenhoven, E.N., Hoyer, J., Sticht, H., Ekici, A.B., Kjaergaard, S., Rauch, A., Stunnenberg, H.G., Uebe, S., *et al.* (2013). De Novo Mutations in the Genome Organizer CTCF Cause Intellectual Disability. *American Journal of Human Genetics* 93, 124-131.

Grounds, M.D. (1998). Age-associated changes in the response of skeletal muscle cells to exercise and regeneration. In *Towards Prolongation of the Healthy Life Span: Practical Approaches to Intervention*, D. Harman, R. Holliday, and M. Meydani, eds., pp. 78-91.

Haddix, S.G., Lee, Y.I., Kornegay, J.N., and Thompson, W.J. (2018). Cycles of myofiber degeneration and regeneration lead to remodeling of the neuromuscular junction in two mammalian models of Duchenne muscular dystrophy. *Plos One* 13.

Hamer, P.W., McGeachie, J.M., Davies, M.J., and Grounds, M.D. (2002). Evans Blue Dye as an in vivo marker of myofibre damage: optimising parameters for detecting initial myofibre membrane permeability. *Journal of Anatomy* 200, 69-79.

Handoko, L., Xu, H., Li, G.L., Ngan, C.Y., Chew, E., Schnapp, M., Lee, C.W.H., Ye, C.P., Ping, J.L.H., Mulawadi, F., *et al.* (2011). CTCF-mediated functional chromatin interactome in pluripotent cells. *Nature Genetics* 43, 630-U198.

Hargreaves, M., and Spriet, L.L. (2020). Skeletal muscle energy metabolism during exercise. *Nature Metabolism* 2, 817-828.

Hark, A.T., Schoenherr, C.J., Katz, D.J., Ingram, R.S., LeVorse, J.M., and Tilghman, S.M. (2000). CTCF mediates methylation-sensitive enhancer-blocking activity at the H19/Igf2 locus. *Nature* 405, 486-489.

Hashimoto, H., Wang, D.X., Horton, J.R., Zhang, X., Corces, V.G., and Cheng, X.D. (2017). Structural Basis for the Versatile and Methylation-Dependent Binding of CTCF to DNA. *Molecular Cell* 66, 711-+.

Hood, D.A., Memme, J.M., Oliveira, A.N., and Triolo, M. (2019). Maintenance of Skeletal Muscle Mitochondria in Health, Exercise, and Aging. In *Annual Review of Physiology*, Vol 81, M.T. Nelson, and K. Walsh, eds., pp. 19-41.

Horowitz, R., and Podolsky, R.J. (1987). THE POSITIONAL STABILITY OF THICK FILAMENTS IN ACTIVATED SKELETAL-MUSCLE DEPENDS ON SARCOMERE-LENGTH - EVIDENCE FOR THE ROLE OF TITIN FILAMENTS. *Journal of Cell Biology* 105, 2217-2223.

Hosokawa, N., Hara, T., Kaizuka, T., Kishi, C., Takamura, A., Miura, Y., Iemura, S.-i., Natsume, T., Takehana, K., Yamada, N., *et al.* (2009). Nutrient-dependent mTORC1 Association with the ULK1-Atg13-FIP200 Complex Required for Autophagy. *Molecular Biology of the Cell* 20, 1981-1991.

Hotamisligil, G.S. (2010). Endoplasmic Reticulum Stress and the Inflammatory Basis of Metabolic Disease. *Cell* 140, 900-917.

Hoyer-Hansen, M., and Jaattela, M. (2007). Connecting endoplasmic reticulum stress to autophagy by unfolded protein response and calcium. *Cell Death and Differentiation* 14, 1576-1582.

Hsieh, A.C., Costa, M., Zollo, O., Davis, C., Feldman, M.E., Testa, J.R., Meyuhas, O., Shokat, K.M., and Ruggero, D. (2010). Genetic Dissection of the Oncogenic mTOR Pathway Reveals Druggable Addiction to Translational Control via 4EBP-eIF4E. *Cancer Cell* 17, 249-261.

Hsieh, T.H.S., Cattoglio, C., Slobodyanyuk, E., Hansen, A.S., Rando, O.J., Tjian, R., and Darzacq, X. (2020). Resolving the 3D Landscape of Transcription-Linked Mammalian Chromatin Folding. *Molecular Cell* 78, 539-+.

Hultstrom, M., Leh, S., Paliege, A., Bachmann, S., Skogstrand, T., and Iversen, B.M. (2012). Collagen-binding proteins in age-dependent changes in renal collagen turnover: microarray analysis of mRNA expression. *Physiological Genomics* 44, 576-586.

Iwata, M., Englund, D.A., Wen, Y., Dungan, C.M., Murach, K.A., Vechetti, I.J., Mobley, C.B., Peterson, C.A., and McCarthy, J.J. (2018). A novel tetracycline-responsive transgenic mouse strain for skeletal muscle-specific gene expression. *Skeletal Muscle* 8.

Jacobs, B.L., Goodman, C.A., and Hornberger, T.A. (2014). The mechanical activation of mTOR signaling: an emerging role for late endosome/lysosomal targeting. *Journal of Muscle Research and Cell Motility* 35, 11-21.

Jarvinen, T., Jarvinen, T.L.N., Kaariainen, M., Kalimo, A., and Jarvinen, M. (2005). Muscle injuries - Biology and treatment. *American Journal of Sports Medicine* 33, 745-764.

Jejurikar, S.S., Henkelman, E.A., Cederna, P.S., Marcelo, C.L., Urbanek, M.G., and Kuzon, W.M. (2006). Aging increases the susceptibility of skeletal muscle derived satellite cells to apoptosis. *Experimental Gerontology* *41*, 828-836.

Jeselsohn, R., Bergholz, J.S., Pun, M., Cornwell, M., Liu, W.H., Nardone, A., Xiao, T.F., Li, W., Qiu, X.T., Buchwalter, G., *et al.* (2018). Allele-Specific Chromatin Recruitment and Therapeutic Vulnerabilities of ESR1 Activating Mutations. *Cancer Cell* *33*, 173-+.

Jing, H.I., Vakoc, C.R., Ying, L., Mandat, S., Wang, H.X., Zheng, X.W., and Blobel, G.A. (2008). Exchange of GATA factors mediates transitions in looped chromatin organization at a developmentally regulated gene locus. *Molecular Cell* *29*, 232-242.

Jungbluth, H., Treves, S., Zorzato, F., Sarkozy, A., Ochala, J., Sewry, C., Phadke, R., Gautel, M., and Muntoni, F. (2018). Congenital myopathies: disorders of excitation-contraction coupling and muscle contraction. *Nature Reviews Neurology* *14*, 151-167.

Kadauke, S., and Blobel, G.A. (2009). Chromatin loops in gene regulation. *Biochimica Et Biophysica Acta-Genes and Cell Regulation* *1789*, 17-25.

Kashyap, M.K., Marimuthu, A., Peri, S., Kumar, G.S.S., Jacob, H.K.C., Prasad, T.S.K., Mahmood, R., Kumar, K.V.V., Kumar, M.V., Meltzer, S.J., *et al.* (2010). Overexpression of periostin and lumican in esophageal squamous cell carcinoma. *Cancers* *2*, 133-142.

Kawabe, Y.-i., Wang, Y.X., McKinnell, I.W., Bedford, M.T., and Rudnicki, M.A. (2012). *Carm1* Regulates *Pax7* Transcriptional Activity through MLL1/2 Recruitment during Asymmetric Satellite Stem Cell Divisions. *Cell Stem Cell* *11*, 333-345.

Kelly, A.M., and Zacks, S.I. (1969). HISTOGENESIS OF RAT INTERCOSTAL MUSCLE. *Journal of Cell Biology* *42*, 135-+.

Klein, S.M., Vykoukal, J., Lechler, P., Zeitler, K., Gehmert, S., Schreml, S., Alt, E., Bogdahn, U., and Prantl, L. (2012). Noninvasive in vivo assessment of muscle impairment in the mdx mouse model - A comparison of two common wire hanging methods with two different results. *Journal of Neuroscience Methods* *203*, 292-297.

Klenova, E.M., Chernukhin, I.V., El-Kady, A., Lee, R.E., Pugacheva, E.M., Loukinov, D.I., Goodwin, G.H., Delgado, D., Filippova, G.N., Leon, J., *et al.* (2001). Functional phosphorylation sites in the C-terminal region of the multivalent multifunctional transcriptional factor CTCF. *Molecular and Cellular Biology* 21, 2221-2234.

Klenova, E.M., Nicolas, R.H., Paterson, H.F., Carne, A.F., Heath, C.M., Goodwin, G.H., Neiman, P.E., and Lobanenko, V.V. (1993). CTCF, A CONSERVED NUCLEAR FACTOR REQUIRED FOR OPTIMAL TRANSCRIPTIONAL ACTIVITY OF THE CHICKEN C-MYC GENE, IS AN 11-ZN-FINGER PROTEIN DIFFERENTIALLY EXPRESSED IN MULTIPLE FORMS. *Molecular and Cellular Biology* 13, 7612-7624.

Knappe, S., Zammit, P.S., and Knight, R.D. (2015). A population of Pax7-expressing muscle progenitor cells show differential responses to muscle injury dependent on developmental stage and injury extent. *Frontiers in Aging Neuroscience* 7.

Krupsky, M., Kuang, P.P., and Goldstein, R.H. (1997). Regulation of type I collagen mRNA by amino acid deprivation in human lung fibroblasts. *Journal of Biological Chemistry* 272, 13864-13868.

Kuang, S., Charge, S.B., Seale, P., Huh, M., and Rudnicki, M.A. (2006). Distinct roles for Pax7 and Pax3 in adult regenerative myogenesis. *Journal of Cell Biology* 172, 103-113.

Kuang, S., Kuroda, K., Le Grand, F., and Rudnicki, M.A. (2007). Asymmetric self-renewal and commitment of satellite stem cells in muscle. *Cell* 129, 999-1010.

Lachmann, A., Xu, H., Krishnan, J., Berger, S.I., Mazloom, A.R., and Ma'ayan, A. (2010). ChEA: transcription factor regulation inferred from integrating genome-wide ChIP-X experiments. *Bioinformatics* 26, 2438-2444.

Lemos, D.R., Babaeijandaghi, F., Low, M., Chang, C.K., Lee, S.T., Fiore, D., Zhang, R.H., Natarajan, A., Nedospasov, S.A., and Rossi, F.M.V. (2015). Nilotinib reduces muscle fibrosis in chronic muscle injury by promoting TNF-mediated apoptosis of fibro/adipogenic progenitors. *Nature Medicine* 21, 786-+.

Levin-Salomon, V., Bialik, S., and Kimchi, A. (2014). DAP-kinase and autophagy. *Apoptosis*

19, 346-356.

Li, G.L., Cai, L.Y., Chang, H.D., Hong, P., Zhou, Q.W., Kulakova, E.V., Kolchanov, N.A., and Ruan, Y.J. (2014). Chromatin Interaction Analysis with Paired-End Tag (ChIA-PET) sequencing technology and application. *Bmc Genomics* 15.

Li, L., Xiong, W.C., and Mei, L. (2018). Neuromuscular Junction Formation, Aging, and Disorders. In *Annual Review of Physiology*, Vol 80, D. Julius, ed., pp. 159-188.

Li, Y., Haarhuis, J.H.I., Cacciatore, A.S., Oldenkamp, R., van Ruiten, M.S., Willems, L., Teunissen, H., Muir, K.W., de Wit, E., Rowland, B.D., *et al.* (2020). The structural basis for cohesin-CTCF-anchored loops. *Nature* 578, 472-+.

Li, Y., and Huard, J. (2002). Differentiation of muscle-derived cells into myofibroblasts in injured skeletal muscle. *American Journal of Pathology* 161, 895-907.

Lieber, R.L., and Ward, S.R. (2013). Cellular Mechanisms of Tissue Fibrosis. 4. Structural and functional consequences of skeletal muscle fibrosis. *American Journal of Physiology-Cell Physiology* 305, C241-C252.

Lieberman-Aiden, E., van Berkum, N.L., Williams, L., Imakaev, M., Ragoczy, T., Telling, A., Amit, I., Lajoie, B.R., Sabo, P.J., Dorschner, M.O., *et al.* (2009). Comprehensive Mapping of Long-Range Interactions Reveals Folding Principles of the Human Genome. *Science* 326, 289-293.

Lobanenkova, V.V., Nicolas, R.H., Adler, V.V., Paterson, H., Klenova, E.M., Polotskaja, A.V., and Goodwin, G.H. (1990). A NOVEL SEQUENCE-SPECIFIC DNA-BINDING PROTEIN WHICH INTERACTS WITH 3 REGULARLY SPACED DIRECT REPEATS OF THE CCCTC-MOTIF IN THE 5'-FLANKING SEQUENCE OF THE CHICKEN C-MYC GENE. *Oncogene* 5, 1743-1753.

Loson, O.C., Song, Z., Chen, H., and Chan, D.C. (2013). Fis1, Mff, MiD49, and MiD51 mediate Drp1 recruitment in mitochondrial fission. *Molecular Biology of the Cell* 24, 659-667.

Lu, J.R., Ruhf, M.L., Perrimon, N., and Leder, P. (2007). A genome-wide RNA interference

screen identifies putative chromatin regulators essential for E2F repression. *Proceedings of the National Academy of Sciences of the United States of America* *104*, 9381-9386.

Magnuson, B., Ekim, B., and Fingar, D.C. (2012). Regulation and function of ribosomal protein S6 kinase (S6K) within mTOR signalling networks. *Biochemical Journal* *441*, 1-21.

Magri, L., Swiss, V.A., Jablonska, B., Lei, L., Pedre, X., Walsh, M., Zhang, W.J., Gallo, V., Canoll, P., and Casaccia, P. (2014). E2F1 Coregulates Cell Cycle Genes and Chromatin Components during the Transition of Oligodendrocyte Progenitors from Proliferation to Differentiation. *Journal of Neuroscience* *34*, 1481-1493.

Mahadevan, M., Tsilfidis, C., Sabourin, L., Shutler, G., Amemiya, C., Jansen, G., Neville, C., Narang, M., Barcelo, J., Ohoy, K., *et al.* (1992). MYOTONIC-DYSTROPHY MUTATION - AN UNSTABLE CTG REPEAT IN THE 3' UNTRANSLATED REGION OF THE GENE. *Science* *255*, 1253-1255.

Masiero, E., Agatea, L., Mammucari, C., Blaauw, B., Loro, E., Komatsu, M., Metzger, D., Reggiani, C., Schiaffino, S., and Sandri, M. (2009). Autophagy Is Required to Maintain Muscle Mass. *Cell Metabolism* *10*, 507-515.

Mauro, A. (1961). SATELLITE CELL OF SKELETAL MUSCLE FIBERS. *Journal of Biophysical and Biochemical Cytology* *9*, 493-&.

Megeney, L.A., Kablar, B., Garrett, K., Anderson, J.E., and Rudnicki, M.A. (1996). MyoD is required for myogenic stem cell function in adult skeletal muscle. *Genes & Development* *10*, 1173-1183.

Meyer, N., Zielke, S., Michaelis, J.B., Linder, B., Warnsmann, V., Rakel, S., Osiewacz, H.D., Fulda, S., Mittelbronn, M., Munch, C., *et al.* (2018). AT 101 induces early mitochondrial dysfunction and HMOX1 (heme oxygenase 1) to trigger mitophagic cell death in glioma cells. *Autophagy* *14*, 1693-1709.

Miniou, P., Tiziano, D., Frugier, T., Roblot, N., Le Meur, M., and Melki, J. (1999). Gene targeting restricted to mouse striated muscle lineage. *Nucleic Acids Research* *27*.

Mishra, P., and Chan, D.C. (2016). Metabolic regulation of mitochondrial dynamics. *Journal of Cell Biology* 212, 379-387.

Mohan, C., Long, K., Mutneja, M., and Ma, J. (2015). Detection of End-Stage Apoptosis by ApopTag (R) TUNEL Technique. In *Apoptosis and Cancer: Methods and Protocols*, 2nd Edition, G. Mor, and A.B. Alvero, eds., pp. 43-56.

Molina-Berenguer, M., Vila-Julia, F., Perez-Ramos, S., Salcedo-Allende, M.T., Camara, Y., Torres-Torronteras, J., and Marti, R. (2022). Dysfunctional mitochondrial translation and combined oxidative phosphorylation deficiency in a mouse model of hepatoencephalopathy due to Gfm1 mutations. *Faseb Journal* 36.

Monroy, J.A., Powers, K.L., Gilmore, L.A., Uyeno, T.A., Lindstedt, S.L., and Nishikawa, K.C. (2012). What Is the Role of Titin in Active Muscle? *Exercise and Sport Sciences Reviews* 40, 73-78.

Moon, H., Filippova, G., Loukinov, D., Pugacheva, E., Chen, Q., Smith, S.T., Munhall, A., Grewe, B., Bartkuhn, M., Arnold, R., *et al.* (2005). CTCF is conserved from *Drosophila* to humans and confers enhancer blocking of the Fab-8 insulator. *Embo Reports* 6, 165-170.

Moore, J.M., Rabaia, N.A., Smith, L.E., Fagerlie, S., Gurley, K., Loukinov, D., Disteché, C.M., Collins, S.J., Kemp, C.J., Lobanenko, V.V., *et al.* (2012). Loss of Maternal CTCF Is Associated with Peri-Implantation Lethality of Cctf Null Embryos. *Plos One* 7.

Mueller, J.S., Baumeister, S.K., Schara, U., Cossins, J., Krause, S., von der Hagen, M., Huebner, A., Webster, R., Beeson, D., Lochmueller, H., *et al.* (2006). CHRND mutation causes a congenital myasthenic syndrome by impairing co-clustering of the acetylcholine receptor with rapsyn. *Brain* 129, 2784-2793.

Nasmyth, K., and Haering, C.H. (2009). Cohesin: Its Roles and Mechanisms. *Annual Review of Genetics* 43, 525-558.

Needham, D.M. (1926). Red and white muscle. *Physiological Reviews* 6, 1-27.

Nicole, S., Azuma, Y., Bauche, S., Eymard, B., Lochmuller, H., and Slater, C. (2017).

Congenital Myasthenic Syndromes or Inherited Disorders of Neuromuscular Transmission: Recent Discoveries and Open Questions. *Journal of neuromuscular diseases* 4, 269-284.

Nicole, S., Desforges, B., Millet, G., Lesbordes, J., Cifuentes-Diaz, C., Vertes, D., Cao, M.L., De Backer, F., Languille, L., Roblot, N., *et al.* (2003). Intact satellite cells lead to remarkable protection against Smn gene defect in differentiated skeletal muscle. *Journal of Cell Biology* 161, 571-582.

Nora, E.P., Goloborodko, A., Valton, A.L., Gibcus, J.H., Uebersohn, A., Abdennur, N., Dekker, J., Mirny, L.A., and Bruneau, B.G. (2017). Targeted Degradation of CTCF Decouples Local Insulation of Chromosome Domains from Genomic Compartmentalization. *Cell* 169, 930-+.

Nora, E.P., Lajoie, B.R., Schulz, E.G., Giorgetti, L., Okamoto, I., Servant, N., Piolot, T., van Berkum, N.L., Meisig, J., Sedat, J., *et al.* (2012). Spatial partitioning of the regulatory landscape of the X-inactivation centre. *Nature* 485, 381-385.

Nuebler, J., Fudenberg, G., Imakaev, M., Abdennur, N., and Mirny, L.A. (2018). Chromatin organization by an interplay of loop extrusion and compartmental segregation. *Proceedings of the National Academy of Sciences of the United States of America* 115, E6697-E6706.

Olguin, H.C., Yang, Z., Tapscott, S.J., and Olwin, B.B. (2007). Reciprocal inhibition between Pax7 and muscle regulatory factors modulates myogenic cell fate determination. *Journal of Cell Biology* 177, 769-779.

Ottaviani, A., Rival-Gervier, S., Boussouar, A., Foerster, A.M., Rondier, D., Sacconi, S., Desnuelle, C., Gilson, E., and Magdinier, F. (2009). The D4Z4 Macrosatellite Repeat Acts as a CTCF and A-Type Lamins-Dependent Insulator in Facio-Scapulo-Humeral Dystrophy. *Plos Genetics* 5.

Ottenheijm, C.A.C., and Granzier, H. (2010). Lifting the Nebula: Novel Insights into Skeletal Muscle Contractility. *Physiology* 25, 304-310.

Oustanina, S., Hause, G., and Braun, T. (2004). Pax7 directs postnatal renewal and propagation of myogenic satellite cells but not their specification. *Embo Journal* 23, 3430-3439.

Pena-Hernandez, R., Marques, M., Hilmi, K., Zhao, T., Saad, A., Alaoui-Jamali, M.A., del Rincon, S.V., Ashworth, T., Roy, A.L., Emerson, B.M., *et al.* (2015). Genome-wide targeting of the epigenetic regulatory protein CTCF to gene promoters by the transcription factor TFII-I. *Proceedings of the National Academy of Sciences of the United States of America* *112*, E677-E686.

Peterson, J.M., Wang, D.J., Shettigar, V., Roof, S.R., Canan, B.D., Bakkar, N., Shintaku, J., Gu, J.M., Little, S.C., Ratnam, N.M., *et al.* (2018). NF-kappa B inhibition rescues cardiac function by remodeling calcium genes in a Duchenne muscular dystrophy model. *Nature Communications* *9*.

Peterson, T.R., Sengupta, S.S., Harris, T.E., Carmack, A.E., Kang, S.A., Balderas, E., Guertin, D.A., Madden, K.L., Carpenter, A.E., Finck, B.N., *et al.* (2011). mTOR Complex 1 Regulates Lipin 1 Localization to Control the SREBP Pathway. *Cell* *146*, 408-420.

Picard, M., White, K., and Turnbull, D.M. (2013). Mitochondrial morphology, topology, and membrane interactions in skeletal muscle: a quantitative three-dimensional electron microscopy study. *Journal of Applied Physiology* *114*, 161-171.

Pidsley, R., Fernandes, C., Viana, J., Paya-Cano, J.L., Liu, L., Smith, R.G., Schalkwyk, L.C., and Mill, J. (2012). DNA methylation at the Igf2/H19 imprinting control region is associated with cerebellum mass in outbred mice. *Molecular Brain* *5*.

Powers, S.K., Lynch, G.S., Murphy, K.T., Reid, M.B., and Zijdwind, I. (2016). Disease-Induced Skeletal Muscle Atrophy and Fatigue. *Medicine and Science in Sports and Exercise* *48*, 2307-2319.

Pugacheva, E.M., Kubo, N., Loukinov, D., Tajmul, M., Kang, S., Kovalchuk, A.L., Strunnikov, A.V., Zentner, G.E., Ren, B., and Lobanenko, V.V. (2020). CTCF mediates chromatin looping via N-terminal domain-dependent cohesin retention. *Proceedings of the National Academy of Sciences of the United States of America* *117*, 2020-2031.

Rao, S.S.P., Huntley, M.H., Durand, N.C., Stamenova, E.K., Bochkov, I.D., Robinson, J.T., Sanborn, A.L., Machol, I., Omer, A.D., Lander, E.S., *et al.* (2014). A 3D Map of the Human

Genome at Kilobase Resolution Reveals Principles of Chromatin Looping. *Cell* 159, 1665-1680.

Rawls, A., Valdez, M.R., Zhang, W., Richardson, J., Klein, W.H., and Olson, E.N. (1998). Overlapping functions of the myogenic bHLH genes MRF4 and MyoD revealed in double mutant mice. *Development* 125, 2349-2358.

Ren, G., Jin, W., Cui, K., Rodriguez, J., Hu, G., Zhang, Z., Larson, D.R., and Zhao, K. (2017). CTCF-Mediated Enhancer-Promoter Interaction Is a Critical Regulator of Cell-to-Cell Variation of Gene Expression. *Molecular Cell* 67, 1049-+.

Robson, L.G., Di Foggia, V., Radunovic, A., Bird, K., Zhang, X., and Marino, S. (2011). Bmi1 Is Expressed in Postnatal Myogenic Satellite Cells, Controls Their Maintenance and Plays an Essential Role in Repeated Muscle Regeneration. *Plos One* 6.

Roman, W., Pinheiro, H., Pimentel, M.R., Segales, J., Oliveira, L.M., Garcia-Dominguez, E., Gomez-Cabrera, M.C., Serrano, A.L., Gomes, E.R., and Munoz-Canoves, P. (2021). Muscle repair after physiological damage relies on nuclear migration for cellular reconstruction. *Science* 374, 355-+.

Roth, S.M., Martel, G.F., Ivey, F.M., Lemmer, J.T., Metter, E.J., Hurley, B.F., and Rogers, M.A. (2000). Skeletal muscle satellite cell populations in healthy young and older men and women. *Anatomical Record* 260, 351-358.

Roy, A.R., Ahmed, A., DiStefano, P.V., Chi, L.J., Khyzha, N., Galjart, N., Wilson, M.D., Fish, J.E., and Delgado-Olguin, P. (2018). The transcriptional regulator CCCTC-binding factor limits oxidative stress in endothelial cells. *Journal of Biological Chemistry* 293, 8449-8461.

Rudnicki, M.A., Schnegelsberg, P.N.J., Stead, R.H., Braun, T., Arnold, H.H., and Jaenisch, R. (1993). MYOD OR MYF-5 IS REQUIRED FOR THE FORMATION OF SKELETAL-MUSCLE. *Cell* 75, 1351-1359.

Sabourin, L.A., Girgis-Gabardo, A., Seale, P., Asakura, A., and Rudnicki, M.A. (1999). Reduced differentiation potential of primary MyoD^{-/-} myogenic cells derived from adult skeletal muscle. *Journal of Cell Biology* 144, 631-643.

Sadeh, M. (1988). EFFECTS OF AGING ON SKELETAL-MUSCLE REGENERATION. *Journal of the Neurological Sciences* 87, 67-74.

Sanborn, A.L., Rao, S.S.P., Huang, S.C., Durand, N.C., Huntley, M.H., Jewett, A.I., Bochkov, I.D., Chinnappan, D., Cutkosky, A., Li, J., *et al.* (2015). Chromatin extrusion explains key features of loop and domain formation in wild-type and engineered genomes. *Proceedings of the National Academy of Sciences of the United States of America* 112, E6456-E6465.

Sancak, Y., Bar-Peled, L., Zoncu, R., Markhard, A.L., Nada, S., and Sabatini, D.M. (2010). Regulator-Rag Complex Targets mTORC1 to the Lysosomal Surface and Is Necessary for Its Activation by Amino Acids. *Cell* 141, 290-303.

Saxton, R.A., and Sabatini, D.M. (2017). mTOR Signaling in Growth, Metabolism, and Disease. *Cell* 168, 960-976.

Schiaffino, S., and Reggiani, C. (2011). FIBER TYPES IN MAMMALIAN SKELETAL MUSCLES. *Physiological Reviews* 91, 1447-1531.

Seale, P., Sabourin, L.A., Girgis-Gabardo, A., Mansouri, A., Gruss, P., and Rudnicki, M.A. (2000). Pax7 is required for the specification of myogenic satellite cells. *Cell* 102, 777-786.

Seo, J., Choi, I.-H., Lee, J.S., Yoo, Y., Kim, N.K.D., Choi, M., Ko, J.M., and Shin, Y.B. (2015). Rare cases of congenital arthrogryposis multiplex caused by novel recurrent CHRNG mutations. *Journal of Human Genetics* 60, 213-215.

Shorstova, T., Marques, M., Su, J., Johnston, J., Kleinman, C.L., Hamel, N., Huang, S.D., Alaoui-Jamali, M.A., Foulkes, W.D., and Witcher, M. (2019). SWI/SNF-Compromised Cancers Are Susceptible to Bromodomain Inhibitors. *Cancer Research* 79, 2761-2774.

Skuk, D., Goulet, M., Roy, B., Chapdelaine, P., Bouchard, J.P., Roy, R., Dugre, F.J., Sylvain, M., Lachance, J.G., Deschenes, L., *et al.* (2006). Dystrophin expression in muscles of Duchenne muscular dystrophy patients after high-density injections of normal myogenic cells. *Journal of Neuropathology and Experimental Neurology* 65, 371-386.

Soshnikova, N., Montavon, T., Leleu, M., Galjart, N., and Duboule, D. (2010). Functional

Analysis of CTCF During Mammalian Limb Development. *Developmental Cell* *19*, 819-830.

Spangenburg, E.E., and Booth, F.W. (2003). Molecular regulation of individual skeletal muscle fibre types. *Acta Physiologica Scandinavica* *178*, 413-424.

Splinter, E., Heath, H., Kooren, J., Palstra, R.-J., Klous, P., Grosveld, F., Galjart, N., and de Laat, W. (2006). CTCF mediates long-range chromatin looping and local histone modification in the beta-globin locus. *Genes & Development* *20*, 2349-2354.

Stedman, W., Kang, H., Lin, S., Kissil, J.L., Bartolomei, M.S., and Lieberman, P.M. (2008). Cohesins localize with CTCF at the KSHV latency control region and at cellular c-myc and H19/Igf2 insulators. *Embo Journal* *27*, 654-666.

Sylvester, J.E., Fischel-Ghodsian, N., Mougey, E.B., and O'Brien, T.W. (2004). Mitochondrial ribosomal proteins: Candidate genes for mitochondrial disease. *Genetics in Medicine* *6*, 73-80.

Tedesco, F.S., Dellavalle, A., Diaz-Manera, J., Messina, G., and Cossu, G. (2010). Repairing skeletal muscle: regenerative potential of skeletal muscle stem cells. *Journal of Clinical Investigation* *120*, 11-19.

Thiery, J.P., Acloque, H., Huang, R.Y.J., and Nieto, M.A. (2009). Epithelial-Mesenchymal Transitions in Development and Disease. *Cell* *139*, 871-890.

Thomas, G.V., Tran, C., Mellinghoff, I.K., Welsbie, D.S., Chan, E., Fueger, B., Czernin, J., and Sawyers, C.L. (2006). Hypoxia-inducible factor determines sensitivity to inhibitors of mTOR in kidney cancer. *Nature Medicine* *12*, 122-127.

Tidball, J.G. (2017). Regulation of muscle growth and regeneration by the immune system. *Nature Reviews Immunology* *17*, 165-178.

Tidball, J.G., Albrecht, D.E., Lokensgard, B.E., and Spencer, M.J. (1995). APOPTOSIS PRECEDES NECROSIS OF DYSTROPHIN-DEFICIENT MUSCLE. *Journal of Cell Science* *108*, 2197-2204.

Tolhuis, B., Palstra, R.J., Splinter, E., Grosveld, F., and de Laat, W. (2002). Looping and interaction between hypersensitive sites in the active beta-globin locus. *Molecular Cell* *10*,

1453-1465.

Uezumi, A., Fukada, S., Yamamoto, N., Takeda, S., and Tsuchida, K. (2010). Mesenchymal progenitors distinct from satellite cells contribute to ectopic fat cell formation in skeletal muscle. *Nature Cell Biology* 12, 143-U116.

Um, S.H., Frigerio, F., Watanabe, M., Picard, F., Joaquin, M., Sticker, M., Fumagalli, S., Allegrini, P.R., Kozma, S.C., Auwerx, J., *et al.* (2004). Absence of S6K1 protects against age- and diet-induced obesity while enhancing insulin sensitivity. *Nature* 431, 200-205.

van der Maarel, S.M., Miller, D.G., Tawil, R., Filippova, G.N., and Tapscott, S.J. (2012). Facioscapulohumeral muscular dystrophy: consequences of chromatin relaxation. *Current Opinion in Neurology* 25, 614-620.

van der Meer, S.F.T., Jaspers, R.T., Jones, D.A., and Degens, H. (2011). TIME-COURSE OF CHANGES IN THE MYONUCLEAR DOMAIN DURING DENERVATION IN YOUNG-ADULT AND OLD RAT GASTROCNEMIUS MUSCLE. *Muscle & Nerve* 43, 212-222.

van Zandwijk, J.P., Bobbert, M.F., Harlaar, J., and Hof, A.L. (1998). From twitch to tetanus for human muscle: experimental data and model predictions for m-triceps surae. *Biological Cybernetics* 79, 121-130.

Verdijk, L.B., Snijders, T., Drost, M., Delhaas, T., Kadi, F., and van Loon, L.J.C. (2014). Satellite cells in human skeletal muscle; from birth to old age. *Age* 36, 545-557.

Vostrov, A.A., and Quitschke, W.W. (1997). The zinc finger protein CTCF binds to the APB beta domain of the amyloid beta-protein precursor promoter - Evidence for a role in transcriptional activation. *Journal of Biological Chemistry* 272, 33353-33359.

Wagers, A.J., and Conboy, I.M. (2005). Cellular and molecular signatures of muscle regeneration: Current concepts and controversies in adult myogenesis. *Cell* 122, 659-667.

Wan, L.-B., Pan, H., Hannenhalli, S., Cheng, Y., Ma, J., Fedoriw, A., Lobanenkoy, V., Latham, K.E., Schultz, R.M., and Bartolomei, M.S. (2008). Maternal depletion of CTCF reveals multiple functions during oocyte and preimplantation embryo development. *Development* 135,

2729-2738.

Wang, H.Z., Melton, D.W., Porter, L., Sarwar, Z.U., McManus, L.M., and Shireman, P.K. (2014). Altered Macrophage Phenotype Transition Impairs Skeletal Muscle Regeneration. *American Journal of Pathology* *184*, 1167-1184.

Weiss, R.B., Vieland, V.J., Dunn, D.M., Kaminoh, Y., Flanigan, K.M., and United Dystrophinopathy, P. (2018). Long-range genomic regulators of THBS1 and LTBP4 modify disease severity in duchenne muscular dystrophy. *Annals of Neurology* *84*, 234-245.

Welle, S. (2002). Cellular and molecular basis of age-related sarcopenia. *Canadian Journal of Applied Physiology-Revue Canadienne De Physiologie Appliquee* *27*, 19-41.

Wosczyzna, M.N., and Rando, T.A. (2018). A Muscle Stem Cell Support Group: Coordinated Cellular Responses in Muscle Regeneration. *Developmental Cell* *46*, 135-143.

Xiao, R.J., Ferry, A.L., and Dupont-Versteegden, E.E. (2011a). Cell death-resistance of differentiated myotubes is associated with enhanced anti-apoptotic mechanisms compared to myoblasts. *Apoptosis* *16*, 221-234.

Xiao, T.J., Wallace, J., and Felsenfeld, G. (2011b). Specific Sites in the C Terminus of CTCF Interact with the SA2 Subunit of the Cohesin Complex and Are Required for Cohesin-Dependent Insulation Activity. *Molecular and Cellular Biology* *31*, 2174-2183.

Xiao, T.J., Wongtrakoongate, P., Trainor, C., and Felsenfeld, G. (2015). CTCF Recruits Centromeric Protein CENP-E to the Pericentromeric/Centromeric Regions of Chromosomes through Unusual CTCF-Binding Sites. *Cell Reports* *12*, 1704-1714.

Yaffe, E., and Tanay, A. (2011). Probabilistic modeling of Hi-C contact maps eliminates systematic biases to characterize global chromosomal architecture. *Nature Genetics* *43*, 1059-U1040.

Yin, M.L., Wang, J.Y., Wang, M., Li, X.M., Zhang, M., Wu, Q., and Wang, Y.L. (2017). Molecular mechanism of directional CTCF recognition of a diverse range of genomic sites. *Cell Research* *27*, 1365-1377.

- Yoon, Y.S., Jeong, S., Rong, Q., Park, K.Y., Chung, J.H., and Pfeifer, K. (2007). Analysis of the H19ICR insulator. *Molecular and Cellular Biology* 27, 3499-3510.
- Yue, L., Wan, R., Luan, S.Y., Zeng, W.S., and Cheung, T.H. (2020). Dek Modulates Global Intron Retention during Muscle Stem Cells Quiescence Exit. *Developmental Cell* 53, 661-+.
- Zhang, D.D., Zhang, W.M., Li, D., Fu, M., Chen, R.S., and Zhan, Q.M. (2015). GADD45A inhibits autophagy by regulating the interaction between BECN1 and PIK3C3. *Autophagy* 11, 2247-2258.
- Zhang, J., Xiao, Z.C., Qu, C., Cui, W., Wang, X.N., and Du, J. (2014). CD8 T Cells Are Involved in Skeletal Muscle Regeneration through Facilitating MCP-1 Secretion and Gr1(high) Macrophage Infiltration. *Journal of Immunology* 193, 5149-5160.
- Zierath, J.R., and Hawley, J.A. (2004). Skeletal muscle fiber type: Influence on contractile and metabolic properties. *Plos Biology* 2, 1523-1527.
- Zoncu, R., Efeyan, A., and Sabatini, D.M. (2011). mTOR: from growth signal integration to cancer, diabetes and ageing. *Nature Reviews Molecular Cell Biology* 12, 21-35.